Aus dem Institut für Virologie
des Fachbereichs Veterinärmedizin
der Freien Universität Berlin

The role of the secreted glycoprotein G (gG) in equine herpesvirus type 1 (EHV-1) immune modulation and virulence

Inaugural-Dissertaion
zur Erlangung des Grades eines
Doktors der Veterinärmedizin
an der
Freien Universität Berlin

vorgelegt von
Nora Mariella Thormann
Tierärztin
aus Fürstenfeldbruck

Berlin 2011

Journal-Nr.: 3517

Gedruckt mit Genehmigung des Fachbereichs Veterinärmedizin

der Freien Universität Berlin

Dekan:	Herr Univ.-Prof. Dr. Leo Brunnberg
Erster Gutachter:	Herr Univ.-Prof. Dr. Klaus Osterrieder
Zweiter Gutachter:	Frau Univ.-Prof. Dr. Gerlinde Van de Walle
Dritter Gutachter:	Herr Univ.-Prof. Dr. Johannes Handler

Deskriptoren (nach CAB-Thesaurus):
Equine herpesvirus 1, Equine herpesvirus 4, horse diseases, immune evasion, glycoproteins, neutrophils, chemotaxis, recombination, bacterial artificial chromosomes

Tag der Promotion: 21. November 2011

Bibliografische Information der *Deutschen Nationalbibliothek*
Die Deutsche Nationalbibliothek verzeichnet diese Publikation in der Deutschen Nationalbibliografie; detaillierte bibliografische Daten sind im Internet über <http://dnb.ddb.de> abrufbar.

ISBN: 978-3-86387-098-0
Zugl.: Berlin, Freie Univ., Diss., 2011
Dissertation, Freie Universität Berlin
D 188

Choriner Str. 85 - 10119 Berlin
verlag@menschundbuch.de – www.menschundbuch.de

„Ach, die Welt ist so geräumig,
und der Kopf ist so beschränkt.“
(Wilhelm Busch)

To my mother and
my stepfather

Table of Contents

List of Abbreviations

aa	Amino acid
APC	Allophycocyanin
ASHV-1	Asinine Herpes Virus 1
BAC	Bacterial artificial chromosome
BAL	Bronchoalveolar lavage
BHV-1	Bovine Herpes Virus 1
BHV-2	Bovine Herpes Virus 2
CK	Chemokine
C	Cysteine
CPE	Cytopathogenic effect
DNA	Deoxyribonucleic acid
eGFP	enhanced green fluorescent protein
EHV-1	Equine Herpes Virus Type 1
EHV-3	Equine Herpesvirus Type 3
EHV-4	Equine Herpes Virus Type 4
EHV-9	Equine Herpes Virus Type 9
ER	Endoplasmatic reticulum
FBS	Fetal bovine serum
FeHV-1	Felid Herpes Virus 1
FITC	Fluorescein
G+C content	Guanine-cytosine content
gG	Glycoprotein G
gp2	Glycoprotein gp2
HSV-1	Herpes Simplex Virus 1
HSV-2	Herpes Simplex Virus 2
IFA	Indirect immunofluorescence assay
ILTV	Infectious Laryngotracheitis Virus
IRs	Internal Repeat short
kDa	kilo Dalton

List of Abbreviations

kbp	kilo base pairs
MEM	Minimum Essential Medium Eagle
MHV-68	Murine Gammherpesvirus 68
MOI	Multiplicity of infection
ORF	Open reading frame
PCR	Polymerase chain reaction
PFU	Plaque forming units
PRV	Pseudorabies Virus
psm	positive selection marker
RFLP	restriction fragment length polymorphism
RT	Room temperature
SDS-PAGE	Sodium Dodecyl Sulfate Polyacrylamide Gel Electrophoresis
TRs	Terminal Repeat short
U_L	Unique long
U_S	Unique short
vCKBP	viral Chemokine binding protein
vCKR	viral Chemokine receptor
VZV	Varicella Zoster Virus

List of Figures and Tables

Immunmodulation und Beeinflussung der Virulenz durch das Glykoprotein G (gG) des Equinen Herpesvirus vom Typ 1

Zusammenfassung

Infektionen durch equine Herpesviren vom Typ 1 und Typ 4 (EHV-1 und EHV-4) treten in Pferdepopulationen weltweit auf. Während eine Infektion mit EHV-4 primär auf den oberen Respirationstrakt beschränkt bleibt, kann eine Infektion mit EHV-1 nach einer Lymphozyten-assoziierten Virämie zu neurologischen Ausfällen und Aborten führen. Einen möglichen Beitrag zur systemischen Verbreitung von EHV-1 liefert das Glykoprotein G, genauer gesagt dessen hypervariable Region, die an Chemokine bindet und dadurch mit der Immunantwort des Wirtes interagieren kann.

In dieser Studie wurde die Hypothese getestet, dass gG einer der bestimmenden Faktoren einer systemischen EHV-1 Infektion ist. Hierzu wurden verschiedene EHV-1-Mutanten konstruiert, in welchen das gesamte gG-Gen oder die hypervariable Region allein, aufwärts von der Transmembranregion gelegen, mit den entsprechenden Sequenzen von EHV-4 substituiert wurden. Basierend auf dem neurovirulenten Stamm Ohio 2003 (OH-03) wurden die folgenden Mutanten generiert: eine gG-Deletionsmutante (vOH-ΔgG), eine Mutante, in welcher das EHV-4 gG an Stelle des EHV-1 gGs inseriert wurde (vOH-4gG), eine Mutante mit der Chemokin-bindenden Region des EHV-1 gG im EHV-4 gG (vOH-4hyp1) sowie eine Mutante, in welcher nur die hypervariable Region des EHV-1 gG durch die variable Region des EHV-4 gGs ersetzt wurde (vOH-1hyp4). Die Virusmutanten wurden durch En passant-Mutagenese in dem als Bacterical Artificial Chromosome (BAC) konstruierten Genom des EHV-1 Stammes OH-03 in *Escherichia coli* generiert. Nach Virus-Rekonstitution wurden die Virusmutanten durch Analyse der Plaquegrößen und Ein-Schritt-Wachstums-Kinetiken *in vitro* charakterisiert. Hier konnte gezeigt werden, dass sowohl der Austausch des gG zwischen EHV-1 und EHV-4 sowie die verschiedenen Mutationen keine Auswirkung auf die Zell-zu-Zell-Ausbreitung sowie die Vermehrung des Virus haben. Im Anschluss daran wurden Chemotaxis-Assays durchgeführt, um zu eruieren, ob die diversen gGs in der Lage sind, die Migration von neutrophilen Granulozyten *in vitro* zu beeinflussen. Bei diesen Experimenten konnte beobachtet werden, dass die gG-Deletionsmutante sowie die das EHV-4 gG enthaltende Mutante den Flux von Neutrophilen nicht zu beeinflussen vermochten. Allerdings wurde auch durch die Restaurierung der vorhergesagten Chemokin-bindenden Region des EHV-1 gG die Fähigkeit zur Hemmung der Migration von Neutrophilen nicht komplett wiederhergestellt. Ebenso ging die Fähigkeit zur Hemmung auch bei Insertion der hypervariablen Region des EHV-4 gG nicht gänzlich verloren.

Im Anschluss an diese Experimente wurden die verschiedenen Mutanten in einem Infektions-Modell in BALB/c Mäusen *in vivo* getestet. Durchflusszytometrische Analysen

wurden ausgeführt, um die Zusammensetzung der Immunzellen in der bronchoalveolären Lavage intranasal infizierter Mäuse und eventuell durch die verschiedenen gG-Varianten erzeugte Unterschiede zu bestimmen. Der größte Einstrom von Neutrophilen an den Infektionsort war bei den Mäusen zu verzeichnen, die mit der vOH-4gG-Mutante infiziert waren, wohingegen der Influx von Neutrophilen bei den mit der Deletionsmutante infizierten Mäuse mehr dem Wildtyp glichen. Wie schon bei den Chemotaxis-Assays zu verzeichnen, zeigten auch hier die zwei Mutanten, in welchen nur die hypervariable Region ausgetauscht wurde, um dem EHV-4 gG die Chemokin-bindende Funktion zu verleihen und diese im EHV-1 gG zu inaktivieren, nicht das erwartete Muster bezüglich des Einflusses der Migration von Neutrophilen. Dies lässt zu der Annahme führen, dass nicht allein die hypervariable Region für das immunmodulatorische Potential des gG verantwortlich ist sondern auch andere Domänen des Proteins an der Ausbildung des Phänotyps beteiligt sind.

The role of the secreted glycoprotein G (gG) in equine herpesvirus type 1 (EHV-1) immune modulation and virulence

Summary

Equine herpesvirus type 1 and 4 (EHV-1 and EHV-4) affects horses worldwide. Infection with EHV-4 usually remains restricted to the upper airways, while EHV-1 infection can result in neurological disorders and abortions following lymphocyte-associated viremia. One of the possible mechanisms allowing systemic dissemination of EHV-1 is the documented ability of EHV-1 gG, more specifically its hypervariable region, to interfere with the host's immune response by binding to chemokines. In this study we tested the hypothesis that gG influences the ability of EHV-1 to cause systemic infection by constructing EHV-1 mutants in which the entire gG or only its hypervariable region upstream of the transmembrane region were exchanged with their EHV-4 counterparts. Based on the neurovirulent strain Ohio 2003 (OH-03), we constructed four recombinant viruses by en-passant mutagenesis of OH-03 cloned as a bacterial artificial chromosome: A gG deletion mutant (vOH-ΔgG), a mutant in which EHV-4 gG was inserted in lieu of authentic EHV-1 gG (vOH-4gG), a mutant harboring EHV-4 gG with the chemokine-binding region of EHV-1 gG (vOH-4gGhyp1) and a mutant harboring the hypervariable region of EHV-4 gG in the EHV-1 backbone (vOH-hyp4). The mutant viruses were characterized *in vitro* by plaque size assays as well as single-step-growth-kinetics and it could be shown that the various mutations in gG did not influence viral cell-to-cell spread or replication *in vitro*. Next, chemotaxis assays were performed to analyze if the various gGs can interfere with neutrophil migration *in vitro.* Here, an increased chemotaxis of neutrophils could be observed when supernatants of cells infected with vOH-ΔgG or vOH-4gG were used. In contrast, re-insertion of the predicted chemokine-binding region of EHV-1 glycoprotein G did not completely restore the ability to inhibit neutrophil migration as well as insertion of the hypervariable region of EHV-4 gG did not lead to complete loss of chemokine-binding function of gG. Finally, the different mutant viruses were tested in an *in vivo* infection model in BALB/c mice. Flow cytometric analyses were performed to determine the composition of immune cells in bronchoalveolar lavages of intranasally infected mice. The largest influx of neutrophils was noted for mice infected with the vOH-4gG virus, whereas here the gG deletion virus behaved more like the OH-03 virus and resulted in a more pronounced inhibition of chemotaxis in infected mice. Again, the two viruses with the exchanged hypervariable region did not show the expected influence on neutrophil migration to the site of infection, suggesting that it is not the hypervariable region alone that determines the immunmodulatory potential of gG.

1. Introduction

1.1. Animal Herpesviruses

The familiy of *Herpesviridae* consists of a diverse group of viruses infecting a variety of different hosts. Herpesviruses are present in virtually every species of birds and mammals and have as well been found in reptiles, amphibians and mollusks [1]. Based on biological properties, gene contents and sequences they are divided into three main subfamilies, the *Alphaherpesvirinae*, the *Betaherpesvirinae* and the *Gammaherpesvirinae* [2]. These subfamilies include all herpesviruses with mammalian, avian and reptilian hosts. Lately, a new family was added, the *Alloherpesviridae,* comprising piscine and amphibian herpesviruses and the channel catfish virus being the first sequenced member of this family [3].

1.1.1. Virion architecture

Herpesviruses are enveloped, double-stranded DNA viruses, around 150 – 250 nm in diameter containing an icosahedral nucleocapsid that measures about 125 nm in diameter. The capsid is composed of 162 capsomers - 150 hexamers and 12 pentamers. The DNA genome is present in the nucleocapsid as a fibrous spool-like core in the shape of a torus, which appears to be suspended by fibrils that are anchored to the inner side of the surrounding capsid and pass through the hole of the torus [4]. The capsid is surrounded by a layer of proteins, called the tegument, which is followed by a typical lipoprotein envelope. The envelope harbors more than 10 different membrane (glyco) proteins, the exact number and relative amounts of these vary in between the different herpesviruses [2]

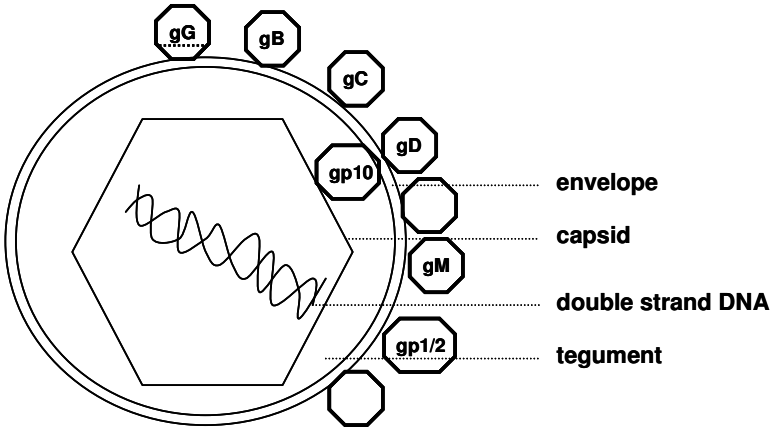

Figure 1: Schematic representation of herpesvirion architecture. Depicted are some of the glycoproteins located in the viral envelope

Herpesvirus genes generally can be divided into three classes: 1) Immediate-early genes which require no viral protein synthesis for their expression, 2) early genes whose expression is independent of viral DNA synthesis and 3) late genes, which are expressed following viral DNA synthesis. The first two classes of genes mainly encode proteins concerned with viral replication as well as enzymes involved in DNA replication and transcription, whereas the third mostly encode for structural proteins [1, 2].

1.2. Equine herpesviruses type 1 and 4

To date, nine different equine herpesviruses have been identified. Equine Herpesvirus type 1 to 5 (EHV-1 to -5) infect horses whereas EHV-6 to -8 or asinine herpesviruses 1 to 3 (AHV-1 to 3) infect donkeys. EHV-9, possibly endemic in zebras, is also able to jump species barriers and was isolated from different animals in zoological collections [5].

1.2.1. Classification and structure of equine herpesvirus type 1 and 4

EHV-1 and EHV-4 are classified as members of the *Varicellovirus* genus of the *Alphaherpesvirinae*, a subfamily of the *Herpesviridae.* The type species of the genus is varicella zoster virus (VZV). The genus is also home to other important pathogens of animals such as BHV-1 and pseudorabies virus, while the prototypical alphaherpesvirus, herpes simplex virus type-1 (HSV-1), is a member of the *Simplexvirus* genus [6]. Virus species belonging to the subfamily *Alphaherpesvirinae* have a variable host range and a relatively short reproductive cycle. They can spread rapidly in cell culture and infected cells are usually destroyed efficiently by lytic replication. The hallmark of herpesviruses is that they undergo a state called latency in which the virus remains in the host for a lifetime. Latency can be established in sensory ganglia as well as in lymphocytes and monocytes, wherefrom viral replication can be reactivated by stress resulting in renewed shedding of virus [2].

Until 1981, EHV-1 and EHV-4 were considered two subtypes of one virus species causing either rhinopneumonitis or abortion. Investigations by Studdert, Simon and Roizman based on restriction endonuclease analyses identified the two viruses clearly as two different species with collinear genomes and a highly homologous genetic structure [7]. The genome of EHV-1 consists of a linear, double-stranded DNA molecule of approximately 150 kbp and a base composition of 57 % G + C, which is significantly higher in the internal and terminal repeats (IR and TR) with 67 % when compared to the unique-long segment (U_L) where it is 55 % or the unique-short segment (U_S) with 52 % G + C content.

On account of the arrangement of the EHV-1 and EHV-4 genomes, they are classified as viruses with a class D genome [4]. The genome is composed of two covalently linked components, designated L and S. The S component is comprised of the U_S flanked by IR and TR. As the U_S can invert relative to the inverted repeats, two isomers of the genome are formed and present in equimolar amounts. The U_L is flanked by very small inverted repeats with variable sequences and no isomerization occurs.

Figure 2: Schematic diagram of sequence arrangement of the EHV-1 and EHV-4 genome. Present are the unique-long (U_L) and unique-short (U_S) sequences, the latter being flanked by inverted repeat sequences termed internal and terminal repeats (IR and TR, respectively).

All sequenced EHV-1 strains share a highly similar genome size of approximately 150 kbp and encode for at least 76 genes [8]. Due to duplications of ORFs in the TR and IR, where at least six different genes have been identified (IR1 to IR6), no less than 80 genes are encoded in total [8, 9]. The genome of EHV-1 has an arrangement similar to those of VZV, PRV and BHV-1. Three possible origins of DNA replication (ori) exist, two of them in the IR and TR at positions corresponding to ori of HSV-1 and VZV.

In comparison, the EHV-4 genome is approximately 145 kbp in size, hence slightly more compact. There are 76 distinct genes; three genes are present in two copies in the internal repeat region (64, 65 and 66) resulting in 79 genes in total. Every gene of EHV-4 has a homologue in the EHV-1 genome, which was used as an aid in locating EHV-4 genes. The amino acid sequence identity between EHV-1 and EHV-4 proteins ranges from 55 % to 96 %, the greatest number of sequence differences could be determined in parts of the U_S, where the 3´ portion of gene 70 (gG) was shown to encode variable regions immediately upstream of the transmembrane anchor. The different epitopes specified by this region also elicit EHV-1- and EHV-4 - specific antibody responses in horses and are used for determination of type-specific immune responses and epidemiological investigations [6, 10].

1.2.2. Glycoproteins in the viral envelope

Some of the glycoproteins of EHV-1 located in the viral envelope are important for initiating infection as they are the first and determining factors for attachment to and penetration into susceptible cells. Furthermore, they account for strain variation and play an important role as the host humoral immune response is mainly directed against the distinct envelope glycoproteins [11, 12]. Twelve glycoproteins were identified in EHV-1, 6 major and 6 minor [13]. The major glycoproteins were designated gp2, gp10, gp13 (gC), gp14 (gB), gp18 (gD) and gp21/22 (gM), all of these glycoproteins are located in the viral envelope except gp10, which was later shown to encode a tegument protein [14-16]. The major glycoproteins located in the envelope of EHV-1 and EHV-4 carry type-common and type-specific epitopes [14, 15]

Glycoproteins are essential for virus entry. The principal mechanisms as well as the glycoproteins involved were studied extensively for HSV-1 and PRV. The entry mechanism of EHV-1 is comparable to those of the former two viruses, and the functions of distinct glycoproteins in EHV-1 virions were evaluated with the help of numerous deletion mutants [17-21]. It could be shown that gC and, in some cases gB bind to cell surface proteoglycans providing the basis for initial attachment. This event is followed by tight interaction of gD and a cell surface receptor such as MHC class I resulting in a more stable binding [22]. Fusion of the viral envelope to the plasma membrane of the cell is mediated by gB, gD and the gH-L complex [23].

1.2.3. The glycoprotein G

Glycoprotein G is conserved in most alphaherpesviruses [24]. Homologues of the protein were identified in EHV-1 and -4 as well as for bovine herpes virus type 1 and 5 (BHV-1 and BHV-5), herpes simplex virus 2 (HSV-2), PRV, infectious laryngotracheitis virus (ILTV) and felid herpes virus 1 (FeHV-1), all of them are at least partially secreted into the medium of infected cells [25-31]. Due to point mutations, deletions and/or insertions of DNA segments, the genes encoding gG are very heterogeneous and the resulting amino acid sequences differ widely from 699 aa of HSV-2 gG to 298 aa of ILTV gG [28, 29] [32]. In the following paragraphs, the characteristics and functions of different gGs expressed by animal alphaherpesviruses will be described in more detail:

a. BHV-1 gG and BHV-5 gG

In the case of BHV-1 and BHV-5, gG constitutes a minor glycoprotein encoded by US4 in the U_s segment comprising 444 and 440 amino acids, respectively, which is secreted into the supernatant of infected cells as a 65 kDa polypeptide. Also, a diffusely migrating glycoproteoglycan of 90 – 250 kDa can be detected, resulting from addition of chondroitin-sulfate side chains during intracellular transport [26, 27]. BHV-1 gG is not essential for viral growth in cell culture but appears to be required for efficient cell-to-cell spread [33, 34]. BHV-1 gG deletion mutants showed reduced plaque sizes *in vitro* [33, 34] and a first *in vivo* study showed that a BHV-1 gG deletion mutant is slightly attenuated in cattle [35]. BHV-1 gG was also suggested to function in maintaining cell-to-cell-junctions and adhesion during BHV-1 infection [36]. Finally, secreted BHV-1 and BHV-5 gG bind to most human and mouse CC chemokines as well as to some CXC chemokines. Recombinant His-tagged gG of both viruses was proven to inhibit CCL3-induced chemotaxis of human neutrophils [37].

b. EHV-3 gG

Glycoprotein G of EHV-3, a protein of 488 aa, was also shown to be secreted into the medium of infected cells [38]. Comparing the sequences of EHV-3, EHV-1, EHV-4 and AHV-3 gG an overall identity of around 40 % could be noted with the EHV-3 gG being very similar to EHV-1 and EHV-4 gG. EHV-3 gG specifies a strongly immunogenic, variable region at the C-terminal part of the protein [38]. It was demonstrated to bind to chemokines of human origin but to date there is no data available regarding further functions of this protein [37].

c. FeHV-1 gG

FeHV-1 gG, encoded by US4 located in the unique short between PK (US3) and gD (US6), has an overall size of 434 aa and was shown to be a secreted protein with a molecular weight of approximately 52 kDa [25]. A membrane-bound form as well as its presence as a structural component on the surface of virion particles could also be demonstrated [25, 39]. Each of these forms have the capability of binding to a broad range of chemokines of human origin, acting either as a soluble viral chemokine binding protein (vCKBP) or as a CK decoy receptor on the surface of virions [39].

d. ILTV gG

The gG homologue of ILTV is located in the unique short between UL47 and gJ and consists of 298 aa. Interestingly, while in most alphaherpesvirus the UL47 is inclosed in a gene cluster within the U_L, in the genome of ILTV it is translocated to the U_S region [40, 41]. In western blot analyses of infected-cell supernatants, three bands of approximately 40, 60 and 70 kDa

with the 40 kDa being the most dominant form can be detected [28, 42]. ILTV gG was described as a virulence factor as infection of SPF chickens with a gG deletion mutant showed attenuation in terms of clinical signs, weight loss and mortality [40] . In contrast, an increased infiltration of immune cells to the site of infection could be noted [42]. Furthermore, SPF chickens infected with the gG deletion mutant were protected against subsequent challenge with ILTV wild type virus [43]. ILTV gG was proven to interact with CXCL and CCL chemokine subfamilies of human and mice. Additionally, it could be demonstrated that heterophil chemotaxis towards a supernatant of LPS-stimulated monocytes containing various chemoattractants was inhibited in presence of ILTV wild-type or ILTV gG rescuant virus whereas the gG-deletion mutant could not interfere with chemotaxis [42].

e. PRV gG

PRV gG, previously termed gX, is also encoded by US4 and expressed early in the infectious cycle, first as a cell associated precursor that is secreted into the medium of infected cells after processing and glycosylation as a protein of approximately 95 kDa [30, 44]. PRV gG is a type I integral membrane protein composed of a hydrophobic signal sequence of around 20 aa at the N-terminal site followed by a 438 aa extracellular part, a 25 aa membrane spanning domain and a 16 aa comprising cytoplasmic domain [30] resulting in a total size of 498 amino acids. A stretch of only 81 aa of the whole protein show similarity to HSV-2 gG [29]. PRV gG was demonstrated to bind to various chemokines of human origin (CL1, CC and CXC), interacting preferentially but not exclusively with the receptor-binding domain of the chemokines and thereby inhibiting chemokine-induced chemotaxis of monocytes *in vitro.* A possible interaction of PRV gG with chemokines of suid origin *in vitro* as well as the gG-chemokine interaction in the natural host has not been investigated so far [45].

f. EHV-1 gG and EHV-4 gG

The predicted aa sequence for EHV-1 is 411 [8] and that for EHV-4 is 405 aa [31]. EHV-1 and EHV-4 gG are encoded by gene 70 located in the U_s segment of the genome. Based on *Bam*HI restriction mapping of the entire genome of EHV-1 and EHV-4, the EHV-1 gG encoding open reading frame is located in the fragment designated D [6, 8, 46, 47].

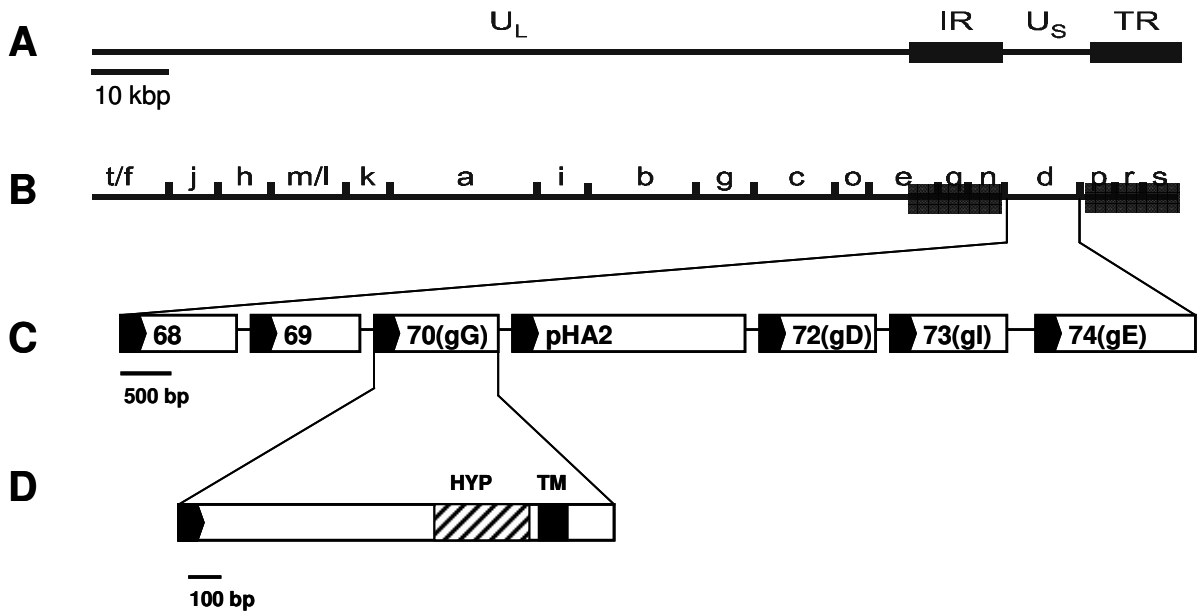

Figure 3: Schematic representation of the location of the gG gene in the EHV-1 genome. (A) Overall genome organization of the BAC pOH-03 (B) *Bam*HI restriction map of the EHV-1 sequence (C) Organization of the Unique short segment showing ORF 70 encoding gG and the adjacent genes ORF 69 coding for a Protein kinase and the gene 71 replacing mini-F plasmid sequences pHA2 (D) Schematic representation of gG with the transmembrane domain (closed box, TM) and the hypervariable region (cross-hatched box, HYP) indicated (modified from [10, 48])

Glycoprotein G of EHV-1 is under control of early promoters [49] and so some functions early in the infectious cycle were suggested. Hydrophilicity and -phobicity analysis of EHV-1 and EHV-4 gG classified them to the group of type I membrane proteins. A stretch of hydrophobic amino acid residues at the N-terminus represent an ER signal sequence that is followed by a proteolytic cleavage site. The membrane spanning domain consists of another hydrophobic region whereas the intracellular anchor domain is characterized by basic amino acids. The external domain harbors three asparagine-linked glycosylation sites conserved in EHV-1 and EHV-4 gG as well as in the gG of asinine herpesvirus 3 (AHV-3) assuming these three molecules to fold in a similar fashion [8, 31, 50].

When comparing the amino acid sequences of EHV-1 and EHV-4 gG, an overall identity of 58 % is noted with the C-terminal region being more divergent than the N-terminal region. Amino acids 1 to 286 (EHV-4 gG) and aa 1 to 287 (EHV-1 gG) are 75 % identical, but the hypervariable regions comprising aa 287 to 382 (EHV-4 gG) and aa 288 to 350 (EHV-1 gG) share only 21 % sequence identity. The hypervariable region near the C-termini of the molecules is encompassing the antigenic sites which were shown to elicit type-specific antibody responses in horses [10]. Expression of the hypervariable region of gG as fusion

proteins in *E.coli* allowed detection of type-specific equine antibodies by western blotting and ELISA and opened new possibilities for broadly based seroepidemiological surveys of EHV-1 and EHV-4 infections [10, 51].

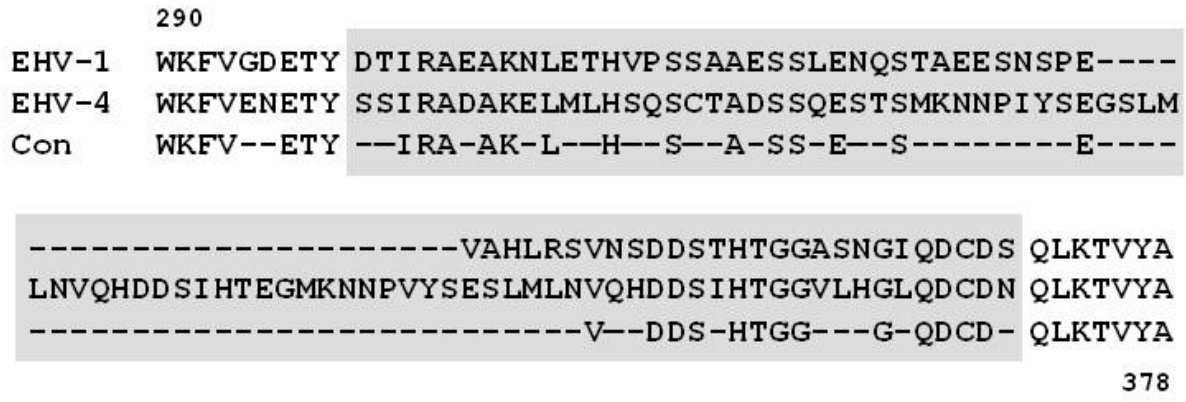

Figure 4: Amino acid comparison of the section of EHV-1 and EHV-4 gG comprising the hypervariable region (framed)

EHV-1 and EHV-4 gG exist in three isoforms, the full-length 68 kDa membrane-bound form, the 60 kDa secreted and the 12 kDa virion-associated form resulting from posttranslational cleavage of the polypeptide. Native SDS-PAGE, where samples were prepared without denaturing reagents, revealed the oligomeric structure of virion-associated gG isoforms as 140 kDa and 20 kDa whereas that of the secreted form was 120 kDa. All three gG-related species are thought to be disulphide-linked homodimers [52].

It was shown that gG of various EHV-1 strains, in contrast to EHV-4 gG, can bind to chemokines not only of equine but also of human and mouse origin. Recombinantly expressed gG can act as a viral chemokine binding protein and blocks interaction of chemokines with both specific receptors and glycosaminoglycans (GAGs) [37]. Glycoprotein G of EHV-1 is dispensable for viral cell-to-cell spread and infectivity [53], a reduction of plaque size of an EHV-4 gG deletion mutant compared to parental virus, however, is probably due to some sequence deletion in the adjacent gene 71 encoding gp2 [54]. EHV-1 gG displayed the ability to inhibit neutrophil chemotaxis in *in vivo* experiments [48]. By designing hybrid molecules, in which the hypervariable region of EHV-1 gG was substituted by EHV-4 hypervariable region and vice versa, it could be demonstrated that the epitopes comprising amino acids 301 to 340 of EHV-1 gG are responsible for binding to chemokines [55].

1.2.4. Pathogenesis of EHV-1 and EHV-4 infection

EHV-1 and EHV-4 are endemic in horse populations worldwide. Virus transmission takes place via shedding from the nasal cavity of infected horses to neighbouring horses via virus containing droplets in aerosols or through direct contact. Alternative routes are infection with virus coming from aborted foetuses and placenta [11]. Primary infection and viral replication takes place in the upper respiratory tract, where nasopharyngeal epithelial cells are the site of virus entry. Direct destruction of the affected cells and tissues in the respiratory tract due to lytic viral replication results in inflammation and the first clinical signs of EHV-1- and EHV-4-induced rhinopneumonitis, which are acute fever, coughing, anorexia as well as nasal and ocular discharge. The listed symptoms occur in various degrees of severity and in various combinations. Virus transport to the regional lymphoid tissue and infection of leukocytes can result in a leukocyte-associated viremia, a condition seen almost exclusively in the case of EHV-1 infections. Thus, EHV-1 can further spread to other organ systems and infect endothelial cells lining end vessels, where viral replication results in vasculitis and multifocal thrombosis. Especially in the last trimester of pregnancy, EHV-1 infection can lead to abortion or neonatal foal death [11, 56]. Vasculitis of end vessels supplying the central nervous system (CNS) and the spinal cord following infection with some EHV-1 strains can lead to a reactive myeloencephalopathy characterized by partial paralysis or complete paraplegia. Affected animals can also show behavioural changes such as head pressing, impaired proprioception, ataxia and circling as well as loss of bladder function [11, 57, 58].

EHV-1 and EHV-4 can establish latency in neurons, especially in cells of the trigeminal ganglion (cranial nerve V), but more frequently in lymphoid cells, primarily monocytes and CD8+ and CD4+-T-lymphocytes. Virus replication can be reactivated by stress-inducing treatments like corticosteroid application, weaning, castration, transportation and training [11, 59, 60].

1.2.5. Diagnosis of EHV-1 and EHV-4 infection

For diagnosis of EHV-1 or EHV-4 infection, virus cultivation from nasal swabs during the febrile stage of infection is applied and still the method of choice if further molecular characterization of the virus is considered necessary. In culture, EHV-1 grows in various cell culture systems whereas EHV-4 has a relatively restricted host range and only replicates in equine cells. The *in vitro* properties can give a first hint to differentiate both viruses. Also, EHV-1 and EHV-4 can be detected and discriminated by their DNA restriction enzyme patterns which, however, requires DNA isolation and is not feasible for routine diagnostics

[11, 61]. A fast and very efficient method to detect EHV-1 or EHV-4 infection is by polymerase chain reaction (PCR), especially the lately established real time PCR (qPCR), determining the viral load in order to differentiate between lytic and latent phase and in addition distinguishing between EHV-1 and EHV-4 infection [62, 63].

All serological methods, which require paired serum samples from the acute and convalescent stage, and include serum neutralization assays, complement fixation or ELISA are not ideal because they are confounded by high antigenic similarity and cross-reactivity of EHV-1 and EHV-4 [11, 64]. Hence, serological discrimination between the two viruses is hard to accomplish.

Since the 1980´s there were several attempts to distinguish between EHV-1 and EHV-4 infection by direct means, first with the help of monoclonal antibodies in enzyme immunofiltration and indirect immunofluorescence assays, later, a type-specific ELISA was developed based on fusion proteins representing the highly variable region of glycoprotein G of either virus [51, 65].

1.2.6. Current vaccines for EHV-1 and EHV-4

Currently, there are only two inactivated combination vaccines available in Germany, only one containing inactivated EHV-1 and EHV-4 antigen. Just one of these two is licensed for protection against EHV-1-induced abortion when administered in the 5th, 7th and 9th month of pregnancy (Duvaxyn®EHV-1, -4 Fort Dodge). The other inactivated combination vaccine, which in addition to EHV-1 and EHV-4 antigen contains antigen of three different equine influenza virus isolates, only claims protection for rhinopneumonitis or a decrease in clinical symptoms in case of respiratory infection (Resequin®NNplus Intervet). There is one modified live vaccine available containing exclusively the attenuated EHV-1 strain RacH but this vaccine as well only is stating reduction of clinical symptoms after infection of the respiratory tract (Prevaccinol®Intervet). [Paul-Ehrlich-Institut:http://www.pei.de/cln_170/nn_151790/DE/arzneimittel/vet-mittel/pferde/] [66-68]

Immunity to EHV-1 seems to be mainly based on cytotoxic T-cell (CTL) responses and neutralizing or complement-fixing antibodies seem to play a minor role. This finding is probably a reflection of the virus´ ability for systemic spread via cell-to-cell contact, more specifically from virus-infected lymphocytes directly to endothelial cells, which renders the virus inaccessible to antibody neutralization [69, 70]. It was seen that, in the presence of high levels of circulating antibodies after many vaccinations, pregnant mares still developed viremia and aborted after experimental challenge [71].

To date, there is no vaccine licensed for protection against the EHV-1-induced neurological form of infection [66] and there is no established marker vaccine for EHV-1 where a number of glycoprotein deleted marker vaccines are in use to facilitate diagnosis in the case of PRV and BHV-1 [72].

1.3. Bacterial artificial chromosomes (BACs)

1.3.1. BACs in general

The recently developed BAC technology has brought remarkable advances in virus research as it enables stable maintenance of large DNA molecules in *E.coli* and allows efficient mutagenesis of viral genomes using bacterial recombination systems [73]. The technology is based on the f-factor of *E. coli,* whose replication is tightly controlled. A plasmid carrying the f-factor is stably maintained in the bacteria as one or two copies per cell and was shown to maintain bacterial DNA fragments as large as one mega base pairs. A BAC vector containing the f-factor and a resistance gene can be used as a cloning vehicle and inserted into the viral genome by homologous recombination in eukaryotic cells [73, 74]. *E. coli* can then be transformed with the large plasmids by electroporation and the existence of the foreign DNA as a supercoiled circular plasmid permits easy isolation and manipulation of the large DNA in solution with minimal strand breaks [75]. Finally, virus incorporating the introduced mutations can be easily reconstituted by transfecting viral BAC plasmid into susceptible cells by electroporation or chemical methods [74, 76].

1.3.2. BACs in Virology

Murine cytomegalovirus with its 230-kbp genome is used as a model to study pathogenesis of human cytomegalovirus infection and was the first animal herpesvirus to be cloned by insertion of the BAC cassette into the viral genome through homologous recombination. Mutation of the immediate-early gene 1 and successful reconstitution of infectious virus proved this method as a very useful tool that is especially applicable for viruses which are difficult to grow in cell culture systems [74]. Since the original description, numerous BACs of human and animal viruses have been cloned and reams of (deletion) mutant viruses have been constructed [76, 77]. Ten EHV-1 strains were cloned as BACs to date, in most of them the mini-F plasmid sequences were inserted in place of gene 71 [66]. Several of these BACs harbor the additional insertion of a gene conferring chloramphenicol resistance which

facilitates selection in bacteria culture as well as the introduction of green fluorescent protein (*egfp*) allows selection for green plaques after transfection of BAC DNA into susceptible cells [78]. Deletion of gp2 resulted in impaired growth of EHV-1 in cell culture after transfection compared to infection with wild-type virus. Co-transfection of the mutated BAC DNA and a plasmid maintaining the gp2 sequence could reconstitute fully infectious virus [53, 78]. Recently, EHV-4 strain Th20p has been cloned as a BAC as well and the first mutant viruses were reported [79, 80].

1.4. Chemokines

Chemokines (CK), small proteins of 8 – 15 kDa in size with chemoattractant properties, are released by different cell types in response to infection or physical damage. Various CKs have been explored to date. Based on their primary aa sequence they can be divided in four families regarding conserved N-terminal cysteine motifs: CC CKs are characterized by two adjacent cysteine residues and mainly promote migration of monocytes and lymphocytes, CXC CKs, where the two cysteines are separated by a single aa, mostly promote migration of neutrophils from the bloodstream to surrounding tissues. In addition, a family named XCL1, where a single cysteine residue is located at the N-terminus, as well as the CX3C family, where the cysteine residues are separated by three spacer aa were characterized recently [81, 82]. CKs are part of the innate immune system where they play important roles in recruitment of cells but they are also considered to bridge innate and adaptive immunity by guiding lymphocytes to the site of damage or immune reactions. Furthermore, they are involved in lymphocyte development and angiogenesis [82]. In the case of neutrophil chemotaxis, CKs are involved in two ways: First, they convert “rolling” of neutrophils along the vascular wall into stable binding to surface molecules present on endothelial cells, second, the extravasation of neutrophils to the site of inflammation is induced by a gradient of CKs [82].

1.5. Viral chemokine binding proteins of other viruses

Viruses have evolved numerous strategies for immune evasion and interfering with the cytokine and chemokine pathways is one amongst them. There are three different ways of interference with the cytokine and chemokine pathways: 1) expression of viral chemokine

receptor homologues mimicking the cellular receptor, 2) expression of viral chemokines with functional or structural homology to cellular proteins and 3) the expression of viral chemokine binding proteins (vCKBP) showing no sequence similarity to known chemokines or chemokine receptors [83, 84]. The soluble viral chemokine binding proteins found to date are divided into four families [85]:

The M-T7 protein of myxoma virus is classified as a vCKBP type 1 and alters chemotaxis of leukocytes in infected tissues. An *in vivo* experiment with a virus unable to express M-T7 led to increased migration of leukocytes to the sites of infection [86]. It was shown that M-T7 binds to C, CC and CXC CKs, a process, which could be blocked by heparin treatment [87]. Furthermore, binding was demonstrated to function through CK-proteoglycan-binding domains, thereby sterically hindering the interaction of CK with cell surfaces and extracellular matrices [81].

Type 2 vCKBP are encoded by several members of the poxvirus family, amongst them is the M-T1 protein of myxoma virus as well as the 35 kDa protein of vaccinia virus [84, 88, 89]. These proteins bind with high affinity to CC CKs and only with low affinity to CXC CKs in a non-species specific fashion [84]. The CC CK-mediated recruitment of inflammatory cells into infected tissues in the initial phase of poxvirus infection is inhibited. Furthermore, direct inhibition of CK-receptor binding could be shown [81, 84].

The 44 KDa secreted M3 protein of murine gamma-herpesvirus 68 is the only known member of the vCKBP type 3 family to date [90]. Binding of M3 to CC, CXC, C and CX3 CKs results in competitive inhibition binding of CKs to their respective receptors and therefore prevents signaling through cognate receptors [91]. It was suggested that, by inducing conformational changes at the C-terminal of CKs, M3 prevents their binding to GAG [92].

Recently, several alphaherpesviruses have been shown to express a chemokine-binding protein, which exists in a membrane-bound form and is also secreted into the medium of infected cells. By binding to various chemokines in a species-independent fashion, an ability to interfere with the host´s immune system was suggested [25, 37, 93]. These proteins, classified as vCKBP type 4, were demonstrated to block CK-receptor and CK-GAG interactions to the same extent [37, 85]. EHV-1 gG, a protein classified as a vCKBP-4 [85], is further examined in this study and compared to its counterpart in EHV-4.

1.6. Murine respiratory model

The first small laboratory animal model for experiments with equine abortion virus was the Syrian hamster, which, despite providing a basis for further research, was not the optimal model for studying virus properties, as the pathogenesis in the model organism differs remarkably from that in the natural host [94]. The first infection of mice was performed in newborns, which were inoculated intracerebrally and turned out to be susceptible to EHV-1 infection. However, as the cerebral route is not the natural path of infection, the clinical outcome was not comparable to that after natural infection of horses by the respiratory route [95]. An infection experiment of BALB/c mice inoculated by the intranasal route with EHV-1 strain AB4 proved the mouse model a suitable form to study EHV-1 pathogenesis. 48 h post-infection (p.i.), infected mice showed clinical signs like ruffled fur, weight loss lasting for 4 to 5 days, irregularities in breathing and even some mild neurological symptoms like dragging of hind limbs. Death occurred from days 4 to 7 p.i. but might have been due to the high infectious dose of 10^7 pfu per mouse used in this initial description [96]. Virus could be isolated from nasal tissues, trachea, and lungs as well as occasionally from CNS, eye and liver. In addition, histological examination showed evidence of viral replication in the lung as well as the infiltration of inflammatory cells into the lung and loss of normal alveolar structure. A cell-associated viremia could be demonstrated by infectious centre assays [96]. Mice developed a specific antibody response to EHV-1 detectable on day 12 p.i., which peaked at day 25 post infection. Subcutaneous injection of hyperimmune rabbit polyclonal-anti EHV-1 neutralizing antibody decreased the severity of challenge infection [96]. Immigration of neutrophils into the alveaolar septs of infected mice were noted by days 1-2 p.i., which was replaced by cells of the mononuclear compartment from day 4 p.i. [97]. However, an important and noteworthy difference to horses is the fact that transmission or spread of EHV-1 from mouse to mouse was not documented so far [98]. Thus, it is possible to perform infection experiments of mice with different EHV-1 strains or recombinant viruses in shared air space. Certainly, the murine respiratory model cannot replace experiments in the natural host, the horse, but as a first line of *in vivo* experiments it is still a valuable method to investigate pathogenesis of EHV-1 infection [99]. In a previously performed infection experiment, BALB/c mice were proven susceptible to infection with neurovirulent EHV-1 strain OH-03 [66, 100] and showed weight losses up to 15 % [K. Tsujimura, L. B. Goodman, K. Osterrieder, personal communication] and for that reason this mouse strain was chosen to perform the studies reported here.

1.7. Hypothesis

Previous work by Van de Walle and co-workers showed that amino acids 301 to 340 comprising the hypervariable region of EHV-1 gG is able to bind to chemokines *in vitro* [55].

The aim of this study was to further test the hypothesis, that the hypervariable region of EHV-1 is indeed the determining factor for binding of EHV-1 gG to chemokines and therefore capable of inhibiting neutrophil chemotaxis *in vivo*. For that purpose, different EHV-1 gG mutant viruses were constructed by Red-mediated en passant mutagenesis and tested *in vivo* and *in vitro*. Based on the neurovirulent strain OH-03, various EHV-1 mutants were created in which the entire gG ORF, or the region coding for the hypervariable region only, was exchanged with the EHV-4 counterparts. Recombinant viruses were characterized *in vitro* regarding their growth properties and their immunomodulatory potential was analyzed in *in vitro* and *in vivo* infection experiments. Based on previously performed experiments with an EHV-1 RacL11 gG deletion mutant [48, 53] and recombinant expressed chimeric gGs [55] we hypothesized that the gG deletion mutant as well as EHV-1 expressing EHV-4 gG or the hypervariable region of EHV-4 gG would act as loss–of-function proteins and, hence, influence on neutrophil migration would be mitigated or absent. In contrast, parental EHV-1 gG as well as the mutant, in which the hypervariable region of EHV-1 gG was re-inserted into the EHV-4gG backbone, were expected to act as gain-of-function mutants. Therefore, binding to chemokines and further inhibition of neutrophil chemotaxis was expected.

2. Materials and Methods

2.1. Materials

2.1.1. Buffers and solutions

Buffers and solutions	**Composition**
10X Laemmli stock solution (SDS-PAGE)	1.25M Tris-HCL pH 6.8 10% SDS 0.2% bromophenol blue
20X SSC	3M NaCl 0.3 M Na Citrate, pH 7
2X HEPES buffered saline	140mM NaCl 1.5mM $Na_2EDTAx2H_2O$ 50mM HEPES, pH 7.05
4X Laemmli loading buffer (cell lystates and supernatants):	400µl 10X Laemmli 400µl 100% Glycerol 200 µl DTT or mercaptoethanol (concentrations!)
Denaturing solution (Southern blot)	1.5 M NaCl 0.5 M NaOH
Depurination buffer (Southern blot)	O.25 mM HCl
FACS buffer	PBS 0.2 % BSA
Freeze-thaw-buffer (SDS-Page sample preparation)	25ml of 1mM MgCl2, 1 tablet protease inhibitor

LB	1% Bacto-Tryptone 0.5% Bacto-Yeast extract 0.5% NaCl
Lysis buffer (viral DNA preparation)	80µl Tris 1M 80µl EDTA 500mM 250µl SDS 10% 6µl RNase
Neutralization buffer (Southern blot)	1M Tris, pH 7.4 1.5 M NaCl
P1 (plasmid DNA preparation)	50mM Tris 10mM EDTA, pH 8.0
P2 (plasmid DNA preparation)	0.2N NaOH 1% SDS
P3 (plasmid DNA preparation)	3M K Acetate, pH 5.5
PBS	2mM KH_2PO_4 10mM Na_2HPO_4 137mM NaCl 2.7 mM KCl, pH 7.3
PBS/T	PBS 0.1% Tween-20

RIPA buffer I (SDS-Page sample preparation)	20 mM Tris-HCl, pH 7.5 150 mM NaCl 1% Nonidet P-40 (NP 40) 0.5% Na-desoxycholate 0.1 % SDS
RIPA buffer II (SDS-Page sample preparation)	20 mM Tris-HCl, pH 7.5 150 mM NaCl 1% Nonidet P-40 (NP 40) 0.5% Na-desoxycholate 0.1 % SDS 1mM EDTA
SDS-PAGE running buffer (cell lysates and supernatants)	19.2M glycine 5M Tris (pH 8.9) 10% SDS
TAE	50mM Tris-base 2.5mM $Na_2EDTAx2H_2O$ 25mM Acetic acid 99%, pH 8
TE	10mM Tris-base 1mM $Na_2EDTAx2H_2O$
TE	10mM Tris-base 1mM $Na_2EDTAx2H_2O$, pH 7.5
Transfer buffer 10X (Cell lysates), used 1X (900ml H_2O, 100ml 10Xbuffer)	30.4 g Tris 144.3 g glycine ad 1 l H2O

Transfer buffers supernatants:	90% (v/v) 0.3 M Tris, pH 10.4
Anode buffer I	10 % methanol 90% (v/v) 25 mM tris, pH 10.4
Anode buffer II (Western blot transfer)	10 % methanol (v/v) 25 mM tris, pH 9.4
Cathode buffer (Western blot transfer)	40 mM 6-amino-n-caproic acid 10 % methanol (v/v)

2.1.2. Antibiotics

Antibiotics	**Stock solution**	**Final concentration**	**Manufacturer**
Ampicillin	100 mg/ml in ddH2O	100 µg/ml	ROTH
Chloramphenicol	30 mg/ml in ddH2O	30 µg/ml	ROTH
Kanamycin	50 mg/ml in ddH2O	50 µg/ml	ROTH
Penicillin	0.1 mg/ml	100 U/ml	Fisher-Scientific
Streptomycin	0.1 mg/ml	100 U/ml	Sigma-Aldrich

2.1.3. Media and supplements

Media and supplements	**Manufacturer**
Fetal bovine serum (FBS)	Biochrom AG
Minimal Essential Medium (MEM)	Biochrom AG
Non-essential amino acids (NEAA)	Biochrom AG
Na-pyruvate	GIBCO / Invitrogen

2.1.4. Chemicals and biochemicals

Chemicals/biochemicals	**Manufacturer**
Agarose	Roth
Arabinose	Sigma
Chloroform	AppliChem
$CaCl_2$	Roth
$C_2H_3KO_2$	Merck
Crystal violet	Merck
DMSO	Merck
Easycoll Separation solution	Biochrom
EDTA	Merck
Acetic acid	AppliChem
Ethidium bromide	Roth
Ethanol	Merck
Glucose	Merck
Glycerin	Merck
HBSS	Biochrom
HCl	ROTH
Isopropanol	Merck
KCl	Merck
$Na_2EDTA \times 2H_2O$	Serva
NaOH	Merck
NaCl	Merck
Methanol	Appli-Chem
Methylcellulose	Sigma-Aldrich

$MgCl_2$	Merck
$MgSO_4$	Merck
Phenol/Chloroform	AppliChem
SDS	Serva
Tris-base	AppliChem
6-Amino-Caproic-Acid	Sigma-Aldrich

2.1.5. Enzymes

Enzymes	**Manufacturer**
Antarctic Phosphatase	NEB
Quick-Ligase	NEB
Restriction enzymes	NEB
Restriction enzymes	NEB
RNase A	AppliChem
T4-Ligase	NEB
Taq-Polymerase	Genescript Peqlab
Trypsin	GIBCO

2.1.6. Equipment

Product	**Model/type**	**Manufacturer**
Bunsen burner	Typ1020	Usbeck
Cell counter	Neubauer improved	Assistent

Cell incubator	Excella ECO-1	New Brunswick Scientific
Centrifuges	Centrifuge 5424 Centrifuge 5804R Galaxy Mini	Eppendorf Eppendorf VWR
Chemiluminescent imager	Chemi-Smart 5100	Peqlab
Cryo storage system	Cryo1℃ Freezing container	NALGENE
Electroporator	GenePulser Xcell	Bio-Rad
Fluorescence microscope	Axiovert S 100	Zeiss
Freezer	-20℃ -80℃	Liebherr GFL
Fridge	4℃	EBD
Gel electrophoresis chamber	Mini Elektrophorese System SUB-Cell GT	VWR Bio-Rad
Ice machine	AF100	Scotsman
Laminar flow		Bleymehl
Microscope	Axiovert S100 AE 20	Zeiss Motic
Microwave		Bosch
Nanodrop spectrophoto-meter	Nanodrop 1000	Peqlab
Nitrogen tank	ARPEGE70	Air liquide

PCR cycler	T-Gradient GeneAmp PCR System 2400	Biometra Perkin-Elmer
pH-meter	HI 223 Calibrations Check	Hanna Instruments
Pipettor	Accu-jet pro	BRAND
Power supply (gels)	Power Source 250V	VWR
Roller mixer (Southern blot) and UV-cross linker	HL-2000 HybriLinker	UVP
Scales	ALC-2100.2 ALC-1100.2	ALC ALC
SDS-Page chamber	Mini-PROTEAN TetraCell	Bio-Rad
Software	Vision-Capt ND-1000 V.3.0.7. Cell Quest Pro Vector NTI	PeqLab PeqLab BD Biosciences Invitrogen
Thermomixer	Thermomixer 5326 Thermomixer comfort Thermomixer compact	Eppendorf Eppendorf Eppendorf
Ultracentrifuge	L8-70M	BECKMAN
UV detection system / Gel documentation	Transiluminator Bio-Vision-3026 Printer P93D	PeqLab Mitsubishi
Vacuum aspirator	Vacumat130	H.Saur

Venous blood collection: Holder Multiple sample needle Blood collection tube	BD Vacutainer® One Use Holder BD Vacutainer PrecisionGlide 20G x 1.5” (0.9 x 38 mm) BD Vacutainer® Blood Collection Tubes, 143 USP Units of Sodium Heparin	BD Biosciences
Vortexer	VTY-3000L	Hartenstein
Water bath	TW8 Water Bath Shaker C76	Jubalo New Brunswick Scientific

2.1.7. Consumables

Consumables	**Manufacturer**
Cell culture flasks	TPP
Cell culture plates (6-, 12-, 24-, 96-well) 10 cm cell cuture dishes	TPP
Centrifuge tubes	Hartenstein
Cryo tubes	Hartenstein
Expendable cuvettes	Biodeal
Filter paper	Whatman
Gloves, gloves nitril	Flexam, Roth
Membranes : Nylon (Hybond-N) for Southern blot PVDF for Western blot	 Amersham Biosciences ROTH

Petri dishes	Hartenstein
Pipette tips	VWR
Pipettes	TPP
Polypropylene tubes	TPP / Hartenstein
PVDF membrane	ROTH
Reaction tubes	Hartenstein
Scalpels	Schreiber Instrumente

2.1.8. Kits

Product	**Manufacturer**
DIG Wash and Block Buffer Set	Roche
ECL Plus Detection Kit	Amersham / GE Healthcare
Hi Yield Gel/PCR DNA Fragments Extraction Kit	SLG
PCR DIG Probe Synthesis Kit	Roche
Qiagen Plasmid Midi Kit	Qiagen
QIAquick Gel Extraction Kit	Qiagen
TOPO TA Cloning Kit	Invitrogen

2.1.9. DNA and Protein marker

Marker	**Range**	**Manufacturer**
Broad range protein marker (Coomassie Blue)	2 – 212 kDa	NEB

ChemiBlot Molecular Weight Markers	15 – 82 kDa	Millipore
Gene ruler 1kb plus DNA ladder	75bp – 20 kbp	Fermentas
Page ruler Plus Prestained protein ladder	10 – 250 kDa	Fermentas

2.1.10. Staining

Staining	**Purpose**	**Composition**
Amidoblack	Irreversible staining of proteins on membranes	0.1 % amido black 25 % isopropanol 10 % acetic acid
Coomassie Blue Destain	Destaining of SDS-gels	10 % acetic acid 40% methanol 10% acetic acid
Coomassie Blue Stain	Staining of gels after SDS-PAGE	0.5% (v/v) Coomassie Blue G-250 50 % methanol
Crystal violet	Stains nuclei in deep purple, used for staining adherent cells after virus titration	0.5% (v/v) crystal violet 25% methanol 75% ddH_2O
Modified Wright´s stain	Performing differential white blood cell counts, contains oxidized mehylene blue and azure B which stains nuclei from blue-purple and eosin Y staining cytoplasm	Wright stain, 0.3%, buffered at pH 6.8 in methanol. Contains stabilizers and surfactant

	orange- pink	
Ponceau S stock 10x, used 1x (900ml H2O, 100ml 10x Ponceau S stock)	Reversible staining of proteins after SDS-PAGE	2% Ponceau S powder 30% trichloracetic acid 30% sulfosalicyclic acid
Trypan Blue	Vital stain that stains dead cells blue, viable cells do not take up the dye	0.4% trypan blue in 0.81% NaCl; 0.06% K_2P0_4

Table 1: Primer for construction of transfer plasmids

Name	**Sequence 5´to 3**	**Purpose**
NT1	atgttggctgtgggagcaac	Amplification EHV-4 gG, for
NT2	ttatgcaacgtactcaagtcgat	Amplification EHV-4 gG, rev
NT3	aaaaaccggt**cccatgccccgctcaaaacctaaacaccaacccct actatttgaa***tagggataacagggtaatcgattt*	I-SceI-aphAI and duplication, AgeI, for
NT4	ttttaccggt*gccagtgttacaaccaattaacc*	I-SceI-aphAI and duplication, AgeI, rev
NT33	aaaatgtaca**gctgattcgtcgcaagaaagcacatctatgaagaata accctatttattc***tagggataacagggtaatcgattt*	I-SceI-aphAI and duplication, BsrGI, for
NT34	aaaatgtacagcca*gtgttacaaccaattaacc*	I-SceI-aphAI and duplication, BsrGI, rev

[a] Underlined are restriction sites, boldface type indicate duplicated sequences, nucleotides in italics annealing to pEP-kan-S2 plasmid

Table 2: Primer used for Red-mediated recombination

Name	**Sequence 5´to 3´**	**Purpose**
NTa	tacagtgccaccaactgtaaagcggtagtaagctgcagtg**cacctgtca aataaaagttt**tagggataacagggtaat*cgattt*	Deletion of EHV1gG, for
NTb	**acaacaatgtttttgatttgaaacttttatttgacaggtg**cactgcagctt actaccgct*gccagtgttacaaccaatta*acc	Deletion of EHV1gG, rev
NT5	gccactgcgctacagtgccaccaactgtaaagcggtagtaagctgcagt g*atgttggctgtgggagcaac*	Amplify transfer construct EHV4 gG,recom.cassette, EHV1 duplication, for
NT6	gttattacagacaacaatgtttttgatttgaaacttttatttgacaggtg*ttatgc aacgtactcaagtcgat*	Amplify transfer construct EHV4 gG,recom.cassette, EHV1 duplication, for
NT31	cagaggggccccaaaccttgttaataggtgcagttggactcagaatactc	Amplify transfer construct(pFastBac 1703 chimera,hypervariable reg. EHV1gG, recom. cassette, EHV4 gG duplication, for
NT32	aggcaaatatacacagttttgagctggttgtcgcagtcttggaggccatg	Amplify transfer construct(pFastBac 1703), rev
NT41	ggttggactcagaatcttggcgcaggcatggaagtttgtc*gaaaatgaaa cctacagcag*	Amplify transfer construct, EHV4gGhypervariable region, recom.cassette, EHV1 gG duplication, for
NT42	caagcaggcatacacagttttgagctgactgtcacagtcctggaggccat g*caacacacc*	Amplify transfer construct, EHV4gG hyp, recom. cassette, EHV1gG duplication, rev

[b] Underlined I-*Sce*I site restriction site, boldface type indicate duplicated sequences, nucleotides in italics annealing to transfer constructs

Table 3: Primer for sequence confirmation / DNA sequencing / Southern blot probe

Name	**Sequence 5´to 3**	**Purpose**
gp2_ seq3	ctttgctgatacccaacaga	Confirmation of gp2 reconstitution
gp2 rev	gaaaaacacgtaccagggcg	Confirmation of gp2 reconstitution
NT11	tgactaacctgtttctggga	Sequencing gG region
NT12	ttgccgcgatttagtatttt	Sequencing gG region
EHV-1 del gG blot,for	aaaatacaactccaaggcagacata	PCR probe for Southern blot deletion of gG
EHV-1-del-gG-blot,rev	tatgtttcgtcaccgacaaacttcc	PCR probe for Southern blot deletion of gG

2.1.11. Cells

The following cells were used for the experiments:

Rabbit kidney cells (RK13) were used for EHV-1 virus amplification, $CaCl_2$ transfections and plaque purification (ATCC, CCL 37).

Equine fibroblasts (NBL6) were utilized for EHV-4 virus amplification and plaque purification (ATCC, CCL 57).

Equine neutrophils were isolated from heparinized horse blood (kindly provided by Klinik für Pferde, Allgemeine Chirurgie und Radiologie of the Freie Universität Berlin) using a discontinuous Percoll gradient, washed twice with 1 X HBSS and used immediately in chemotaxis assays [48, 101, 102].

2.1.12. Viruses and Bacterial Artificial Chromosomes (BACs)

EHV-4 isolate (KT-4, kindly provided by Dr. Kerstin Borchers) [103] was used for DNA extraction and amplification of the full-length glycoprotein G (gG) gene or its hypervariable region. The virus strain was unequivocally identified as an EHV-4 isolate by PCR and DNA sequencing (data not shown).

The previously generated BAC of the neurovirulent EHV-1 strain OH-03 [66] was used as a backbone to construct the mutant viruses given in Table 4.

Table 4: Viruses and BACs used and generated in this study

Virus designation	**Genotype**
KT-4	Equine herpesvirus type 4 - parental virus
OH-03	Equine herpesvirus type 1 - parental virus
pOH03	Bacterial artificial chromosome of EHV-1 strain OH-03
pOH-03ΔgG	OH-03 with ORF70 (gG) deleted
vOH-03ΔgG	OH-03 with ORF70 (gG) deleted, ORF71 (gp2) restored
vOH-03ΔgG	OH-03 with a deletion of the start codon of gG, ORF71 (gp2) restored
pOH-03-4gG	OH-03 with EHV-4 gG inserted

vOH-03-4gG	OH-03 with EHV-4 gG inserted, ORF71 (gp2) restored
pOH-03-4gG-hyp1	OH-03 with hypervariable region of EHV-1 gG inserted in EHV-4 gG
vOH-03-4gG-hyp1	OH-03 with hypervariable region of EHV-1 gG inserted in EHV-4 gG, ORF71 (gp2) restored
pOH-03-hyp4	OH-03 with hypervariable region of EHV-4 gG inserted in EHV-1 gG
vOH-03-hyp4	OH-03 with hypervariable region of EHV-4 gG inserted in EHV-1 gG, ORF71 (gp2) restored

2.1.13. Plasmids

For the generation of recombinant BACs, different transfer plasmids were generated. The transfer plasmids used in this study are shown in Table 5:

Table 5: Plasmids used and generated in this study

	Plasmid designation	**Structure**
1	pUC19-EHV-4gG-Kana(AgeI)	I-SceI-aphAI cassette in EHV-4gG, AgeI restriction site used for construction
2	pFASTBAC11-EHV4sgG chimera kana_in	I-SceI-aphAI cassette in hypervariable region of EHV-4 chimera
3	pcr2.1-TOPO-EHV-4gG-Kana(BsrGI)	I-SceI-aphAI cassette in hypervariable region of EHV-4 gG, BsrGI used for construction

Plasmid number 1 and 3 were constructed in the course of this study, whereas Prof. Gerlinde van de Walle and Dr. Benedikt Kaufer kindly provided the pFASTBAC11-EHV4sgG chimera kana_in plasmid.

2.1.14. Antibodies

2.1.14.1. Western Blot

Glycoprotein G expression or absence of expression was confirmed by use of the following polyclonal antibodies (pAb):

pAb rabbit-anti EHV-1gG-hypervariable region (1: 500 in 1% BSA PBST 0.1%)

pAb rabbit-anti EHV-4gG-hypervariable region(1:500 in 1% BSA PBST 0.1%)

pAb rat-anti EHV-1 gG hypervariable region (1: 500 in 1% BSA PBST 0.1%)

pAb rat-anti EHV-4 gG hypervariable region (1:500 in 1% BSA PBST 0.1%)

All polyclonal antibodies directed against the hypervariable region of either EHV-1 or EHV-4 gG were kindly provided by Dr. Carol Hartley (The School of Veterinary Science, The University of Melbourne, Victoria, 3010, Australia)

Loading controls for the cell lysates:

mAb mouse-anti Na-K-ATPase (1:2,000 in 2.5% skim milk in PBST 0.1%) (Millipore)

mAb mouse-anti actin (1:2,000 in 2.5% skim milk in PBST 0.1%) (Cell Signaling Technology)

The following secondary antibodies were used in this study as follows:

pAb goat-anti rabbit-HRP (1:10,000 in 2.5 % skim milk in PBST 0.1 %) (Promega)

pAb donkey-anti rat-HRP (1:5,000 in 2.5% skim milk PBST 0.1%) (Rockland Immuno-chemicals Inc.)

2.1.14.2. Indirect immunofluorescence assays (IFA)

For IFA, the following monoclonal antibodies (mAb) were used:

mAb mouse-anti gp2 (3B12) hybridoma cell supernatant (1:5 in 1% FCS PBS)

mAb mouse-anti gM (A8) (1:1,000 in 1% FCS PBS) [104]

The following secondary antibodies were used for IFA:

pAb goat anti mouse IgG Alexa fluor 568 (1:1,000 in 1 % FCS-PBS) (Invitrogen)

2.1.14.3. Flow cytometry

For FACS analysis of the composition of cells in bronchoalveolar lavages (BALs) of challenge-infected mice, the following antibodies and isotype controls were used:

Rat-anti mouse Ly-6G - APC (GR1+) [IgG2b] (SouthernBiotech)

Rat-anti mouse F4/80 – FITC [IgG2b] (BIOZOL)

Rat-anti mouse CD45R/B220 – APC [IgG2a] (SouthernBiotech)

Rat-anti mouse CD3 – FITC [IgG2a] (BIOZOL)

Rat IgG2b K Isotype Control APC – eFluor 780 for the neutrophil staining (eBioscience)

Rat IgG2b K Isotype Control FITC for the macrophage staining (eBioscience)

Rat IgG2a K Isotype Control APC for the B- lymphocyte staining (eBioscience)

Rat IgG2a K Isotype Control FITC for the T-lymphocyte staining (eBioscience)

2.1.15. Chemokines

For chemotaxis assays, recombinant equine Interleukin 8 (IL-8) was obtained from AbD Serotec and used at a final concentration of 25 ng /ml diluted in MEM-2% FCS.

2.1.16. Animals

3-to 4-week-old female BALB/C mice were obtained from Charles River Laboratories International, Inc. and housed in the animal facility of the Institute of Microbiology of the Freie Universität Berlin on the campus of the Humboldt-Universität Berlin. Routine care and experimental utilization of the mice were done in accordance with the German animal welfare law. The experimental animal procedures performed as part of this study were approved by the LaGeSo (registration number G424/08).

2.2. Methods

2.2.1. Cell culture

a. Maintenance of cells

RK13 cells were grown and maintained in growth medium MEM supplemented with 5% fetal bovine serum (FBS), 100 U/ml penicillin and 0.1 mg/ml streptomycin. Equine fibroblasts (NBL-6) were grown and maintained in MEM supplemented with 20% FBS, 7.5 ml NEAA, 7.5 ml Na-pyruvate, 100 U/ml penicillin and 0.1 mg/ml streptomycin. Both cell lines were kept at 37°C under a 5% CO_2 atmosphere. When confluent, cells were detached with 0.25% trypsin-EDTA for 10 minutes and resuspended in the appropriate medium. Subsequently, cells were cultivated in a 1:2 (NBL-6) or 1:10 (RK13) ratio, respectively.

b. Cell Counting

To seed a determined amount of cells per well, cells were detached as described above and resuspended in 1ml PBS. The cell suspension (10 µl) was mixed with 10 µl trypan blue. Counting was performed in a Neubauer chamber by counting the cells in the four large squares. The number of cells per ml was determined according to following formula:

$$\text{Cells per ml} = \frac{\text{No. of cells in large squares counted}}{\text{No. of large squares counted}} \times 10^4 \times \text{dilution factor}$$

c. Cryoconservation

Trypsinized cells were resuspended in 1.5 ml MEM followed by adding 3 ml of cryoconservation medium (MEM supplemented with 25% FCS and 20% DMSO) and divided into the appropriate number of cryovials. Cells were frozen at -70°C in cryoconservation containers filled with isopropanol and subsequently stored at -196°C in liquid nitrogen**.**

Cryovials were thawed at 37°C in a water bath. In order to remove DMSO, 5 ml of suitable medium were added and cells were centrifuged for 10 minutes at 1,200 rpm at RT. The pellet was resuspended in growth medium and cells were transferred to cell culture flasks.

d. Transfection and contransfection

To transfect RK13 cells with recombinant BAC DNA, the calcium phosphate precipitation method was applied [78]. Briefly, 0.5 – 2 µg of BAC DNA was adjusted to 50 µl total volume with 10 mM Tris-HCL (pH 7.5), followed by adding 388 µl of ddH_2O and incubation for 1 hour at RT on a rotating shaker at 80 rpm. Subsequently, 62 µl of 2M $CaCl_2$ were added in drop-

wise fashion while gently mixing the tube, and solution was left for incubation at 4°C overnight. After incubation, 500 µl ice-cold 2XHBS were added drop-wise to the sample while gently mixing the tube. Fresh MEM without FCS (500 µl per well) was added, and 500 µl of the transfection mixture was applied in a drop-wise manner to RK13 cells that had been seeded in 6-well plates the day before such they were approximately 80% confluent at the time of transfection. Cells were then incubated with the transfection mixture at 37°C for 4 h, washed once with PBS and treated for 2 minutes with 1.5 ml 1XHBS 15% glycerol. Cells were washed again with PBS and finally fresh medium (MEM, 10% FBS, 1% penicillin/streptomycin) was added and cells were further incubated at 37°C. Medium was changed again after 24 hours and cells were evaluated for cytopathogenic effect (CPE) daily.

2.2.2. Virological methods

a. Preparation of viral stocks

EHV-1 wild-type strain OH-03 and mutant viruses were propagated on RK13 cells. Confluent cells were infected at a multiplicity of infection of 0.01 to 2. When CPE was visible in more than 80% of the cells, culture flasks were freeze-thawed three times to release intracellular virions and viral suspensions were centrifuged for 10 min at 180 x g at RT. Supernatant was frozen down in aliquots at -70°C.

b. Titration

To determine the titer of the various EHV-1 recombinants, 10-fold dilutions were plated on confluent RK13 cells in 24-well plates and incubated for 3 days at 37°C under a 0.8% methylcellulose overlay. At 72 h post infection (p.i.) cells were washed twice with PBS and fixed with 90% acetone for 20 minutes at -20°C. Dried plates were stained with crystal violet for 5 minutes and washed twice with ddH_2O. Plaque numbers were counted under a light microscope and virus titers were calculated according to following formula:

$$\text{Virus titer (pfu/ml)} = \frac{\text{number of plaques}}{\text{volume used (ml)}} \times \frac{1}{\text{dilution counted}}$$

To calculate the geometrical mean, the following formula was used:

$$\text{Virus titer (pfu/ml)} = \sqrt{\text{virus titer 1} \times \text{virus titer 2}}$$

c. Single-step growth kinetics

$1X10^5$ RK13 cells were infected at a multiplicity of infection (m.o.i.) of 3. Virus was allowed to attach for 1 hour at 4°C, followed by a penetration period of 1.5 hours at 37°C. Cells were washed twice with PBS, treated with CBS for 3 minutes to remove all virions remaining on the surface of the cells. Immediately following was another PBS washing step, supernatant and cells of the first time point (0 h p.i.) were harvested, supernatant was centrifuged at 18,407 x g for 1 min and stored at -70°C. Samples of the following time points (4, 8, 12, 24 and 36 hours p.i.) were processed in an identical manner.

Cell-associated and extracellular viral titers were determined by plating 10-fold dilutions onto RK13 cells in 24-well plates and incubation for 2 days at 37°C under a 0.8% methylcellulose overlay. Cells were eventually fixed with 90% acetone, stained with crystal violet and plaques were counted using a light microscope.

d. Immunofluorescence assay (IFA)

For IFA, cells were infected with 100 plaque-forming units (pfu) per well and fixed as described earlier 3 days p.i. Plates were dried at room temperature and unspecific binding was blocked with 1 % FBS in PBS for 1 h on an orbital shaker. The primary antibody was diluted in PBS-FBS and added to the cells for 1h while shaking on an orbital shaker at 80 rpm. Cells were washed three times with PBS and the secondary antibody was added to the cells for 1 h. Cells were washed thoroughly once more with PBS, and plaques were inspected by using an inverted fluorescence microscope (Zeiss Axiovert S 100). For plaque size determinations, at least 50 plaques per (recombinant) virus were photographed (Zeiss Axiovision) and mean plaque areas were determined by using the ImageJ software (http://imagej.nih.gov/ij/download.html).

2.2.3. Molecular methods

a. Preparation of DNA from virus infected cells

To isolate viral DNA, infected cells and supernatant were harvested at 48 h p.i., frozen and thawed three times to release all virions retained in the cells. The suspension was centrifuged at 1,200 rpm for 10 minutes to remove cellular debris. Supernatants were incubated with lysis buffer (80 µl 1M Tris, 80 µl 500 mM EDTA, 250 µl 10% SDS, 6 µl RNaseA) at 37°C for 10 – 12 h. In the next step, 2 ml buffered phenol-chloroform was added to the sample and the mixture was carefully inverted several times before incubation at 4°C for 10 min. The sample was then centrifuged at 4,500 x g for 10 min at 4°C and the liquid

phase was transferred to a new tube. Two milliliters of chloroform were added to the liquid phase and the sample was left at 4℃ for another 10 min before centrifugation at 4,500 x g for 10 min at 4℃. An equal volume of isopropanol was added to the liquid phase and centrifuged at 4,500 x g for 15 minutes at room temperature. The DNA pellet was washed twice with 70% ethanol, dried at 37℃, resuspended in 50 µl TE containing 20 µg /ml RNaseA, and incubated for 30 min at 37℃. Efficiency of DNA isolation was controlled by 1% agarose gel electrophoresis at 100 V for 30 min and DNA concentration was measured using the Nanodrop (Peqlab). DNA was stored at 4℃ or -20℃ until further use.

b. Preparation of plasmid DNA by modified alkaline lysis

Principle: The bacterial cell wall is opened by a strong anionic detergent at high pH, followed by denaturation of chromosomal DNA and proteins and release of plasmid DNA into the supernatant. The denatured material is removed by a centrifugation step and DNA is precipitated from the supernatant.

Method: Bacterial cultures (2-4 ml) were grown in appropriate antibiotics overnight at 32℃ or 37℃ respectively in a rotating shaker (New Brunswick) at 220 rpm. The next day, cultures were centrifuged at 9,500 x g and the remaining cell pellet was resuspended in 300 µl buffer P1 by vortexing vigorously. Then, 300 µl buffer P2 were added for cell lysis and incubated at RT for 5 min. Finally, 300 µl of buffer P3 was added to neutralize the solution and incubation on ice for another 5 min followed. Samples were centrifuged at 20,200 x g to remove cellular debris and supernatant was transferred to a new tube. The same volume of buffered phenol-chloroform was added and the solution mixed by inverting the tube followed by centrifugation at 15,000 x g for 10 min. The upper liquid phase was transferred to a new tube and the same volume of 100% isopropanol was added and mixed by inverting followed by centrifuging at 9,500 x g for 30 min. The DNA pellet was washed twice with 70% ice-cold ethanol and dried at RT. Finally, the pellet was resuspended in 50µl TE-RNAse A and incubated for 30 min at 37℃. DNA was stored at 4 or -20 ℃ until further use.

c. Medium scale preparation of DNA from plasmids for transfection

For BAC DNA preparation the plasmid midi kit (Qiagen) was used. Briefly, 100 ml of medium were inoculated with 100 µl of a starter culture and grown overnight at 32℃ or 37℃ at 220 rpm as described. Bacterial cells were harvested by centrifugation at 6,000 x g for 15 min at 4℃ and the resulting pellet was resuspended in 4 ml of buffer P1. Buffer P2 (4 ml) was added, mixed and the sample was left at RT for 5 min. After adding 4 ml of buffer P3, the sample was mixed thoroughly and incubated on ice for 15 min. The sample was centrifuged at 20,000 x g for 30 min at 4℃, followed by another supernatant centrifugation step at

20,000 x g for 15 min at 4℃. Meanwhile, a Qiagen-tip 100 was equilibrated by application of 4 ml Buffer QBT and the DNA-containing supernatant was allowed to enter the resin by gravity flow. Once all liquid had passed through the column, it was washed twice with 10 ml of buffer QC before eluting the DNA with 5 ml of buffer QF. DNA was precipitated by mixing the sample with 3.5 ml of 100% isopropanol and DNA was pelleted by centrifugation at 15,000 x g for 30 min at 4℃. The DNA pellet was washed with 2 ml of 70% ethanol and air dried before it was dissolved in an appropriate amount of TE buffer and kept at 4℃ until further use.

d. Polymerase Chain Reaction

For amplification of different DNA fragments, a standard PCR reaction was used and modified according to the required amplification reactions:

1 µl template DNA	1. 95 ℃	5 min
0.2 µl taq polymerase	2. 95 ℃	30 sec
1 µl dNTPs	3. X ℃	30 sec
1 µl primer A	4. 72 ℃	X sec → repeat step 2 - 4
1µl primer B		(30 times)
5 µl 10X buffer	5. 72 ℃	7 min
10.8 µl ddH2O	6. 4 ℃	∞
20 µl final volume		

e. Gel electrophoresis

To visualize PCR products or fragments of DNA for restriction fragment length polymorphisms (RFLP), samples were mixed with 6 X DNA loading buffer and loaded into slots of a freshly poured and solidified 1% agarose gel, in which ethidium bromide was present at a final concentration of 0.5 µg/ml. If not indicated otherwise, a voltage of 100 V was applied for 35 min followed by examining the gel under UV light and photographing.

f. Purification of DNA by column purification and recovery of DNA from agarose gels

To purify DNA amplified by PCR, the Hi Yield Gel/PCR DNA Fragments Extraction Kit (SLG) was used according to the manufacturers' instructions. To recover required DNA fragments after agarose gel electrophoresis, DNA containing bands were excised from the agarose gel and QIAquick Gel Extraction Kit was used according to the manufacturers' instructions (Qiagen).

g. Sequencing

To determine DNA nucleotide sequences, plasmids or PCR-amplified DNA fragments were column purified, eluted in ddH_2O and sent for DNA sequencing to StarSEQ Sequencing Company (StarSEQ) in the required amounts. This company is using an ABI 3730 automated capillary sequencer (Applied Biosystems) with an ABI Prism Big Dye Terminator Cycle Sequencing Ready Reaction kit version 3.1. Received sequence data was examined by Vector NTI software (Invitrogen).

h. Restriction Fragment Length Polymorphism (RFLP)

Plasmid or BAC DNA isolated from prokaryotic cells was cleaved with appropriate restriction enzymes in required buffers as recommended by the manufacturers at 37°C for 1 - 5 h and separated either on small 1% agarose gels for 30 to 40 minutes at 100 V or on 0.8% agarose gels for 20 hours at 60 V. Gels were stained in ethidium bromide for 30 min, destained in water, and the resulting DNA band pattern was documented under UV light (Transiluminator Bio-Vision-3026, Peqlab).

i. Cloning methods

1. TOPO TA cloning (Invitrogen)

Principle: Taq-polymerase amplified PCR products ligate efficiently with the linearized TOPO vector, as Taq polymerase adds a single deoxyadenosine to the 3´ end in a template-independent terminal transferase activity and the linearized vector has overhanging deoxythymidine residues. Topoisomerase I from vaccinia virus is covalently bound to the vector and its religating activity is used for this system.

A standard PCR set-up was used to amplify the desired fragment and the PCR product was checked by a standard agarose gel electrophoresis. The PCR product (2 µl) was mixed with 0.5 µl salt solution (1.2 M NaCl, 0.06 M $MgCl_2$) and 0.5 µl of TOPO vector, and the reaction was allowed to incubate for 5 min at RT. LB plates containing 50 µg/ml ampicillin were prepared with X-gal (5-brom-4-chlor-3-indoxyl-β-D-galactopyranosid, 40 mg/ml) for blue-white screening and chemically competent *E. coli* cells (TOP 10) were incubated with 2 µl of the cloning reaction on ice for 30 min before cells were transformed by heat-shock for 30 sec at 42°C. SOC medium was added and the transformation reaction was incubated for 1 h at 37°C before spreading on selective plates and incubation overnight. The following day, white colonies were picked for further analysis.

2. Restriction digest and sticky end ligation for cloning in pUC19 vector

T4 DNA ligase catalyzes formation of phosphodiester bonds between the 3'-OH of one nucleotide and the 5'-PPP of a second nucleotide and such ligates DNA fragments having complementary, so-called ´sticky ends`.

The ends were generated by incorporating the restriction enzyme recognition sites required for cloning into the vector into the forward and reverse PCR primers. Vector and PCR product were digested with the appropriate restriction enzymes according to the manufacturer's instructions to obtain sticky ends. In case only a single restriction site was used for the cloning procedure the vector was dephosphorylated with Antarctic phosphatase (1 µg of DNA in 50 µl reaction volume with 1X Antarctic Phosphatase Reaction Buffer) by incubating for 30 min at 37°C followed by heat inactivation at 65°C for 5 minutes. Phosphatase treatment was applied to avoid self-ligation of the vector. The amount of vector and insert DNA was measured spectrophotometrically using the Nanodrop spectrophotometer (Peqlab) and the ligation reaction was set up according to following formula:

$$\frac{\text{ng of vector}}{\text{kb size of vector}} \times \text{molar ratio of } \frac{\text{insert}}{\text{vector}} = \text{ng of insert}$$

The ligation reaction was mixed and incubated for 3 h at RT before chemically or electrocompetent *E. coli* cells were transformed with 1 to 10 µl of the ligation reaction.

j. Two-step *en passant* Red-mediated recombination

The recent development of BAC technology and two-step Red-mediated recombination allows efficient engineering and modification of sequences in large DNA constructs in *E.coli* [75, 105]. In this study, the *E.coli* strain GS1783, a kind gift of Dr. Gregory Smith, Northwestern University, Chicago, IL, U.S.A., was used [106]. This bacterial strain contains the heat inducible λ prophage recombination enzymes Exo, Beta and Gam [107]. The bacterial strain additionally contains the *i-sceI* gene controlled by an arabinose-inducible promoter. *En passant* mutagenesis is applicable to perform deletions, point mutations or exchanges of large sequences in the BAC background. For the latter, a transfer plasmid has to be constructed previous to the recombination procedure.

j.1. General principle for insertion of sequences

1st Red recombination

In a first step, the gene of interest and the positive selection marker are inserted into BAC DNA. For that purpose, PCR amplified I-*Sce*I-*aphA*I cassette from plasmid pEP-kanS was inserted into a unique restriction site of a plasmid containing the gene of interest. The PCR was done using a forward primer with a 50 bp duplication of the gene of interest and unique restriction sites added to each of the primers to clone the PCR product into the gene of interest. This transfer plasmid was used as a template to perform a PCR with primers that had approximately 50 bp of homology to the respective target sequence and around 20 bp that were complementary to the desired primer annealing site of the constructed plasmid. The resulting linear DNA fragment was gel-purified, the template cleaved with *Dpn*I, and eventually *E.coli* strain GS1783 harboring the pOH-03 sequence was transformed by electroporation. The DNA fragment was inserted into the BAC sequence by classical Red recombination (depicted in Figure 5), and the resulting intermediates were selected on LB agar plates containing kanamycin and chloramphenicol. Kanamycin-resistant intermediates were verified by RFLP and colony PCR.

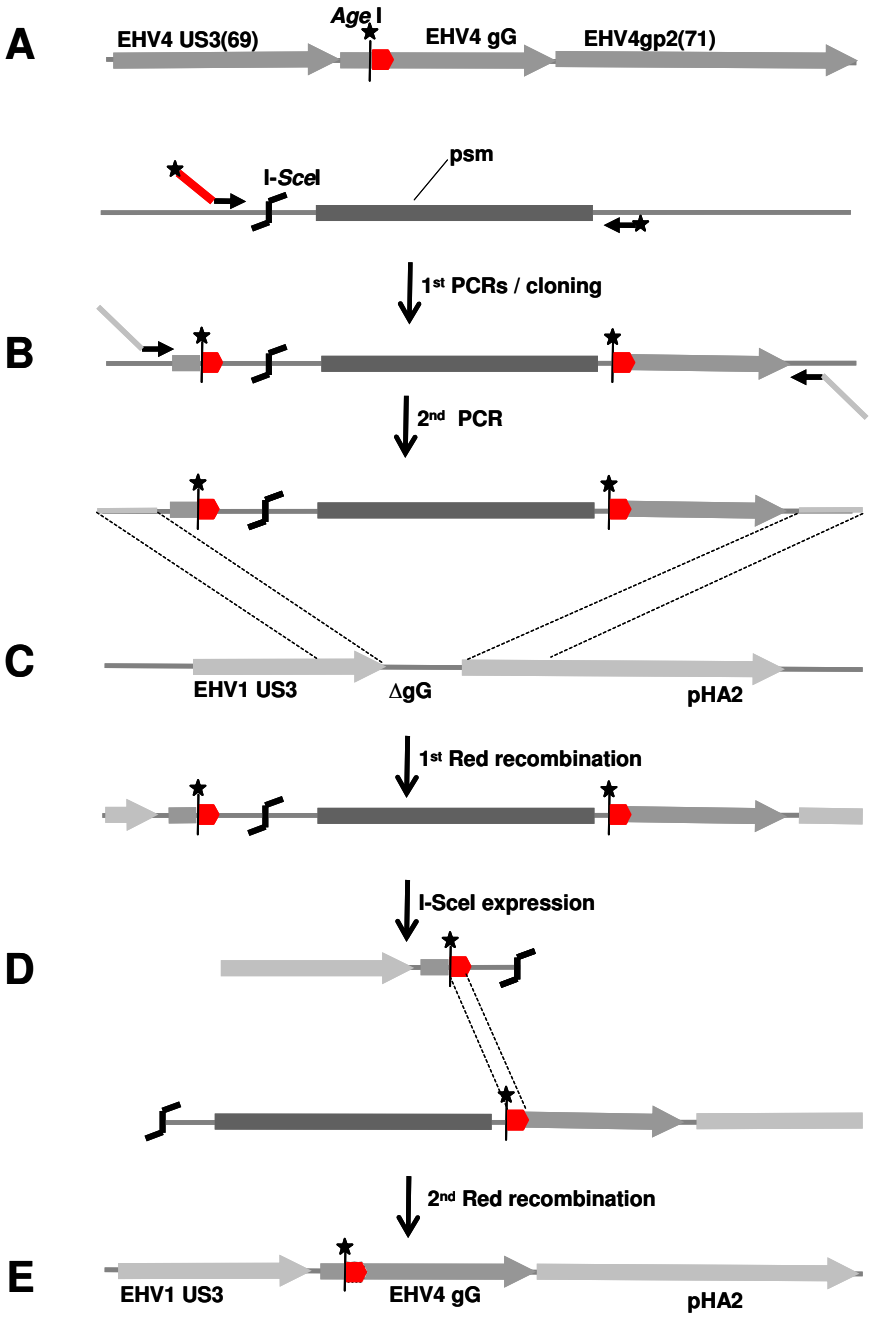

Figure 5: Red recombination – Insertion of DNA sequences (modified from: Tischer, B.K., et al., *Two-step red-mediated recombination for versatile high-efficiency markerless DNA manipulation in Escherichia coli.* Biotechniques, 2006. 40(2): p. 191-7.)

2nd Red recombination

In the second recombination step, the positive selection marker was removed by addition of 1% L-arabinose to the bacterial growth medium, which induced I-SceI expression. Leaving the culture shaking for two hours at 32°C resulted in cleavage at the I-*Sce*I site and double strand breaks in the DNA. Additionally, shaking at 42°C induced Beta, Exo, and Gam expression and initiated the second intramolecular Red recombination, which takes place between duplicated sequences. The culture was incubated at 32°C for an additional period of 2-4 h before spreading serial dilutions on agar plates containing chloramphenicol and 1% arabinose. After 48 h, resulting clones were transferred on replica plates to detect kanamycin sensitivity. Clones that had lost the positive selection marker were further screened by RFLP, colony PCR and finally sent for nucleotide sequencing.

j.2. General principle for deletion of sequences

To delete a sequence in pOH-03, the recombination cassette from plasmid pEP-kanS with primers containing different lengths of overlapping duplications on both ends (see Figure 6) was amplified by PCR. Briefly, in the first step, the linear PCR product was inserted via Red recombination into the target site by positive selection with kanamycin. In the second step, I-*Sce*I cleaved at its recognition site and created a double strand break. The adjacent duplicated sequence was then used as the new substrate for a second, intramolecular Red recombination, which resulted in the loss of the previously introduced marker.

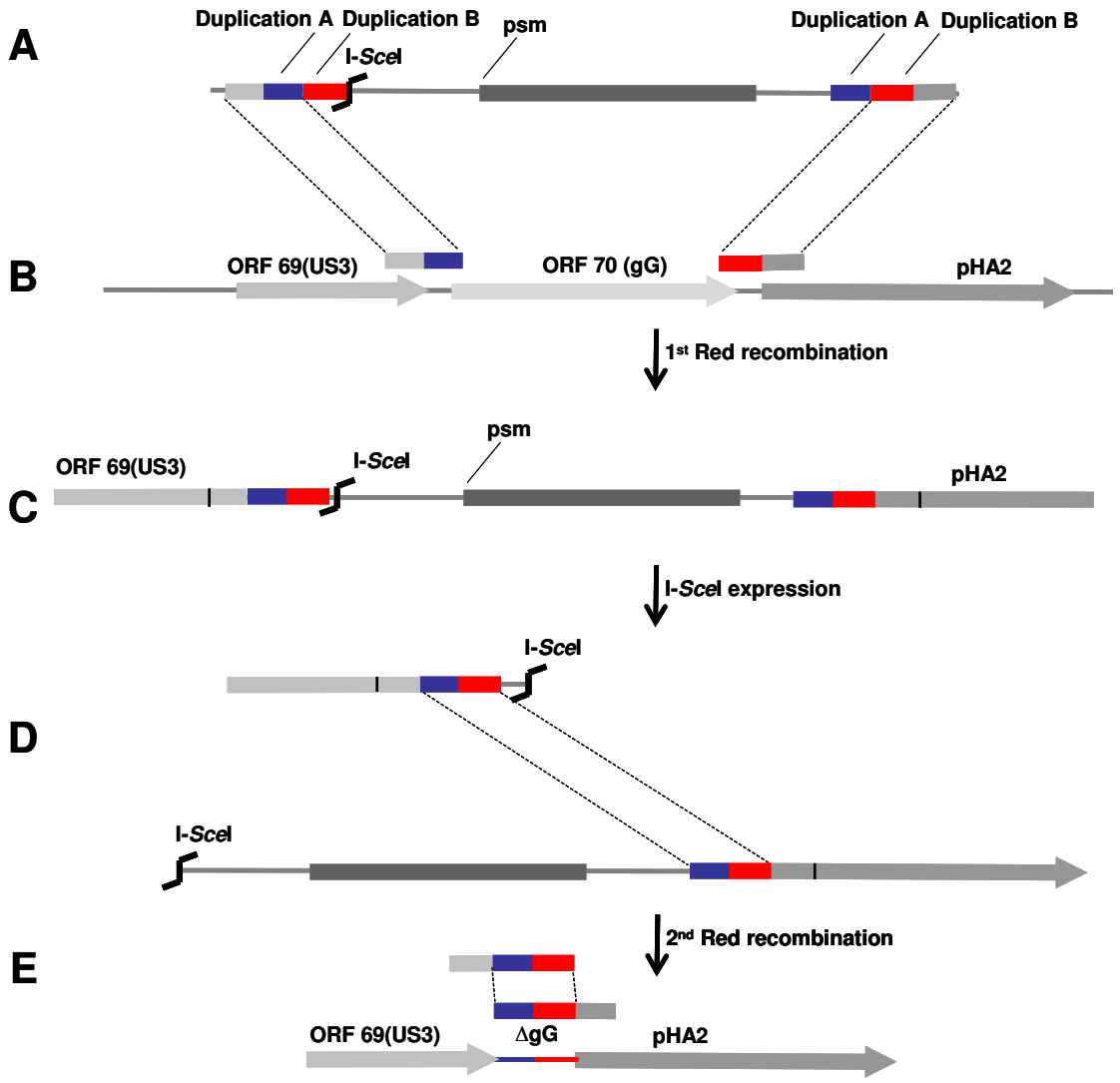

Figure 6: Red recombination – Deletion of DNA sequences (modified from Tischer, B.K. et al., *Two-step Red-mediated recombination for versatile high-efficiency markerless DNA manipulation in Escherichia coli.* Biotechniques, 2006. 40(2): p. 191-7.)

k. Preparation of competent cells and transformation by electroporation

E. coli GS1783 cells containing the pOH-03 were made competent for *en passant* Red-mediated recombination by the following procedure:

An overnight culture of bacteria was grown in the LB containing 30 µg/ml chloramphenicol. After 12 h, 100 µl of the overnight culture was inoculated into 6.5 ml of fresh LB with chloramphenicol and incubated at 32°C at 220 rpm until an OD (600 nm) of 0.5 to 0.7 was reached. Immediately, the culture was transferred into a water bath for 15 min, shaking at 42°C and 220 rpm to induce expression of the Beta, Exo, and Gam enzymes followed by

shaking in ice water for 20 min. Bacteria were centrifuged for 1 min at 17,600 x g at 4°C and resuspended in 1 ml of ice-cold glycerol (10% v/v in ddH_20). Bacteria were centrifuged and resuspended two more times and finally resuspendend in 50 µl of 10% glycerol. Bacteria were then transformed by electroporation with approximately 100 ng of the amplified and purified PCR product in 1 mm cuvettes using a Bio-Rad GenePulserXcell set at 1.8 kV and 25 µF, with the pulse controller set at 200 Ω.

I. Southern blotting

To perform Southern blot hybridization, BAC DNA was digested with restriction enzymes and the resulting fragments separated according to size by standard agarose gel electrophoresis. The DNA was denatured in the gel before transferred and covalently fixed to a nylon membrane after capillary transfer. On the membrane, the DNA was hybridized with a labeled DNA probe and fragments detected by ECL. In the following, the procedure is described in more detail:

1. DIG labeling of PCR probe (PCR DIG Probe Synthesis Kit, Roche)

To DIG-label the PCR probe, a PCR reaction was set up according to the manufacturer´s instructions:

5	µl 10X PCR buffer with $MgCl_2$	1. 95°C	5 min
5	µl PCR DIG labeling Mix	2. 95°C	30 sec
1	µl Forward Primer (EHV-1 blot for)	3. 52°C	30 sec
1	µl Reverse Primer (EHV-1 blot rev)	4. 72°C	90 sec → repeat step 2-4
0.7	µl Enzyme Mix		30 times
2	µl template DNA	5. 72°C	5 min
35.3	µl ddH2O	6. 4°C	∞
50	µl final volume		

After amplification, the PCR probe was checked for correct size on a standard agarose gel and stored at -20°C until further use.

2. RFLP of BAC DNA and electrophoresis

Approximately 10 µg of DNA of the various BAC constructs were fragmented by restriction enzyme digestion in a 30 µl volume and separated by 0.8 % agarose gel electrophoresis at 60 V for 20 h. Five microliters of DIG-labeled Molecular Weight Marker II (Roche) were separated along with 3 µl of standard DNA marker (fermentas). Subsequently, the gel was stained in 0.5 µg / ml ethidium bromide solution for 15 min, destained in ddH_2O for 20 min, and photographedunder UV light (Transiluminator Bio-Vision-3026, Peqlab).

3. Membrane preparation / upward capillary transfer

To improve transfer, DNA was nicked by brief depurination before denaturation. To achieve depurination, the gel was soaked in 0.25 M HCl for 20 min and rinsed in ddH_2O three times. Following denaturation, the gel was soaked in denaturing solution for 45 min with gentle agitation, rinsed with ddH_2O three times and neutralized in Neutralization Buffer (1M Tris, pH 7.4, 1.5 M NaCl) for 45 min. The transfer apparatus was assembled by soaking three filter papers in transfer buffer, laying the gel upside down on top followed by filter and tissue papers to allow capillary suction, which was used to transfer the DNA onto a positively charged nylon membrane (Amersham) for 18 - 24 h. After disassembly of the transfer apparatus, DNA was fixed to the membrane by UV irradiation with an exposure of 1.5 J/cm2 using a UV crosslinker (HL-2000 HybriLinker, UVP) and the membrane was used immediately for hybridization reactions.

4. Hybridization and Detection

The membrane was pre-incubated with DIG Easy Hyb buffer (Roche) in a roller bottle at 42°C for 30 min. Meanwhile the DIG-labeled probe was denatured by heating to 95°C for 5 min and rapid cooling in ice water before it was added to pre-warmed hybridization buffer. The membrane was incubated with the probe in hybridization buffer for 6 - 24 h at 42°C in a roller bottle. After hybridization, the membrane was washed for 5 min in 2 X SSC-0.1 % SDS at RT followed by washing in 0.5 X SSC-0.1 % SDS for 5 min at 68 °C. Meanwhile, the washing and blocking buffers were prepared according to the manufacturer's instructions (Roche) and the membrane was blocked in 1X blocking solution for 30 min. After blocking, the membrane was thoroughly washed and incubated with the antibody solution (anti-DIG-AP 1:10,000) for 30 min, washed twice and incubated with detection solution. Finally, CDP-Star (Roche) was added to the membrane and the chemoluminescent signal was recorded with a luminescent imager (Peqlab, Fusion SL).

m. SDS-Page

For protein analyses, RK13 or NBL-6 cells were infected with wild-type or the different mutant viruses at an m.o.i. of 1 or 2 by adding virus suspension to the culture medium, and cell lysates as well as supernatants were prepared at 24 or 48 h p.i.

Preparation of cell lysates (Enrichment of membrane glycoproteins):

Cells of two infected wells of a 6-well plate were resuspended in 500 µl of Freeze-and-thaw-buffer and frozen and thawed three times followed by centrifugation for 1 h at 15,300 x g and 4°C. The cell pellets were resuspended in 80 µl of RIPA buffer I and 0.5 µl benzonase was added to each sample. After 10 min on ice, 80 µl of RIPA buffer II were added and samples

incubated for another 10 min on ice. Finally, samples were centrifuged for 10 min at 15,300 x g and 4°C, and 40 µl of 4 X loading buffer was added to the supernatant (160 µl).

After incubation for 10 min at 30°C, 30 µl of sample were loaded on an SDS-10% polyacrylamide gel for separation.

Preparation of supernatants:

Twenty-five microliters of 4 X loading buffer was added to 100 µl of infected cell supernatant and the samples were heated at 95°C for 10 min. Samples were kept on ice afterwards and 30 µl were loaded on an SDS-10% polycarylamide gel for separation.

SDS–PAGE – gel preparation:

Glass plates were cleaned with detergent and 70 % ethanol and assembled according to the manufacturer's instructions. Resolving gels containing 7.5% (cell lysates) or 10% (supernatants) were poured, overlayed with isopropanol, and left to polymerize for 30 min. Isopropanol was removed by washing with ddH_20 and the stacking gel was poured on top of the resolving gel and left to polymerize for 20 min.

Resolving gel	**7.5 %**	**10 %**
ddH_20	4.85 ml	4.05 ml
1.5 M Tris-Cl pH 8.8	2.5 ml	2.5 ml
10 % SDS	100 µl	100 µl
30 % acrylamide	2.5 ml	3.3 ml
10 % APS	50 µl	50 µl
TEMED	5 µl	5 µl

Stacking gel	**2 gels**
ddH_20	3.05 ml
1.5 M Tris-Cl pH 8.8	1.25 ml
10 % SDS	50 µl
30 % acrylamide	650 µl
10 % APS	25 µl
TEMED	5 µl

Polymerized gels were loaded with 30 µl of prepared sample per well and gels were run at 30 V for 30 min, 70 V for 30 min and 160 V for 60 to 90 min, until the bromophenol blue indicator dye reached the bottom of the gel.

n. Western blot

1. Semi-Dry Transfer of proteins onto PVDF membranes (supernatant):

The gel was removed from its glass cassette, the stacking gel was removed, and the gel was immersed in cathode buffer for 10 min. The PVDF membrane cut the same size as the gel was soaked in methanol for 15 seconds, then washed in ultrapure water and equilibrated in Anode buffer II for 5 minutes. Five pieces of filter paper with the same dimensions as the gel

were soaked in Anode buffer I, three pieces of filter paper soaked in anode buffer II, and 8 pieces of filter paper slightly smaller than the gel were soaked in Cathode buffer for 2 min. The transfer stack was assembled starting with the Anode electrode plate, followed by filter paper soaked in Anode buffer I, then II, PVDF membrane, gel, filter paper soaked in Cathode buffer and at last the Cathode electrode plate on top of the stack. Air bubbles were removed by carefully rolling a pipette over the surface of all layers. The current was set according to the area of the transfer stack (1.2 mA / cm^2 per h). After transfer, the PVDF membrane was soaked in 100 % ethanol to fix proteins to the membrane and carefully dried between two layers of filter paper (Whatman). To test the efficiency of the transfer, the membrane was stained in Ponceau Red for 5 minutes followed by destaining twice for 5 min in PBS, a procedure that visualized the protein bands in red color.

2. Antigen-antibody reaction

To block unspecific antibody binding, the membrane was incubated at RT in 2.5% of skim milk-1% BSA in PBST for 1 h on an orbital shaker at 80 rpm. Primary antibodies were diluted in 1% BSA-PBST and incubated for 3 h at RT or overnight at 4°C, respectively. After three washing steps with PBST, the membrane was incubated with the HRP-conjugated antibody diluted in 2.5 % skim milk in PBST for 1 h at RT, followed by three more washing steps with PBST. Specific protein bands were detected by using the Amersham ECL Plus detection reagent and exposing the membrane to a luminescent imager (Chemi-Smart 5100, peqlab) for 20 s up to 20 min.

o. Neutrophil isolation from equine blood

Equine neutrophils were isolated by density centrifugation of heparinized blood from healthy horses on a discontinuous Percoll gradient [101]. A gradient was produced in a 15 ml Falcon tube by carefully overlaying 4 ml of Biocoll (75 %) with 4 ml of Biocoll (59 %). Five milliliters of heparinized horse blood were layered onto the Biocoll layers and samples were centrifuged at RT for 30 min at 400 x g. The neutrophil layer was taken off and washed twice with 1 X HBSS without Ca^{2+} or Mg^{2+}. Cells were counted in a Neubauer chamber and purity of each cell population was confirmed by cytospins where 100 µl of cell suspension were centrifuged on glass slides at 700 x g for 4 min at RT, dried for 5 min and stained with modified Wright´s stain according to the manufacturer's instructions (Sigma-Aldrich). Finally, cells were resuspended in MEM at $1x10^5$ cells/ml and used immediately for further experiments.

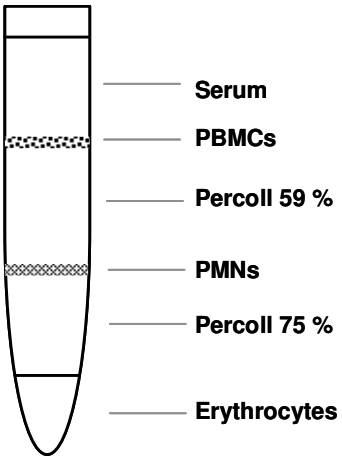

Figure 7: Illustration of cell separation from equine venous blood using a discontinuous Percoll gradient.

p. Chemotaxis assays

To examine the function of secreted gG on neutrophil migration, chemotaxis assays were established previously by Van de Walle et al. [55, 102]. Here, chemotaxis assays were applied to analyze further the function of gG expressed by the various mutant viruses. To obtain the various forms of secreted gG, cells were washed twice with MEM and inoculated for 24 h with virus suspension at an m.o.i. of 1. Virus and cellular debris was removed from supernatants by ultracentrifugation at 100,000 x g for 1 h and cleared supernatants were subsequently used in chemotaxis assays.

Chemotaxis assays were performed as follows: In the lower compartments of the wells of a 12-well Transwell plate (Costar) 300 µl of ultracentrifuged supernatant of infected cells were pre-incubated with 300 µl of equine IL-8 at a final concentration of 25 ng/ml in MEM for 30 min at 37°C. The lower chambers were then covered with a polycarbonate membrane with a 3 µm pore size to allow migration of neutrophils, and 100 µl of the cellular suspension (containing 1 x 10^4 neutrophils) was added to the top chamber. The assay plate was incubated at 37°C for 45 min. Chambers filled with chemokine or medium alone served as positive and negative controls, respectively. After incubation, the polycarbonate membrane insert was removed; plates were centrifuged at 2,400 x g for 3 min at RT. Cells in the lower chambers were stained with modified Wright´s stain and counted under a light microscope.

2.2.4. Animal experiments

a. Animals

3- to 4-week-old female BALB/c mice were obtained from Charles River Laboratories International, Inc. and housed in the animal facility of the Institute of Microbiology of the Freie Universität Berlin on the campus of the Humboldt Universität Berlin. Animals were housed and treated according to Germany's animal welfare law.

b. Animal care and housing

Mice were separated in groups of six to nine mice per cage and allowed to recover from transportation for one week. Mice were kept in Makrolon type III cages with free access to pelleted food and water.

c. General procedures, infection, health parameters

For the infection procedure, mice were anaesthetized by intraperitoneal injection of 0.1 ml/10 g mouse of a xylazine-ketamin-mixture (1 ml ketamine [100 mg/ml] and 0.5 ml xylazine [20mg/ml] in 8.5 ml aqua ad injectionem). Mice were infected by intranasal instillation with the various mutant viruses ($1x10^5$ pfu of virus/mouse) suspended in 40 µl growth medium. Mice were examined daily for clinical signs of infection such as ruffled fur, hunched posture, increased respiratory rates, ataxia and hypersensitivity to external stimuli. Individual weights were determined daily from the day of infection (day 0) until day 14 and percentages of body weight losses were determined.

d. Sacrificing animals

For euthanasia, mice were overdosed with a xylazine-ketamin mixture and unconsciousness of mice was controlled before cervical dislocation and final bleeding was performed.

e. BAL and tissue sampling

After sacrificing the animals, the pleural cavity was exposed, the trachea was cut just below the larynx and a blunted 20-gauge 1.5 inch needle was inserted into the trachea. The needle was fixed in place by tying with a filament. BAL fluid was obtained by using a 1 ml syringe to flush the lungs three times with 1ml of PBS. Recovered BAL fluid was kept on ice until further

use. The lung was removed completely and one part of the lung was fixed in 4 % formaldehyde and submitted to the Institute of Pathology for histopathological examination, whereas the other part was frozen at -70°C for subsequent determination of the virus titers.

f. Flow cytometry

The different composition of immune cells within the BALs of mice infected with the EHV-1 mutants constructed in this study was determined by flow cytometry.

BAL cells were washed twice in PBS before blocking and staining. All steps were carried out in a 96-well plate. Unspecific binding of immunoglobulins to Fc receptors was blocked by rat anti-mouse CD16/CD32 mAb 2.4G2 (BD Biosciences; 10 µg / ml diluted in PBS-0.2% BSA) for 10 min at 4°C. Subsequently, BAL cells were stained with fluorescently labeled rat anti-mouse monoclonal antibodies against surface markers on neutrophil (Gr-1+-APC, SouthernBiotech), macrophages (F4/80-FITC, BIOZOL), B lymphocytes (B220-APC, SouthernBiotech) and T lymphocytes (CD3-FITC, BIOZOL) at a final concentration of 10 µg antibody/ml diluted in PBS-0.2% BSA. Isotype controls applied at the same concentrations were used for each of the antibodies separately, which were rat IgG2b K Isotype Control APC for neutrophil staining, rat IgG2b K Isotype Control FITC for macrophage staining, rat IgG2a K Isotype Control APC for the B lymphocyte staining and rat IgG2a K FITC for T lymphocytes. Staining was carried out at 4 °C for 45 min in the dark. After staining, cells were washed twice with 200 µl PBS-0.2% BSA and finally resuspended in 300 µl PBS-0.2% BSA before flow cytometric analyses were performed. On day 2 p.i., 100,000 events were recorded using a FACSCalibur flow cytometer (BD Biosciences) and, owing to a generally decreasing number of cells in the BALs on day 4 p.i., 50,000 events were measured. Data were analysed using Cell Quest software (BD Biosciences) as well as FlowJo V.7.6.3.

g. Histology

After BAL, lungs were removed and fixed in 4% formaldehyde. Lungs were then embedded in paraffin, cut into 4 µm sections, and stained with hematoxylin-eosin. Lungs were inspected under a light microscope to examine the state of inflammation and to evaluate the influx and character of invading immune cells. Lungs of a non-infected mouse were stained as well and used as control.

h. Titration of virus from tissues

MEM was added to the frozen lung parts according to the determined weight and the tissue was homogenized. Virus titers were determined by standard titration on RK13 cells with a 1.6 % methylcellulose overlay [108].

i. Statistics

For graphs and statistics Microsoft Office Excel 2007, IBM SPSS Statistics 19 or GraphPad Prism 5 were applied. Based on the small number of samples, one-way analysis of variance (ANOVA) by multiple comparisons of the groups was applied at first. To test for statistically significant differences in the plaque size and chemotaxis assays, Bonferroni adjustment was exercised. Bonferroni adjustment was also applied to determine statistically significant differences in weight losses of mice after infection as well as in viral titers of the mouse lungs [109].

3. Results

3.1. Generation of mutant viruses

It was previously demonstrated that gG of EHV-1 is able to interfere with neutrophil chemotaxis *in vivo* [48, 53]. Furthermore, the hypervariable region of EHV-1 gG comprising amino acids 301 to 340 was shown to bind to chemokines *in vitro*. In contrast, EHV-4 gG, specifying a different sequence in the variable region of gG when compared to EHV-1, was not able to bind to chemokines or interfere with neutrophil chemotaxis [48, 55]. In order to test the hypothesis based on the *in vitro* experiments that the hypervariable region is in fact the determining part in binding to chemokines and exerting gG's functions, this study aimed to construct several recombinant gGs in the EHV-1 background that would be tested *in vivo*. A recently isolated neurovirulent EHV-1 strain, Ohio-03 (OH-03) cloned as a bacterial artificial chromosome was used as a backbone to create a set of gG mutants including a null mutant (vOH-03ΔgG), a mutant in which EHV-4 gG was inserted in lieu of authentic EHV-1 gG (vOH-03-4gG), a mutant harboring EHV-4 gG substituted with the hypervariable region of EHV-1 gG (vOH-03-4gGhyp1), and a mutant harboring the hypervariable region of EHV-4 gG in the EHV-1 backbone (vOH-03-hyp1). A list of all primers used in this study for construction of the transfer plasmids as well as for Red-mediated recombination is given in the Materials and Methods section (2.1, Table 1 and 2).

3.1.1. Deletion of glycoprotein G in EHV1 (vOH-03-ΔgG)

a. Transfer constructs

To construct a gG deletion virus, two-step *en passant* Red mutagenesis was applied (see Methods, 2.2.3.j). The primers NTa and NTb, designed to include overlapping duplications of sequences directly adjacent to gG facilitating recombination (designated A and B in Figure 8), were used to amplify the recombination cassette (1108 bp). The plasmid pEPkanS1 served as a template for the PCR reaction. The resulting PCR product was column purified and used for transformation.

Figure 8: PCR product for deletion of gG with recombination cassette including the positive selection marker (psm, dark grey box), homologues flanks to the target sequence (light and medium grey boxes), and duplicated sequences (blue and red boxes) for removal of the psm.

b. Recombination

GS1783 *E. coli* cells containing pOH03 were made electrocompetent and transformed with ~100 ng PCR product as described in 2.2.3. The gG sequence was replaced by the prokaryotic selection marker gene *aph*AI conferring kanamycin resistance in the first recombination step and its correct insertion was confirmed by restriction fragment length polymorphism (RFLP) and PCR. In the second recombination step, the positive selection marker (psm) was removed by SceI cleavage and subsequent homologous recombination events. The resulting sensitivity to kanamycin of successfully resolved clones was confirmed by replica-plating on appropriate selection plates. A schematic representation of the resulting pOH-ΔgG is given in Figure 9.

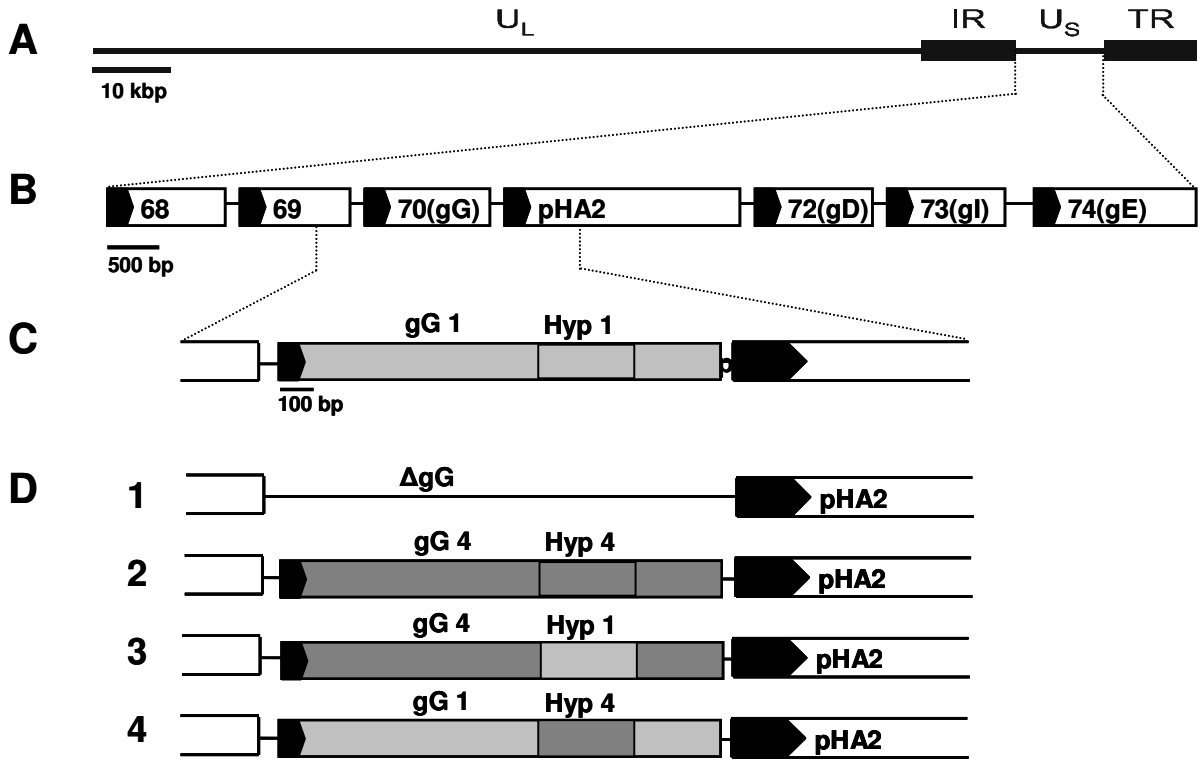

Figure 9: Schematic representation of the gG gene and its various constructed mutations in the EHV-1 strain OH-03
(A) Overall genome organization of pOH-03 with the unique-long and -short segements flanked by internal and terminal repeat regions (B) Organization of the unique-short segment of pOH-03 with ORF 70 encoding gG and upstream ORF 69 encoding the US protein kinase (US3) and the downstream mini-F cassette pHA2, which replaces gene 71 (C) Schematic representation of gG with its hypervariable region at the C-terminus. (D) Schematic representation of the four constructed mutants which are 1) pOH-03 with gG deleted, 2) pOH-03 with EHV-4 gG, 3) pOH-03 with EHV-4gG and the hypervariable region of EHV-1 and 4) pOH-03 gG containing the hypervariable region of EHV-4 gG

The deletion of the gG ORF was confirmed by RFLP with *Eco*RI restriction enzyme digestion and Southern blotting using a DIG-labeled PCR probe generated with primers EHV-1delgG blot forward and reverse (Table 3, 2.1.1.). The insertion of the 988 bp kanamycin cassette in intermediate clones resulted in a shift of the gG containing fragment from 5.24 kb down to 5.03 kb. Furthermore, this fragment was shortened to 4 kb after complete deletion of gG, as depicted in Figure 10. Finally, the fragment comprising the gG sequence was amplified using primers NT11 and NT12 and sequenced to confirm the complete deletion of the gG sequence.

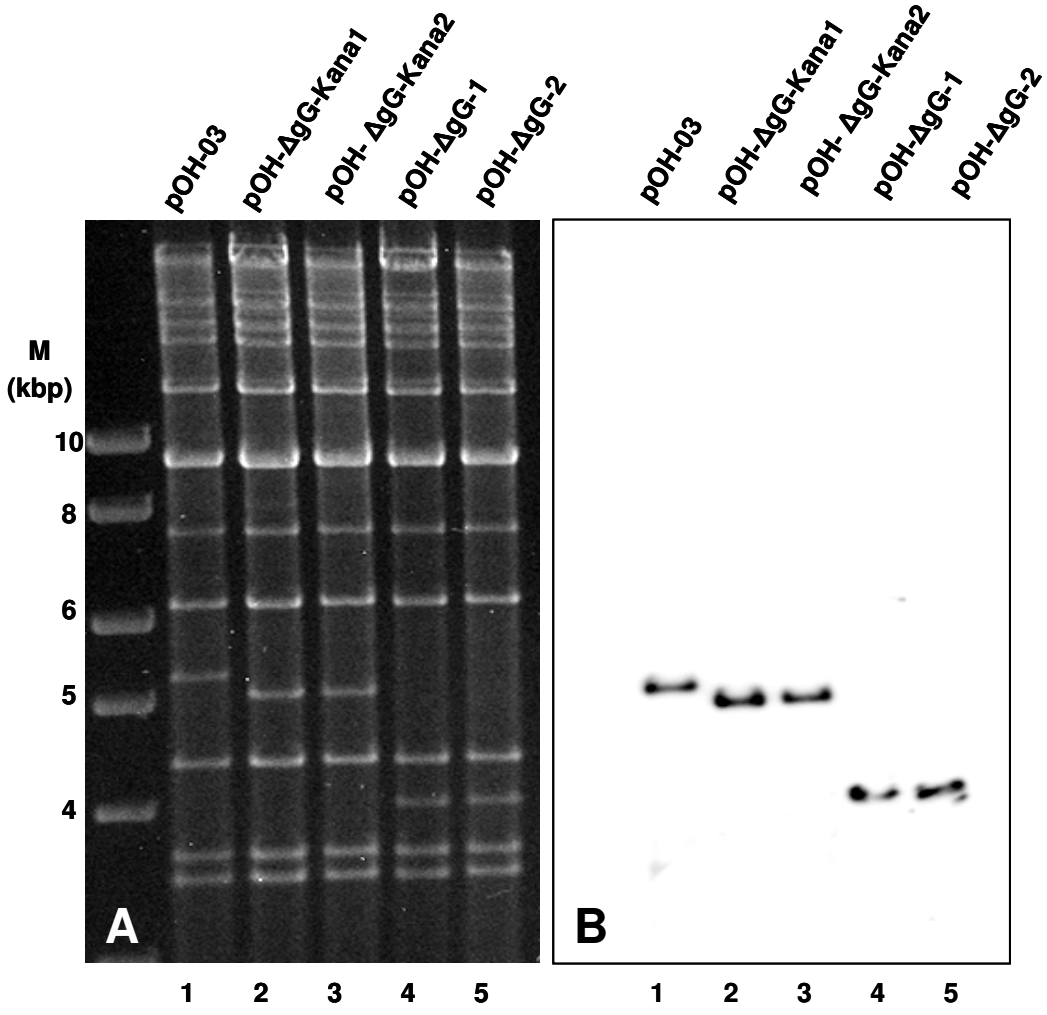

Figure 10: RFLP by EcoRI and Southern blot analysis of pOH-03 (1), pOH-ΔgG-Kana intermediates (2, 3) and pOH-ΔgG(4,5). (A) DNA was digested by EcoRI at 37°C for 4 hours and fragments were separated on a 0.8% gel for 20 h at 60 V, the gel was stained with ethidium bromide (EB) and photographed. (B) After confirmation of the correct restriction pattern DNA was denatured and transferred to a nylon membrane. For hybridization a probe was used that hybridized to sequences 500 bp upstream of gG which was prepared with primers EHV-1delgG blot -for and -rev (Table,3 in 2.1.1.)

3.1.2. Insertion of EHV-4 gG into EHV1 (vOH-03-4gG)

a. Transfer construct

Glycoprotein G of EHV-4 strain KT-4 (kindly provided by Dr. Kerstin Borchers) was amplified by PCR using primer NT1 and NT2 (Table 1, 2.1.1.). The PCR product (1308 bp) was gel-purified and cloned into the vector pcr2.1-TOPO using the TOPO TA Cloning Kit and TOP 10 chemical competent cells for transformation (Invitrogen). Correct clones were determined by triple digestion with *Eco*RI, *Nhe*I and *Xho*I (NEB). Finally, the correct sequence was confirmed by sequencing.

A second PCR using primers NT3 and NT4 and plasmid pEPkanS1 as template was performed. This PCR amplified the I-SceI-aphAI recombination cassette plus 50 bp of duplicated sequences located downstream of the chosen restriction site (AgeI). The primer also included *Age*I restriction sites on both ends to facilitate cloning into the gene of interest.

The PCR product (1053 bp) was gel purified and cloned into the pcr2.1TOPO-4gG plasmid using the *Age*I restriction site (see Figure 11).

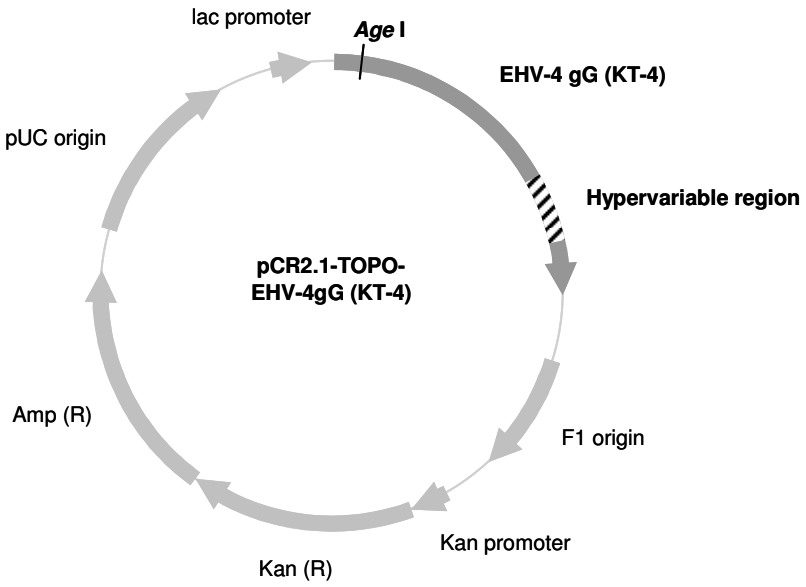

Figure 11: First step of transfer plasmid construction: EHV4 gG was cloned into pcR2.1TOPOvector resulting in pcr2.1TOPO-EHV-4gG, marked the *Age*I restriction site essential for cloning of the universal transfer construct

As the pcr2.1TOPO vector already contained a kanamycin resistance gene, the cloned product was released by *Eco*RI digestion and cloned into the pUC19 vector which had been digested with *Eco*RI as well as dephosphorylated with Antarctic phosphatase (NEB). Thus, selection for resistance to ampicillin and kanamycin was possible. Correct transfer plasmid

clones were confirmed by RFLP, PCR and sequencing (schematic presentation of the universal transfer construct in Figure 12).

Finally, the PCR product for recombination was amplified using the constructed universal transfer plasmid pUC19-4gG-Kana with primers NT5 and NT6 (2553 bp).

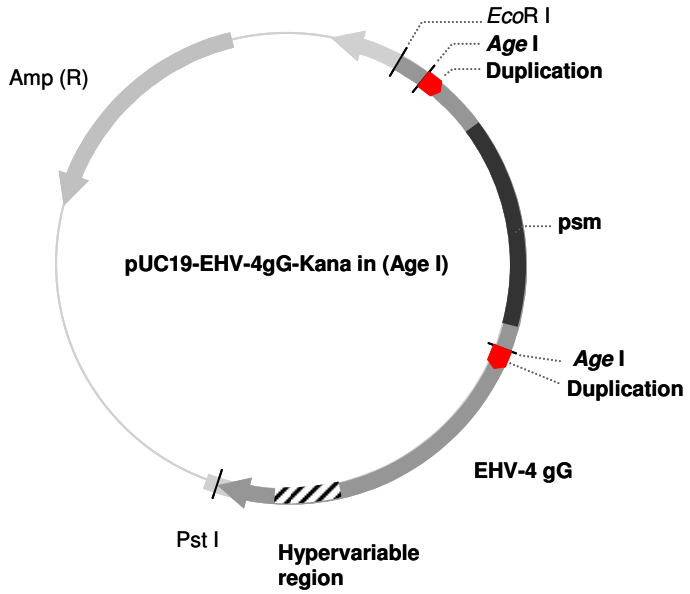

Figure 12: Schematic representation of universal transfer construct pUC19-EHV4gG-Kana in: Depicted are the positive selection marker (psm, dark grey), the hypervariable region (striped) and the *Age*I restriction site used for cloning

b. Recombination

Electrocompetent *E.coli* GS1783 cells containing pOH-03ΔgG were transformed by electroporation with ~ 100ng of PCR product and subsequently plated on chloramphenicol/ kanamycin selective plates. After 48 h, colonies were picked, grown overnight in chloramphenicol/kanamycin selective LB medium and BAC DNA was prepared as described in 2.2.3.b. BAC DNA of the generated intermediate clones was screened by RFLP. For removal of the kanamycin cassette, 1% arabinose was added to overnight cultures in order to induce I-SceI expression, which results in cleavage at the I-SceI site and a double strand break in the DNA. Incubation at 42°C, inducing the expression of *beta*, *exo*, and *gam*, initiates the second intramolecular Red recombination taking place between the inserted duplication and its counterpart in the genome. Bacterial cultures were plated on chloramphenicol selective plates and resulting colonies were replica-plated on kanamycin selective plates for detection of kanamycin-sensitive clones. BAC DNA of clones sensitive for kanamycin was prepared, screened by RFLP with *Bam*HI, *Eco*RI, and *Hind*III followed by sequence analysis (See Figure 15).

3.1.3. Re-insertion of the hypervariable region of EHV-1 into the EHV-4 gG (vOH-03-4gG-hyp1)

a. Transfer constructs

The transfer plasmid pFASTBAC11-EHV-4sgG chimera kana_in was kindly provided by Prof. Gerlinde van de Walle and Dr. Benedikt Kaufer. The positive selection marker of this recombinant plasmid is located within the hypervariable region of an EHV-4 gG chimeric sequence, which comprises the EHV-4 gG sequence with the hypervariable region of EHV-1 gG.

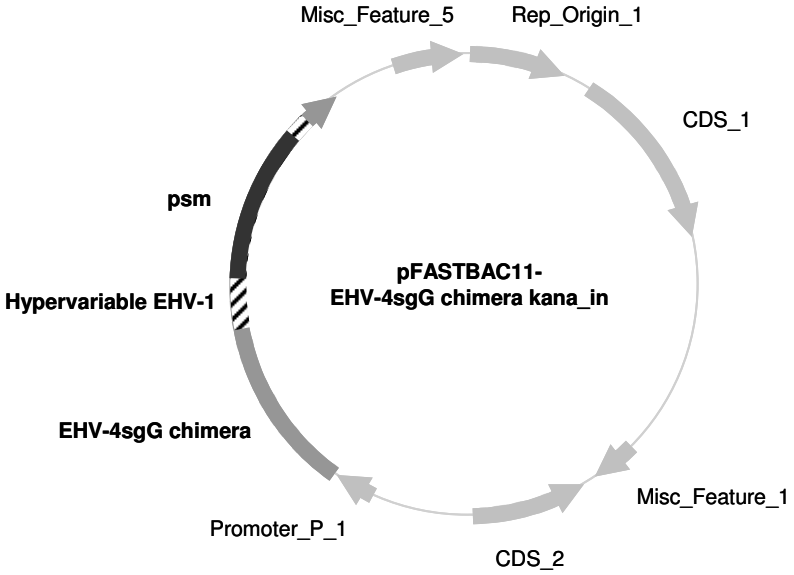

Figure 13: Schematic representation of pFASTBAC11-EHV-4sgG chimera kana_in, comprising a chimeric EHV-4 gG (medium grey) that contains the hypervariable region of EHV-1 gG (striped) with the psm (dark grey) inserted.

b. Recombination

PCR was performed using primer NT31 and NT 32 and resulted in a PCR product (1338 bp) that was purified and used for transformation of pOH-03-4gG. Resulting kanamycin-resistant intermediates were screened by RFLP and clones harboring the correct insertion of the kanamycin cassette were used for resolution of the co-integrates. Resolved kanamycin sensitive clones were controlled for correct insertion of the EHV-1 hypervariable region into the EHV-4 gG by RFLP and by DNA sequencing (See Figure 15).

3.1.4. Insertion of EHV-4 gG hypervariable region into EHV-1 gG (vOH-03-hyp4)

a. Transfer constructs

The gG gene of an EHV-4 strain (KT4) was directly amplified from isolated viral DNA using primers NT1 and NT2 and the resulting PCR product was cloned into the pcr2.1TOPO-vector (Invitrogen).

A second PCR to amplify the I-SceI-aphAI recombination cassette was performed using pEPkanS1 as a template using primers NT33 and NT34. The forward primer contained 50 bp of duplicated sequences located downstream of the chosen restriction site (*Bsr*GI) and restriction sites on either end for cloning into EHV-4 gG (1058bp). The PCR product of the second PCR was cloned into pcr2.1TOPO- 4gG using *Bsr*GI as the restriction site, which is located in the hypervariable region only. Correct clones were determined by colony PCR, RFLP and sequencing.

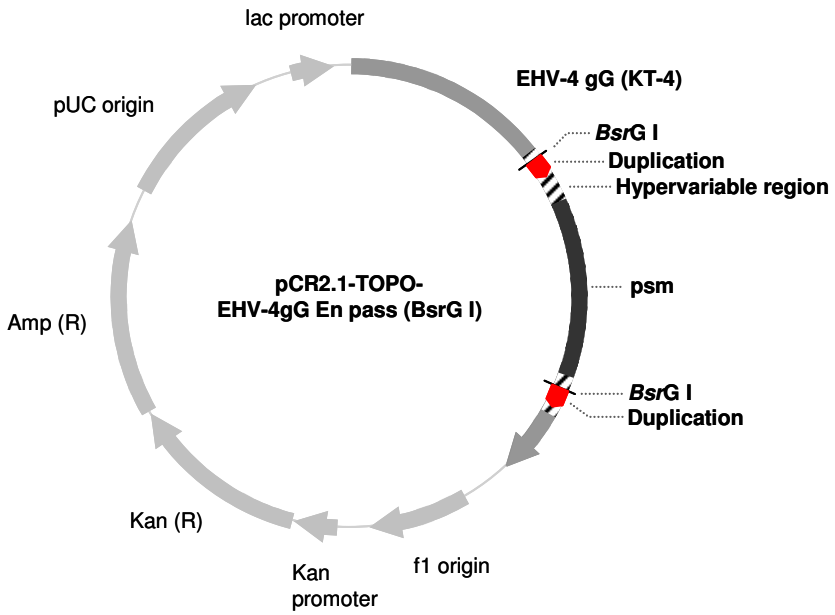

Figure 14: Schematic representation of pcr2.1TOPO-EHV-4gG-kana_in comprising EHV-4 gG with the psm (dark grey) inserted into its respective hypervariable region (striped) by using a *Bsr*GI restriction site and duplications for removal of the psm (red)

b. Recombination

The hypervariable region of EHV-4 gG containing the kanamycin cassette was amplified using primers NT41 and NT42 and the resulting PCR product (1390 bp) was column-purified and subsequently used for transformation of pOH-03. Resulting kanamycin-resistant

intermediates were screened by RFLP with *Eco*RI and clones harboring the positive selection marker were resolved. Resolved kanamycin-sensitive clones were controlled for correct insertion of the EHV-4 gG hypervariable region by RFLP and by DNA sequencing. The resulting recombinant BAC is schematically depicted in Figure 15.

3.1.5. RFLP of recombinant BACs

To confirm the genotypes of all generated mutants, BAC DNA was isolated from bacterial cultures, cleaved with restriction enzymes *Bam*HI, *Eco*RI or *Hind*III and separated on 0.8% agarose gels for 20 hours at 60 V. Changes in the restriction pattern resulting from insertion or deletion of the positive selection marker are marked by orange arrowheads in part B of Figure 15.

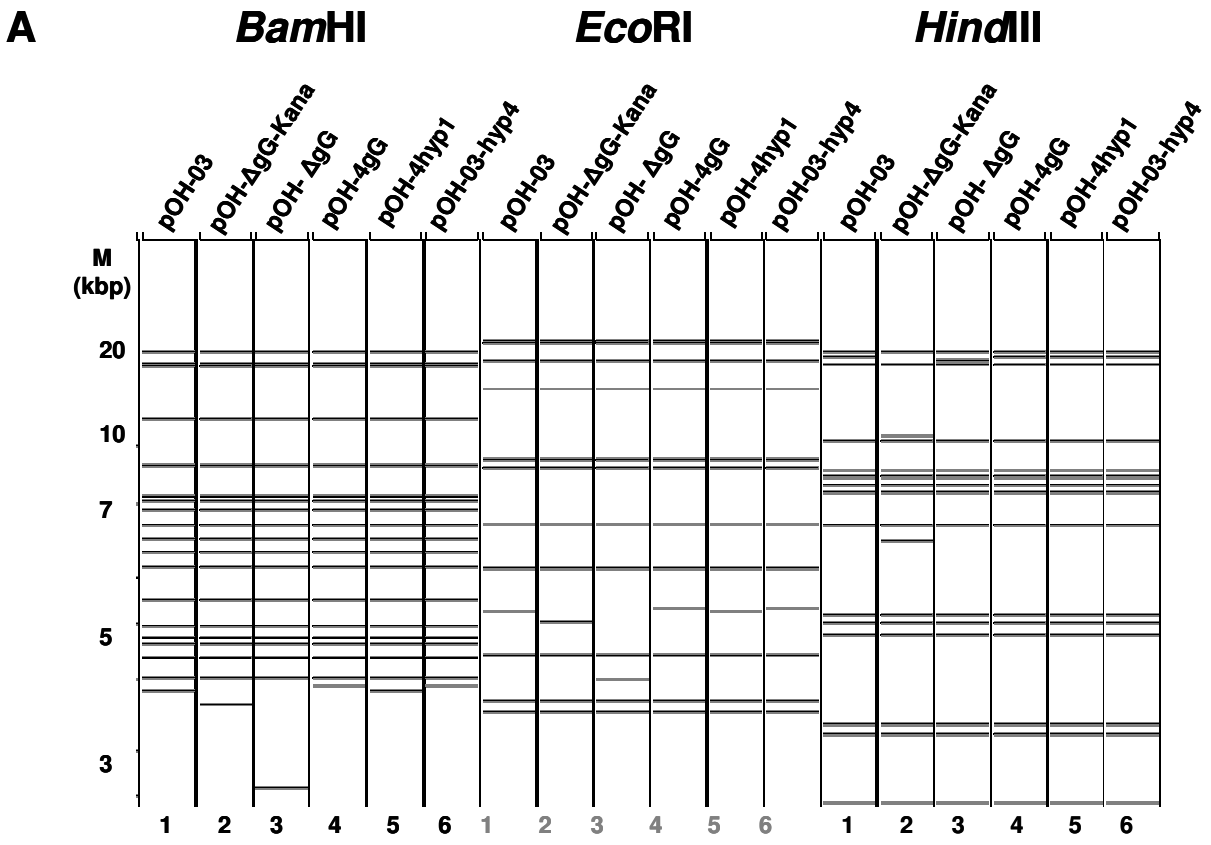

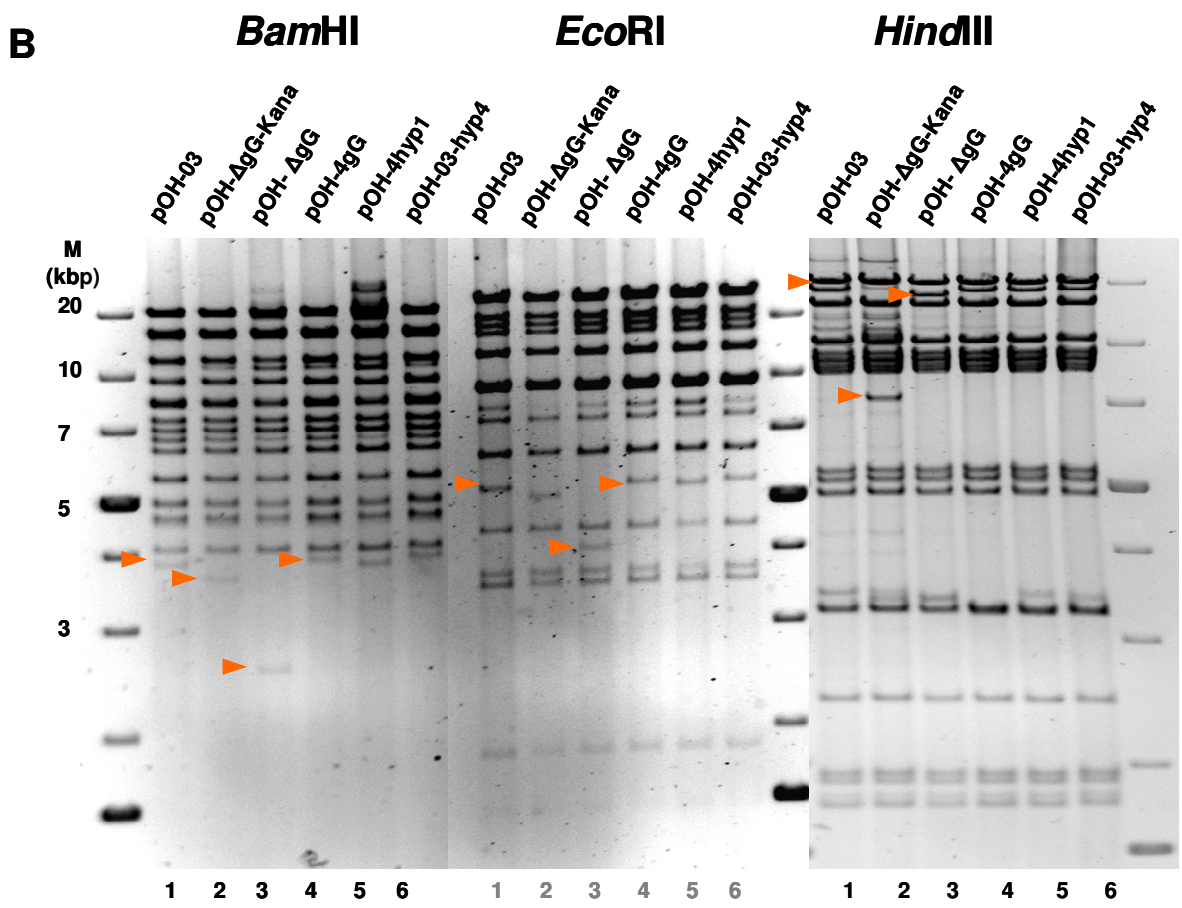

Figure 15: (A) VectorNTI-based prediction of restriction enzyme patterns of pOH-03 and derived mutants digested with *Bam*HI, *Eco*RI or *Hind*III. The recombinant BAC clones were loaded as indicated (B) Resulting DNA fragments were run for 20 hours in a 0.8% agarose gel at 60 V.

3.1.6. Reconstitution of gp2

Glycoprotein gp2, which was previously replaced in pOH-03 by the pHAII sequence that comprises the mini-F plasmid sequences and also contains the egfp and chloramphenicol resistance genes in order to maintain the viral DNA as a BAC was restored by co-transfection of BAC DNA and plasmid pEHV1gene71-Ab4 cloneA as described previously [53, 78]. Glycoprotein gp2 reconstituted mutant viruses, which were generated by homologous recombination between pOH-03 and gene71 sequences upon transfection did no longer express egfp, induced non-fluorescent plaques that could be picked and virus was purified by three rounds of plaque purification. Expression of gp2 in the reconstituted viruses was confirmed by PCR, performed on supernatants of RK13 cells infected with the various recombinant viruses using primers seq gp2-3 and gp2 rev (Table 3, 2.1.1.) resulting in a specific fragment of 1kb in length (see Figure 16).

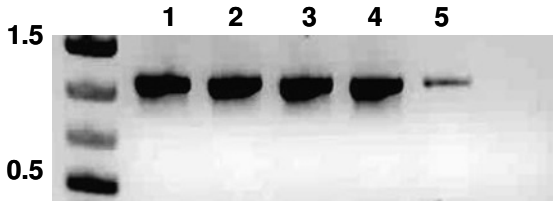

Figure 16: For confirmation of gp2 reconstitution, PCR was performed on supernatants of RK13 cells infected with vOH-03 (1), vOH-03-ΔgG(2), vOH-03-4gG(3), vOH-03-4hyp1(4) and vOH-03-hyp4(5) using Taq polymerase and primers gp2_seq3 and gp2 rev resulting in a 1kb fragment.

Further confirmation of correct reinsertion of gp2 (ORF71) was achieved by an indirect immunofluorescence analysis (IFA) of RK13 cells infected with the various recombinant viruses using monoclonal anti-gp2 antibody 3B12 [110, 111]. Expression of gp2 could be shown for wild-type EHV-1 OH-03 virus as well as for all mutants but no signal could be detected for mock-infected RK13 cells used as control (Figure 17).

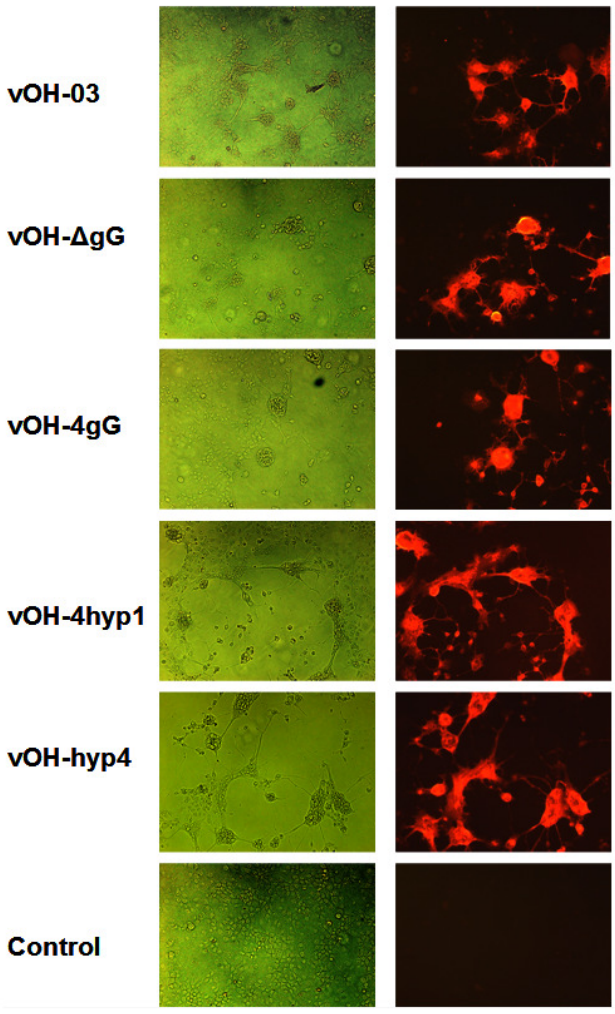

Figure 17: Indirect immunofluorescence analysis for confirmation of gp2 expression. RK13 cells were infected with the various recombinant viruses at 100 pfu / well and IFA was performed using mouse anti-EHV-1 gp2 mAb 3B12 in a 1:5 dilution in 1%FCS-PBS as the primary antibody and Alexa 568-conjugated goat anti-mouse IgG as the secondary antibody in a 1:1000 dilution in 1%FCS-PBS.

3.2. Characterization of mutant viruses

3.2.1. Western blot

Western blot analysis of infected-cell lysates and supernatants containing the secreted gG proteins purified by ultracentrifugation were performed. Cells were infected at an moi of 1 and cell lysates and purified supernatants were prepared at 24 hours p.i. (2.2.3. m, n). The expression of the secreted and the membrane-bound form of the various recombinant gG's, in addition to the authentic EHV-1 and EHV-4 gG's could be detected by use of polyclonal antibodies. The former were expected to range between 55- to 60-kDa and the latter at approximately 68-kDa. The antibodies used here specifically bind to the hypervariable region of either EHV-1 or EHV-4 gG [10]. As expected, no signal could be detected for the gG deletion mutant (Figure 18, B). The secreted form of gG ranged from 50- to 60-kDa in size (Figure 18, A and B), whereas the membrane-bound form was detectable in the 60- to 70-kDa range (Figure 18, C and D). Predicted sizes of the proteins were 412 amino acids for vOH-03 gG, 436 aa for vOH-4 gG, 411 aa for vOH-4hyp1 gG and 437 aa for vOH-hyp4 gG.

To ensure an equal sample loading on SDS-polyarcylamide gels, two different loading controls were applied. In the case of the cell lysate, analysis of the cellular transmembrane protein Na-K-ATPase (approx. 100 kDa) and actin (45 kDa) were detected with specific antibodies. No differences in terms of sample loading could be detected by western blotting using the control antibodies (Figure 18, C and D).

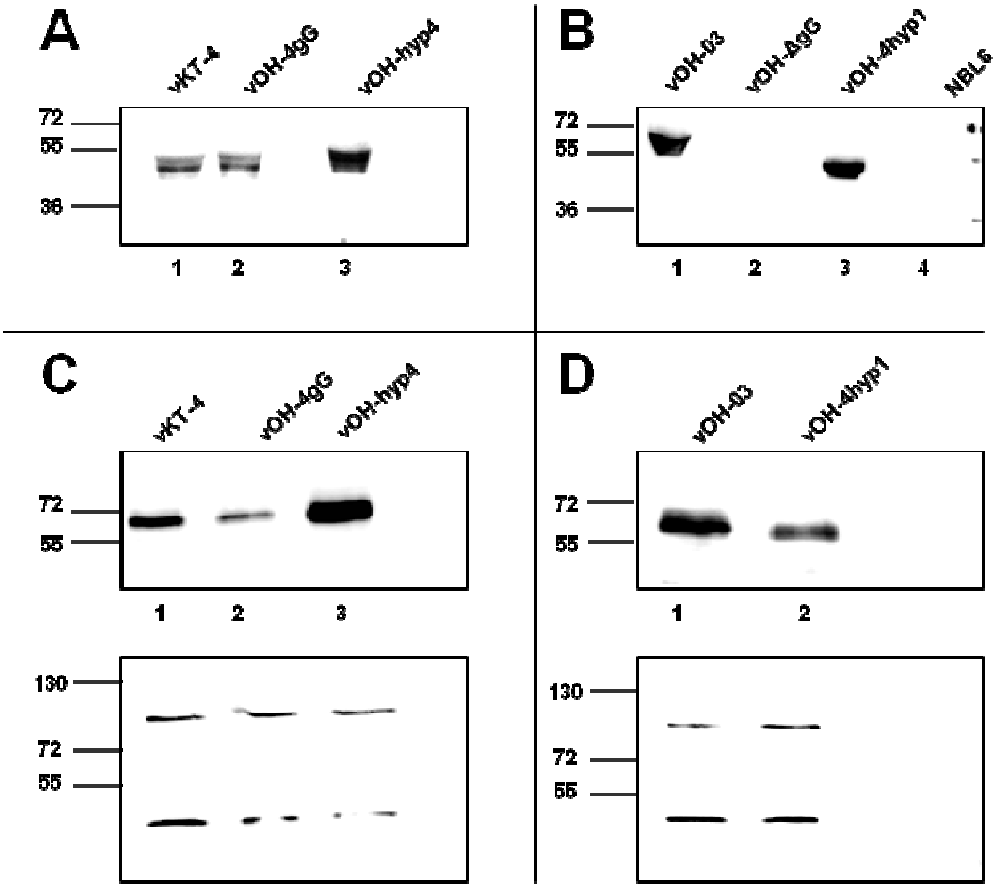

Figure 18: Western blot of secreted or virion-associated forms of gG of the different recombinant viruses. The upper panel shows ultracentrifuged supernatants collected 24 hours p.i. from NBL6 cells infected at an moi of 3 with EHV4 (KT-4), vOH-4gG, vOH-hyp4 (A) or vOH-03 wild type, vOH-ΔgG and vOH-4gGhyp1 (B). The lower panel shows cell lysates of NBL6 cells prepared 24 hours p.i. with EHV4 (KT-4), vOH-4gG and vOH-hyp4 (C) or vOH-03 wild type, vOH-ΔgG and vOH-4gGhyp1 (D) as well as the respective loading controls Na-K-ATPase and actin. Polyclonal Abs(pAbs) rat-anti EHV-1- or EHV-4 gG hyp [10] were used at 1:500 dilution in PBS-T 0.1%, pAb donkey-anti rat at a dilution of 1:10,000 in 2.5% skim milk in PBS-T 0.1%, mAb mouse-anti Na-K-ATPase at a 1:2,000 dilution in 2.5 % skim milk PBS-T 0.1%, and mouse-anti actin mAb at 1:2,000 dilution in 2.5 % skim milk PBS-T 0.1%

After RFLP, PCR and sequencing, the genotypes of all generated virus mutants could be confirmed. IFA and Western blot analysis of all recombinants showed correct restoration and expression of the adjacent glycoprotein gp2 as well as presence or absence of gG and its various mutant forms in the respective viruses.

3.2.2. Plaque size assay

The *in vitro* growth properties of the generated recombinant viruses in comparison to wild-type EHV-1 virus were examined by plaque size assay. In this experiment, any possible impact of the mutated gG on cell-to-cell spread could be evaluated by quantification of plaque areas. In Figure 19, the resulting mean plaque areas of three independent experiments are summarized. No significant differences between OH-03 wild-type and the gG recombinant viruses regarding plaque sizes were observed suggesting no influence of gG on direct cell-to-cell spread *in vitro*.

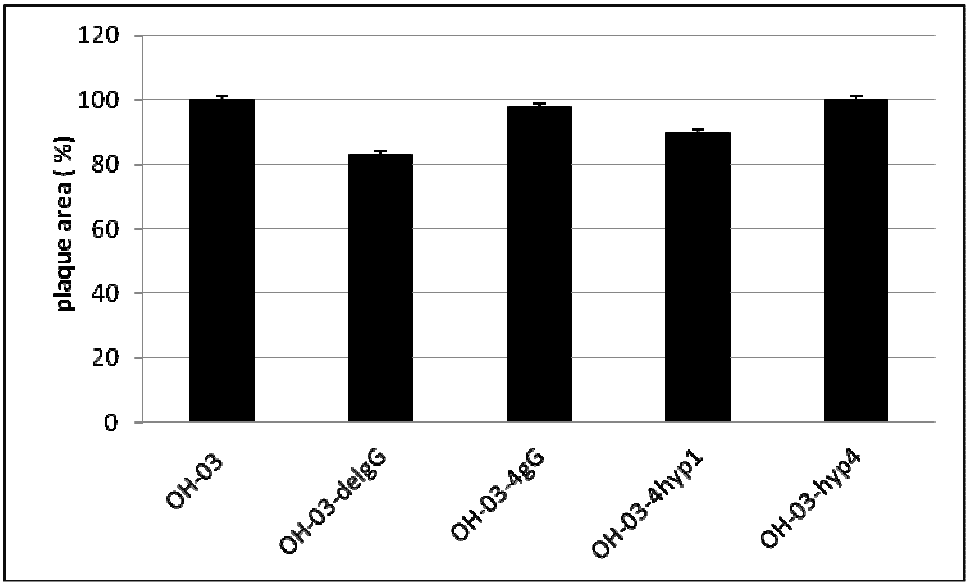

Figure 19: Plaque size assay of vOH-03 wild-type and recombinant viruses. RK13 cells were infected with 100 pfu per well, fixed on day 3 p.i. and stained with anti gM Ab [112] at a 1:50 dilution as the primary and Alexa fluor goat anti mouse 488 (1:1,000 dilution) as the secondary antibody. Shown are mean plaque areas of three independent experiments of all mutant viruses in comparison to plaque sizes of OH-03, set at 100 %. Statistical analysis was done by Kruskal-Wallis-test of independent samples and revealed no significant differences (p-value 0.062).

3.2.3. Single-step growth kinetics

To further assess any possible impairment in virus growth, single-step growth kinetics were conducted. Titers of cell-associated as well as cell-free viruses in the supernatant were determined at different timepoints after infection of RK13 cells. The various recombinant viruses all grew to titers in the same range as parental vOH-03 virus and no statistically significant differences could be revealed between the different viruses at any time p.i. (Figure 20 and 21).

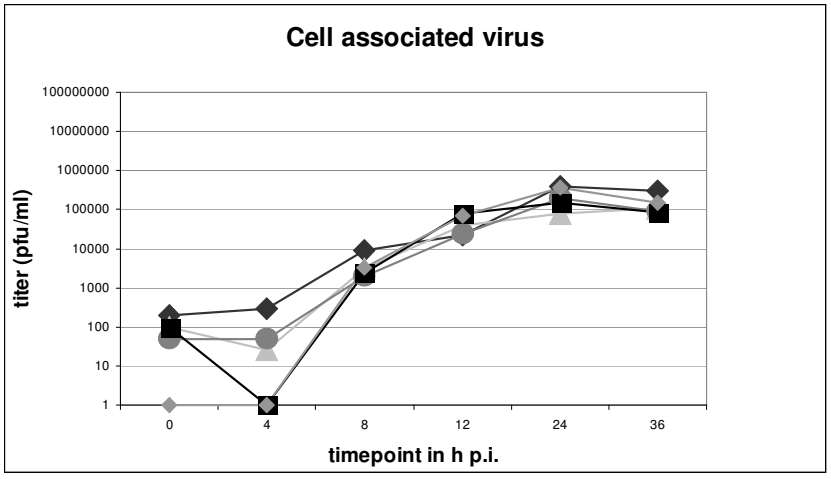

Figure 20: Single-step growth kinetics – cell associated virus. RK13 cells were infected at an moi of 3 and at the indicated time points, cells were collected by trypsinization. After three freeze-thaw cycles, cell-associated viral titers were determined by standard titration on RK13 cells. Statistical analysis was performed by analysis of Variance (ANOVA) followed by the Kruskal-Wallis-test of independent samples and revealed no significant differences.

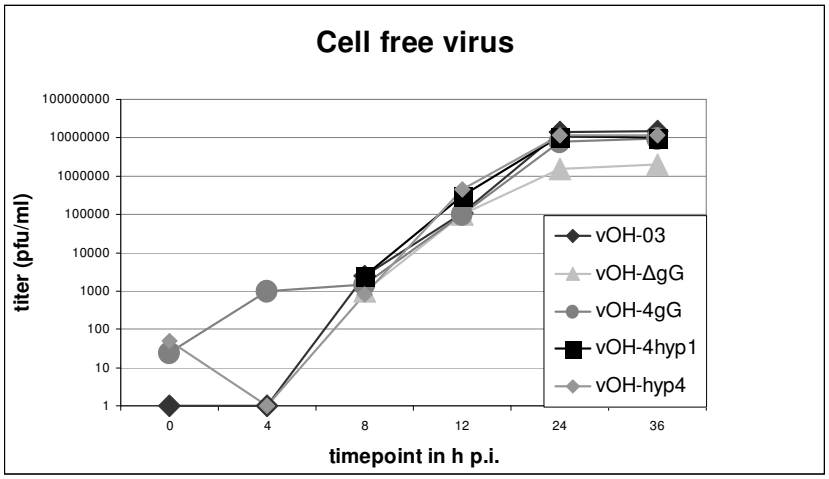

Figure 21: Single-step growth kinetics – cell free virus. RK13 cells were infected at an moi of 3, and at the indicated time points, supernatants were collected and frozen at -70°C. Cell-free virus titers were determined by standard titration on RK13 cells. Statistical analysis was performed by analysis of Variance (ANOVA) followed by the Kruskal-Wallis-test of independent samples and revealed no significant differences.

3.3. In vitro experiments

3.3.1. Chemotaxis assays

Glycoprotein G of EHV-1 strain RacL11 was previously shown to inhibit neutrophil chemotaxis in migration assays *in vitro* [48]. In the chemotaxis experiments employed in these studies, eIL-8 in the lower compartment of a transwell plate was added to attract the neutrophils placed in the upper compartment of the plate and, due to the chemotactic effect of the chemokines; neutrophils migrated through the 3 µm pore-size membrane into the lower compartment. To analyze the role of the constructed recombinant gGs in the OH-03 background with respect to neutrophil migration, the chemotaxis assays were carried out. Supernatants containing the various gGs expressed by the recombinant viruses were added to the lower compartment and migration of neutrophils from the upper compartment was examined in order to assess a potential of vCKBP activity of the secreted gGs. Binding of CKs would lead to a loss of the cytokine gradient for which reason a decrease in neutrophil migration is expected.

First, to adjust the optimal concentration of eIL-8 required to induce neutrophil migration from the upper compartment of the transwell plates, a chemotaxis assay was done using eIL-8 at concentrations of 25, 50 and 100 ng/ml. In the upper compartment, 100 µl of freshly isolated equine neutrophils were applied (containing $1x10^4$ cells in total). The percentages of migrated neutrophils in the presence of increasing eIL-8 concentrations did not differ and the lowest concentration of eIL-8 (25 ng/ ml) proved to efficiently induce migration of neutrophils (data not shown). Thus, all following experiments were carried out using an eIL-8 concentration of 25 ng /ml.

RK13 cells were infected with wild-type EHV-1 or the various recombinant viruses at an moi of 1. At 24 hours p.i., supernatants were collected and cleared of any remaining cell debris and virus particles by ultracentrifugation. Hence, only the role of the different gGs secreted from infected cells were investigated in this experiment. Equine IL-8 was pre-incubated with the supernatant containing the various gG proteins for 30 minutes before freshly isolated equine neutrophils were added to the upper compartment. Medium containing 2% FCS was used as negative control and eIL-8 without any gG as a positive control, respectively. After 45 minutes, the transwell plates were centrifuged to allow attachment of migrated cells to the wells before drying and staining with Modified Wrights´ stain. The number of migrated neutrophils was counted under a light microscope. In Figure 22, the means of migrated neutrophils (duplicates) per horse of a total of three different horses are shown. A clear difference can be seen between negative and positive controls for all three horses, although in the negative control a number of migrated cells could be detected as well. Mean numbers

of migrated neutrophils showed tendencies of differences between the wild-type vOH-03 and the recombinant viruses vOH-ΔgG and vOH-4gG. Supernatants from vOH-03 were able to interfere with chemotaxis most efficiently, while those collected from cells infected with the gG deletion virus or EHV-1 expressing EHV-4 gG did not reach the efficiency observed with parental EHV-1. However, in our experiments, the hypervariable region of EHV-1 gG (vOH-4hyp1) apparently was not sufficient to inhibit neutrophil migration, as even a higher number of cells was detected in the lower compartment with this gG variant when compared with vOH-hyp4 gG, where we had predicted that insertion of the hypervariable region of EHV-4 gG should lead to a failure in chemokine binding and, therefore, to higher numbers of migrating neutrophils. In spite of the trend of the inhibitory function noted for the vOH-03 supernatants, no statistically significant differences between the supernatants collected from cells infected with the various recombinant viruses could be determined here.

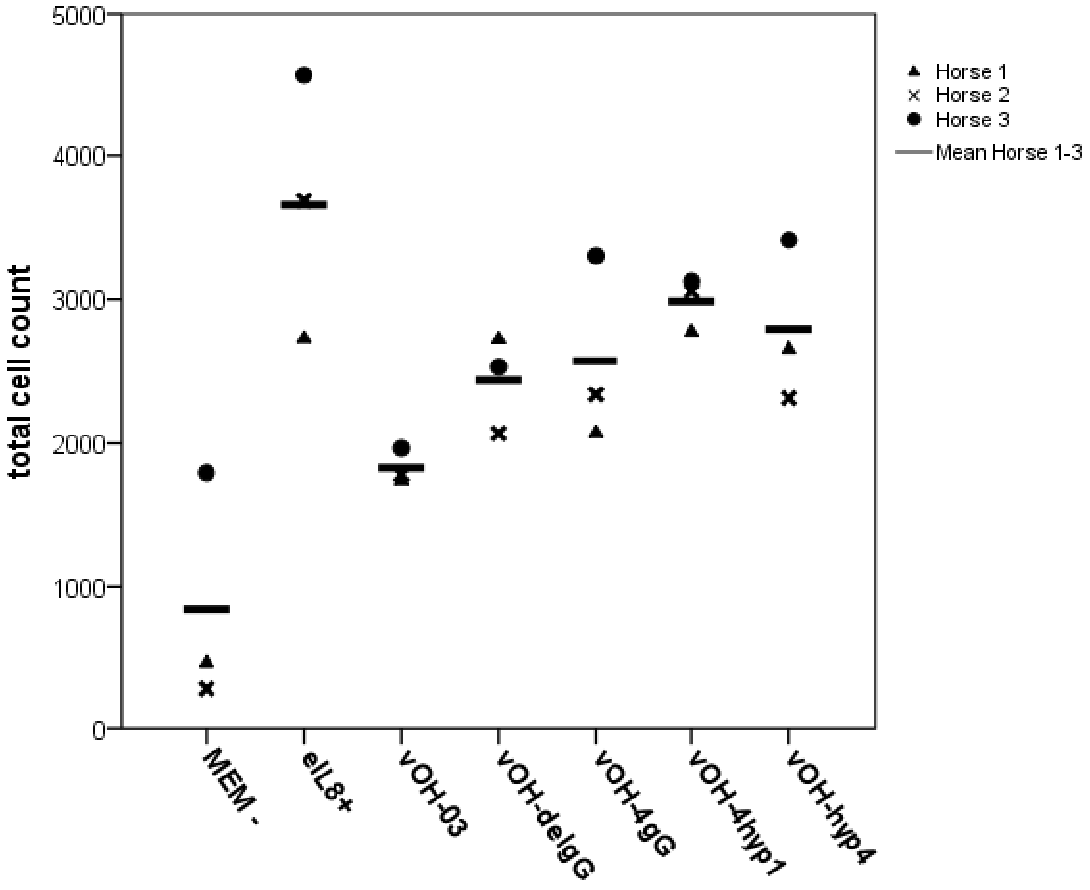

Figure 22: Chemotaxis assays analyzing eIL-8 induced migration of equine neutrophils in the presence of wild-type EHV-1 or recombinant gG, thus in presence or absence of predicted vCKBP activity. Supernatants of infected cells containing the various forms of gG were preincubated with eIL-8 for 30 min before equine neutrophils were added to the upper compartment and allowed to migrate to the lower compartment for 45 min. Migrated cells were stained with modified Wright´s stain and counted under a light microscope.

3.4. In vivo experiments

3.4.1. Mouse experiment I (Pilot experiment)

A preliminary experiment was done to obtain information on the optimal infectious dose for BALB/c mice used in this study and to account for differences in pathogenicity that were previously reported in work from Europe and USA. In these studies different infectious doses between 1 x 10^3 to 1 x 10^7 pfu per mouse were used and it had been suggested that differences in disease outcome might be dependent on different mouse strains [96].

a. Back titration of virus used for infection

Mice were infected with 2x10^5 pfu per mouse in 40µl MEM (5 x10^6 pfu / ml). Back titration of the virus dilutions used for infection was done by standard titration on RK13 cells and the following titers were determined:

OH-03:	2.7x10^6 pfu/ml
OH-03-delgG:	3.5x10^6 pfu/ml
OH-03-4gG:	5.5x10^6 pfu/ml
OH-03-4hyp1:	4.8x10^6 pfu/ml
OH-03-hyp4:	3.4x10^6 pfu/ml

b. Clinical examination

Prior to infection, mice were allowed to rest for one week to exclude any transport-induced stress influencing the infection experiments. Mice were infected intranasally with 2x10^5 pfu of vOH-03, vOH-ΔgG, vOH-4gG, vOH-4hyp1, vOH-hyp4 or MEM medium alone as control, respectively. Following infection, mice were observed daily for clinical signs of virus infection. On days 2 to 4 p.i. virus-infected mice showed signs of illness such as respiratory distress (dyspnea), crouching and ruffled fur. In contrast, no clinical signs could be observed in the control group at any time point p.i. After day 4 p.i., no evident clinical signs of infection were detectable in any of the groups.

c. Weight loss mice

Individual body weights of mice were determined immediately before and every day following infection at the same time of day to record disease related body weight loss. Shown in Figure 24 are the mean body weights of each group at the indicated time point. Three mice per group were sacrificed on days 2 and 4, respectively. Consequently, the means shown here include the body weights of 9 animals on day 2 p.i., 6 animals from days 2 to 4 p.i. and 3 animals from day 4 to the end of the experiment. In correlation with the observation of clinical signs of disease, a decrease of body weights up to 15 % could be detected as early as day 2

p.i. in all groups of mice infected with EHV-1 wild-type or recombinant viruses. In contrast, animals of the control group gained weight over the course of the experiment without any detectable reduction (Figure 23). In our experiment, mice infected with the gG-deletion virus (vOH-ΔgG) were noted to show the most abundant weight loss of all groups over the examined period in contrast to mice infected with the virus, where the hypervariable region of EHV-1 has been reinstalled (vOH-4gGhyp1), which lost the least weight. However, none of the weight losses were statistically significant when all groups were compared. All mice reached pre-infection weights latest at day 6 post infection.

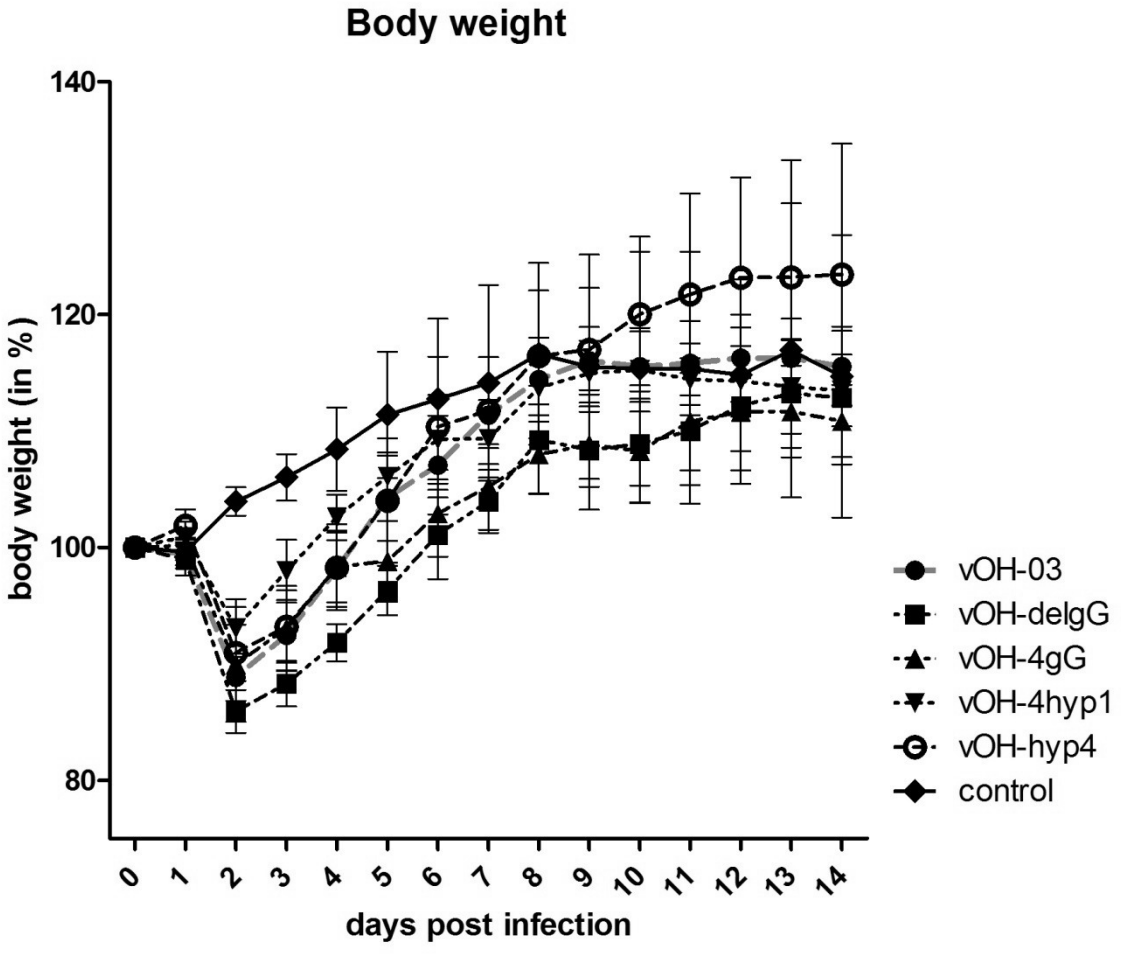

Figure 23: Mean body weight losses of infected and control mice. Nine mice per group were infected intranasal with $2x10^5$ pfu with vOH-03, vOH-ΔgG, vOH-4gG, vOH-4hyp1, vOH-hyp4 and MEM medium alone as control.

d. Virus titers in lungs

After infection, virus titers were determined in lung homogenates of mice on days 2 and 4 p.i. by standard titration on RK13 cells (Figure 24). According to previously published work [48, 53, 102], days 2 and 4 were chosen for detection of viral titers in lungs since titers were below the detection limit (10 pfu/lung) at later time points of the experiment. On day 2 p.i., viral titers in lungs reached from 10^4 up to 10^6 pfu/g lung tissue in mice infected with the various recombinant viruses whereas no virus could be detected in mock-infected mice on day 2 or day 4 p.i. Statistical analysis of the virus titers revealed no significant differences between the mouse groups infected with the different EHV-1 mutants on day 2 or day 4 p.i.

On day 4, virus load was generally decreased and ranged from 10^3 to 10^4 pfu/g lung tissue in lungs of infected mice, most likely due to the efficient clearance of the virus at the site of infection. Determination of virus titers in lungs obtained from mice on day 12 p.i. revealed no detectable virus loads (data not shown).

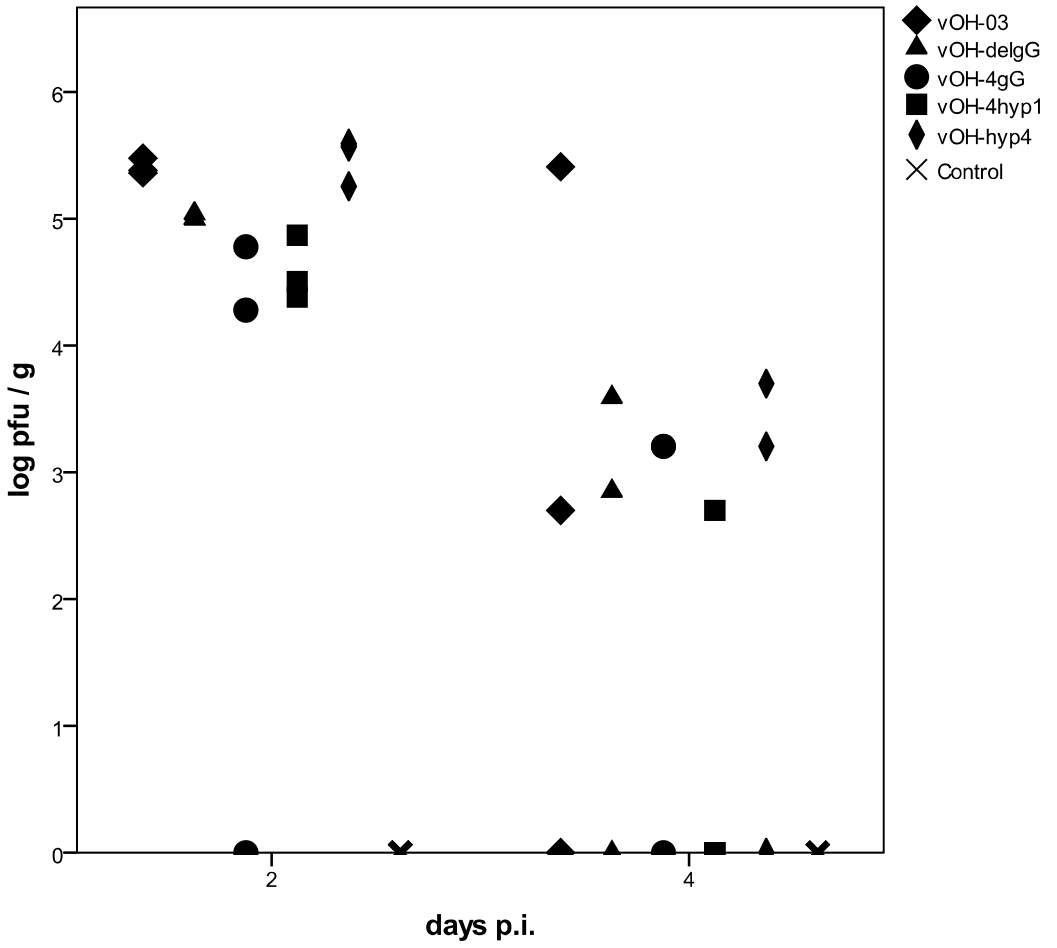

Figure 24: Virus titers in mice lungs on days 2 and 4. Mice were infected intranasally with vOH-03 (diamonds), vOH-ΔgG (triangles), vOH-4gG (dots), vOH-4hyp1 (squares), vOH-hyp4 (flat diamonds) and MEM medium alone (crosses). Three mice per each group were sacrificed on day 2 and 4 p.i., lungs were homogenated and viral titers were determined by standard titration on RK13 cells

e. Pathology

Lungs from sacrificed mice were prepared on days 2, 4 and 14 post infection. After removal, lungs were fixed in 4% formaldehyde, embedded in paraffin and sections were stained with hematoxylin-and-eosin (H&E) for histopathological examination.

Microscopical analysis of the lung sections revealed broncho-interstitial pneumonia in mice of all groups, except for the negative control group, on days 2 and 4 p.i. Detected alterations were often distributed in a multifocal fashion in the tissues. Lungs of mock-infected mice did not have pathological changes throughout the experiment.

On day 2 p.i., we found acute changes in the tissue architecture that are typical for virus infection including necrosis of the alveolar epithelia (Figure 25). Activated alveolar macrophages could be detected in the lumen of the alveoles. Perivascular inflammation consisted mostly of neutrophil granulocytes as well as lymphocytes. In the interstitial space, only few cellular infiltrates comprised of neutrophils, eosinophils, histiocytes and lymphocytes were observed.

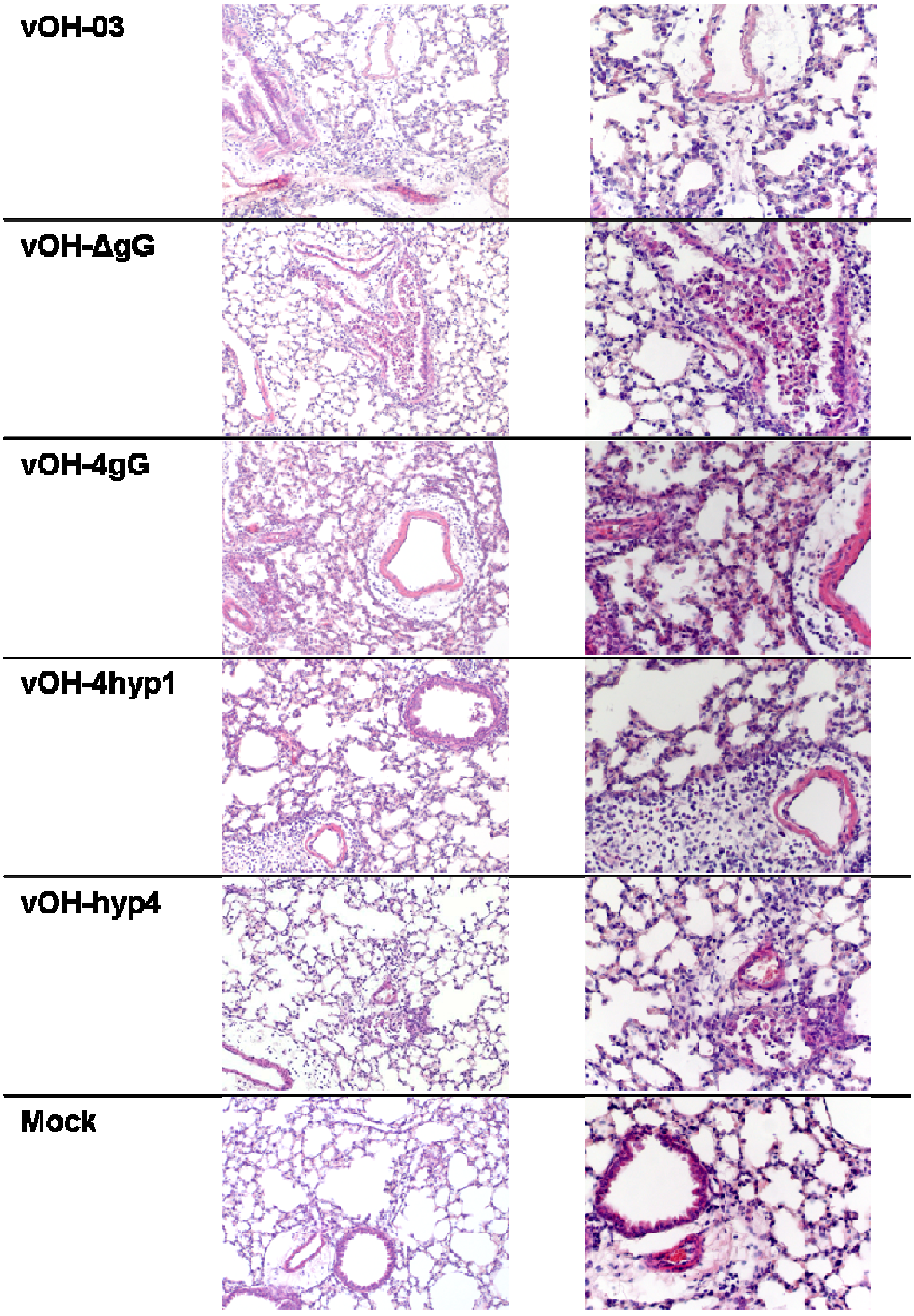

Figure 25: HE-stained sections of lung sections in 10X (left panels) and 20 X magnifications (right panels). Lungs were prepared from mice at day 2 after infection with vOH-03, vOH-ΔgG, vOH-4gG, vOH-4hyp1 or vOH-hyp4 or after mock infection.

On day 4 p.i., the quantity of infiltrating granulocytes and histiocytes in lungs of infected mice was decreasing in all cases, whereas only a mild increase of lymphocyte numbers was observed (Figure 26).

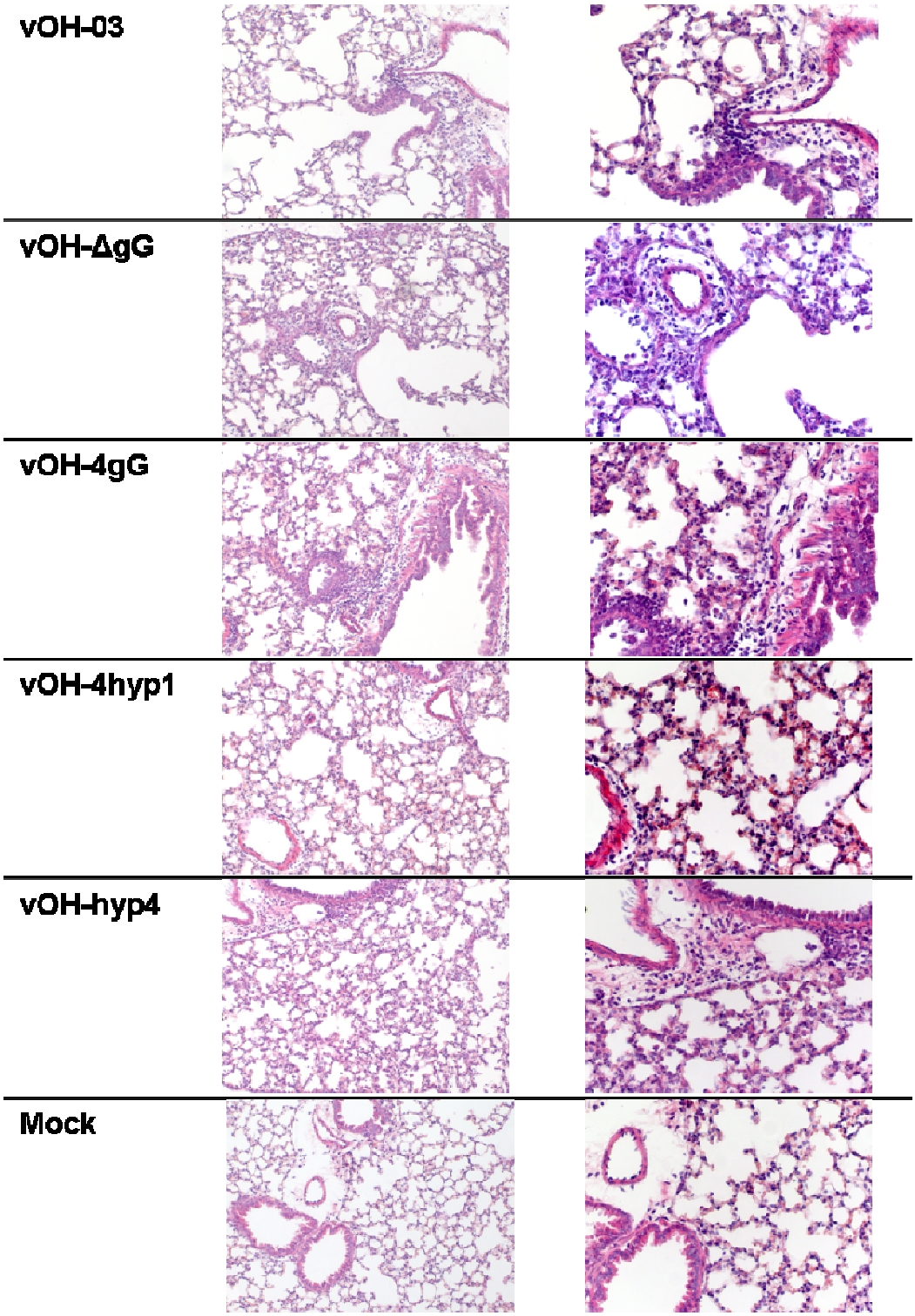

Figure 26: HE-stained sections of lung sections in 10X (left panels) and 20 X magnifications (right panels). Lungs were prepared from mice at day 4 after infection with vOH-03, vOH-ΔgG, vOH-4gG, vOH-4hyp1 or vOH-hyp4 or after mock infection.

On day 14 p.i., lung sections of mice infected with the various viruses were indistinguishable from those of the mock-infected group (Figure 27). Hence, full restitution of the lesions was observed.

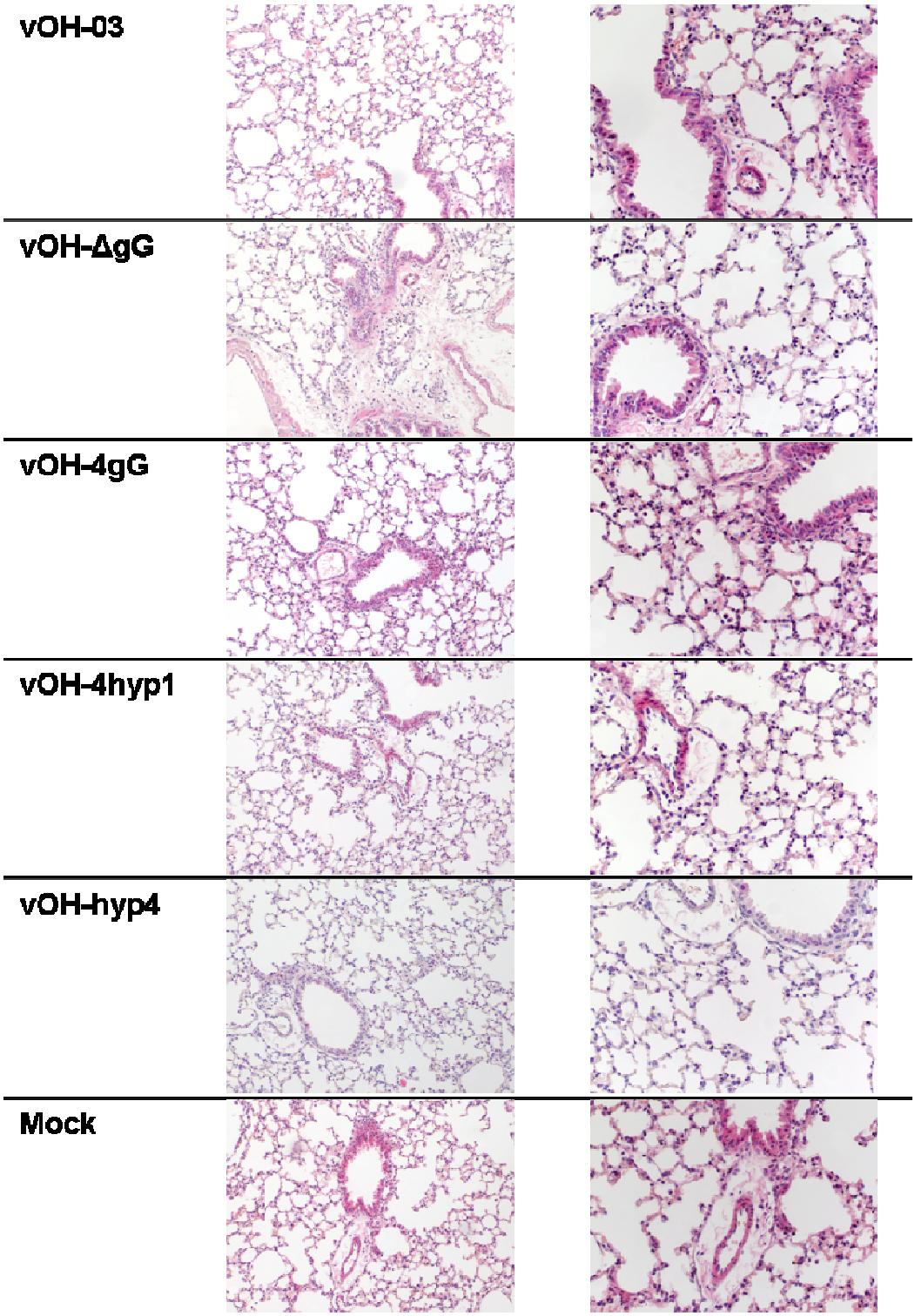

Figure 27: HE-stained sections of lung sections at a 10X magnification (left panels) and 20X magnification (right panels). Lungs were prepared from mice at day 14 after infection with vOH-03, vOH-ΔgG, vOH-4gG, vOH-4hyp1 or vOH-hyp4 or after mock infection.

Taken together, due to the multifocal distribution of inflammation within individual lung sections, no significant or clinically relevant difference of inflammation patterns in mice infected with the various gG recombinant viruses could be demonstrated in this study.

3.4.2. Mouse experiment II

Based on the results of the pilot experiment and previously published data [48], days 2 and 4 p.i. were chosen for investigating the influence of infection with the various recombinant EHV-1 viruses on pathogenicity in the mouse model. At later time points, the amount of cells required for appropriate flow cytometric analysis could not be obtained by pooling the bronchoalveolar lavages (BALs) of 3 mice. Also, viral loads in lungs were below the detection limit on all days after day 4 p.i.(data not shown).

a. Clinical examination

All mice were allowed to rest for one week before infection. In line with the pilot experiment, mice showed signs of respiratory distress after intranasal inoculation of the respective viruses lasting from day 2 to 4 p.i. These observations were in contrast to mock infected mice that did not show any clinical symptoms at any time of observation. Virus-infected mice were hunched, crouched together and their fur was ruffled. None of the infected mice died as a consequence of virus infection. By day 4 to 5 p.i., all mice had recovered and clinical signs of disease could no longer be observed. No difference in the clinical symptoms could be observed in mice infected with the different recombinant viruses.

b. Weight loss

Development of mean body weights of mice after infection was determined on the day of infection (day 0) up to day 4 p.i. BALB/c mice were infected intranasally with 2×10^5 pfu of the respective viruses per mouse. In contrast to the pilot experiment, clear weight loss was only observed in mice infected with vOH-4gG, vOH-4gGhyp1 and vOH-hyp4, respectively, whereas mice infected with vOH-03 wild type or the deletion mutant vOH-ΔgG did not lose any weight in this experiment (Figure 28).

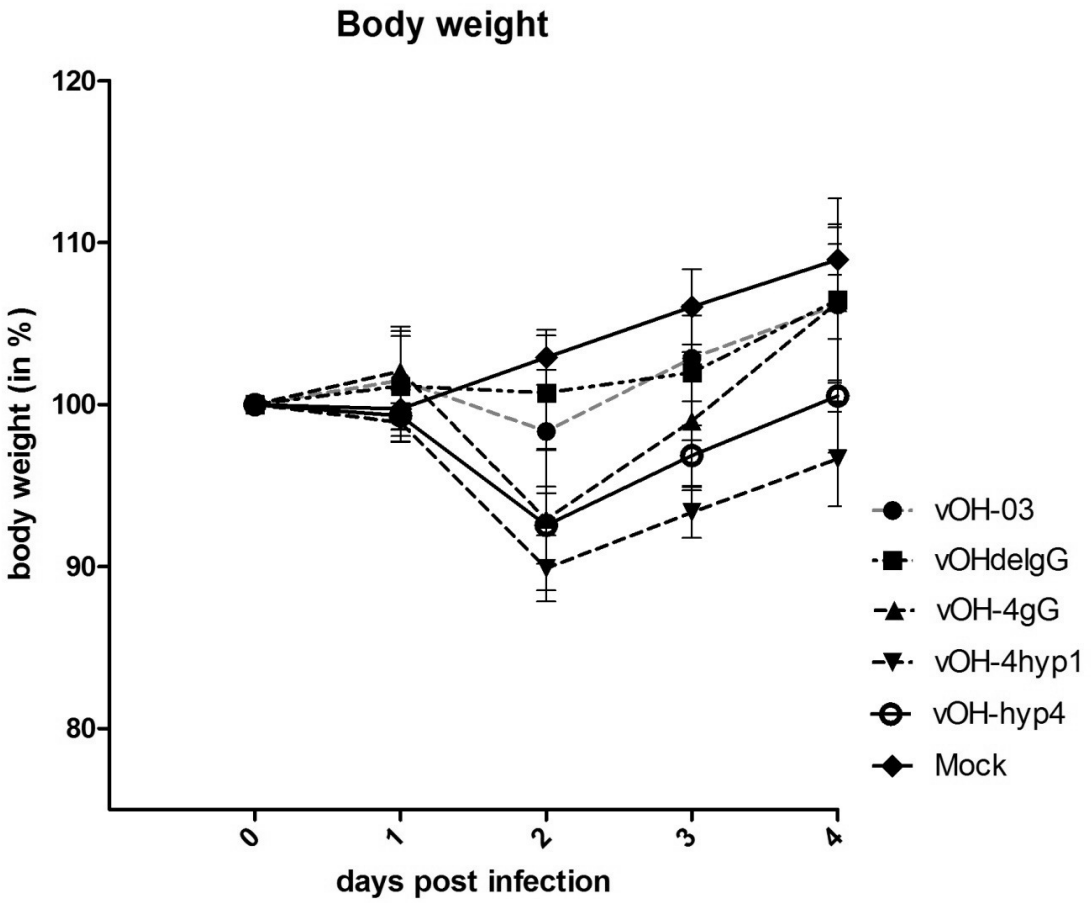

Figure 28: Summarized results of mean body weight loss of infected and mock-infected mice in two independent experiments (infection dose 2 x10^5 pfu in 40 µl). Mice were infected intranasally with vOH-03, vOH-ΔgG, vOH-4gG, vOH-4hyp1, vOH-hyp4 or medium as control. Percentages of mean body weights are shown from the day of infection (day 0) until the end of the experiment (day 4), results of days 1 and 2 represent means of weights of 12 mice, whereas results of day 3 and 4 are means of 6 mice.

c. Virus titers in lungs

Virus titers were determined in lungs of virus- and mock- infected mice on days 2 and 4 p.i. by standard titration on RK13 cells. The limit of detection was 10 pfu/g lung tissue. On day 2 p.i., viral titers between 10^4 and 10^5 pfu/g lung tissue were detectable in mice infected with the various recombinant viruses. In mock-infected mice, no virus could be detected on day 2 or 4 p.i. On day 4, virus load was generally decreased in all infected animals and ranged from 10^2 to 10^3 pfu/g lung tissue, probably as a consequence of efficient clearance of the virus at the site of infection. In this context, very efficient clearance of virus vOH-hyp4 led to no detectable virus in lungs on day 4 p.i.

Statistical analysis of the virus titers, however, revealed no difference of viral lung titers between the different mouse groups on day 2 or day 4 p.i.

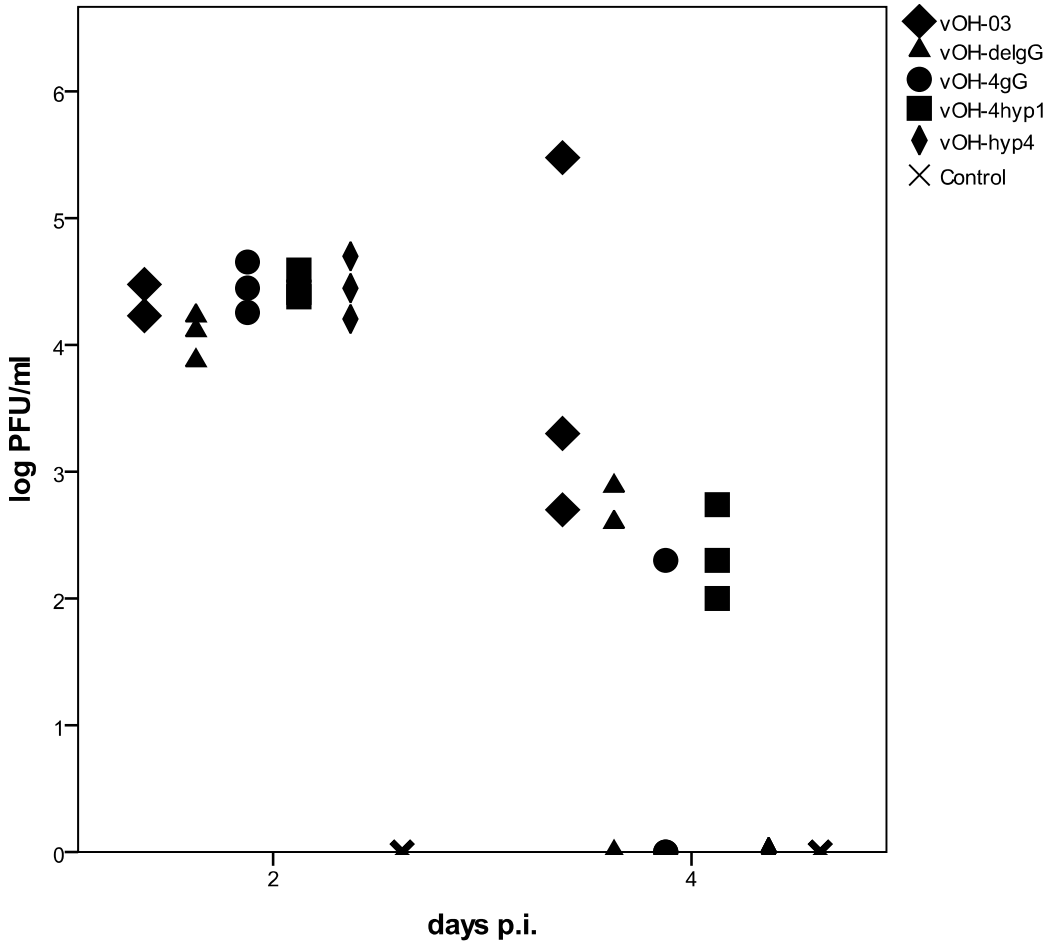

Figure 29: Virus titers in mice lungs on days 2 and 4 p.i. Mice were infected intranasally with vOH-03 (rhombs), vOH-ΔgG (triangles), vOH-4gG (dots), vOH-4hyp1 (squares), vOH-hyp4 (flat rhombs) or MEM (crosses). Three mice per each group were sacrificed on days 2 and 4 p.i., lungs were homogenized, and viral titers were determined by standard titration on RK13 cells.

d. FACS analyses

Bronchoalveolar lavages (BALs), collected from 3 mice per group on day 2 and day 4 after infection, were pooled and the composition of immune cells was analyzed by flow cytometry. We used fluorescently labeled rat-anti mouse monoclonal antibodies against surface markers of neutrophils (Gr-1+-APC), macrophages (F4/80-FITC), B (B220-APC) and T lymphocytes (CD3-FITC). The BALs consisted of a very heterogeneous cell population including granulocytes, lymphocytes as well as some erythrocytes, so an oval-shaped gate was set to focus on the cell population presumably comprising the cells of interest and to sort out cellular debris by size (Figure 30).

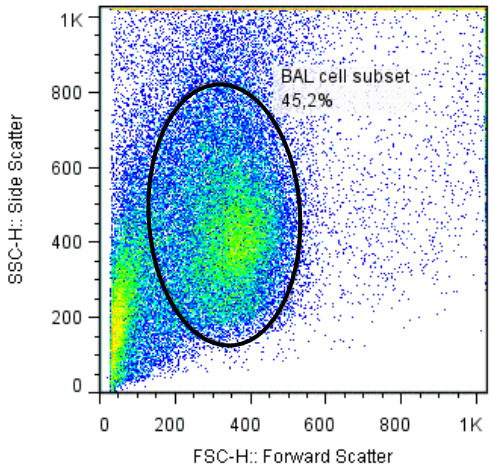

Figure 30: Dot blot of BAL cells and gating of heterogeneous BAL cell population including leukocytes.

First, unstained BAL cells obtained on day 2 after infection were measured for each group (Figure 31, red line). In addition, isotype controls with rat IgG2b-APC for neutrophil staining, rat IgG2bK-FITC for macrophage staining, rat IgG2a-APC for the B-lymphocyte staining and rat IgG2aK-FITC for the T-lymphocytes were performed (Figure 31, blue line). An example of a histogram for a positive staining of each cell type is also shown in Figure 31 (orange line), where primary and secondary antibodies were added to the samples.

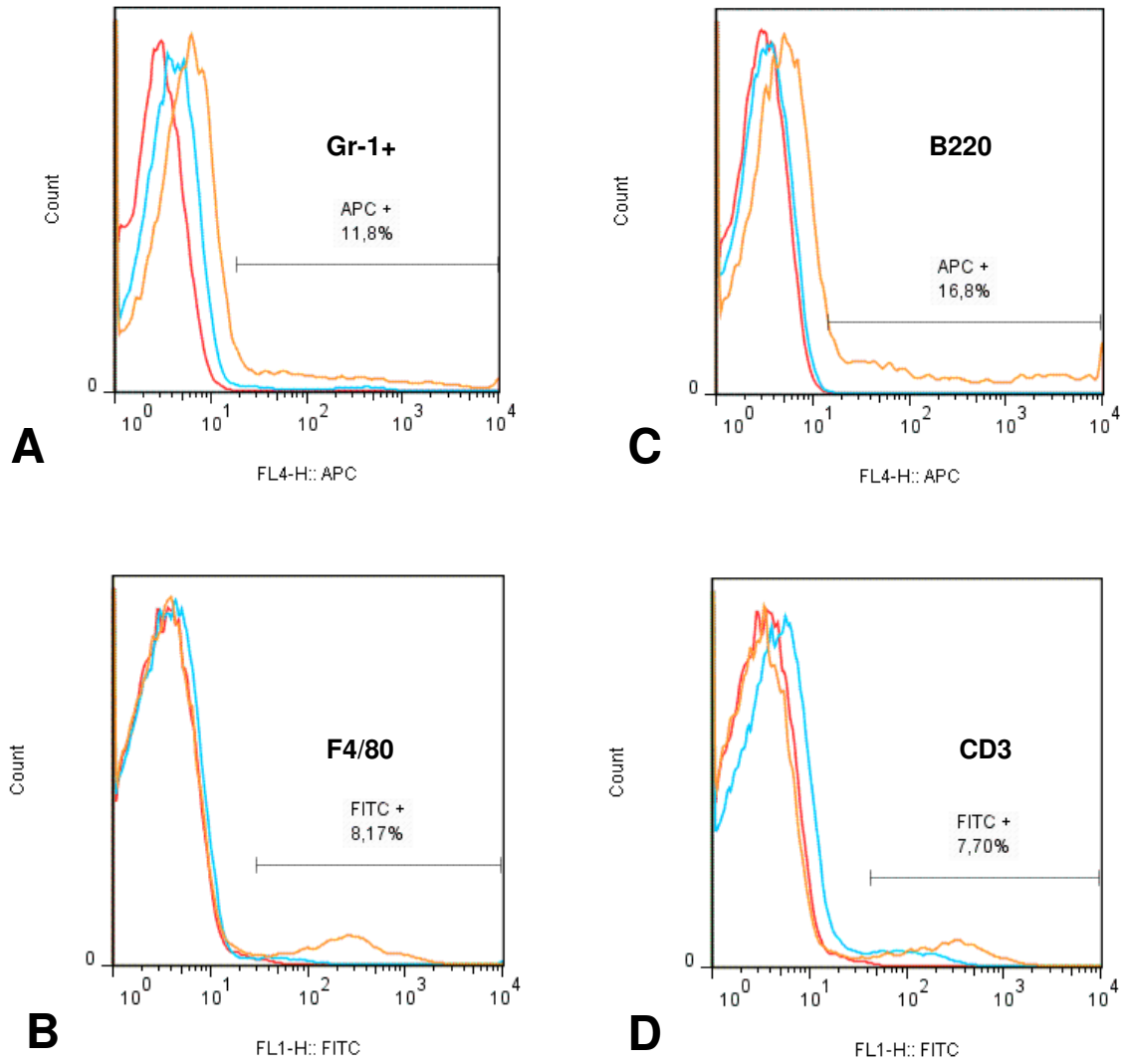

Figure 31: Flow cytometric analysis of BAL cells stained with fluorescently labeled rat-anti mouse monoclonal antibodies against surface markers of (A) neutrophils (Gr-1+-APC), (B) macrophages (F4/80-FITC), (C) B lymphocytes (B220-APC) and (D) T lymphocytes (CD3-FITC). Shown here are examples of unstained cells (red line), isotype controls (blue lines) and cells stained with the respective primary and secondary antibodies (orange line).

In Figure 32, the mean percentages of leukocyte subpopulations on days 2 and 4 p.i. are depicted as bar diagrams. Combined here are the results of two independent animal experiments. In each experiment, 3 mice per group were sacrificed on day 2 or 4 p.i. BALs were taken, pooled and flow cytometric analysis was accomplished as described.

On day 2 p.i., the percentage of neutrophils in BALs of infected mice was generally increased when compared to the mock-infected control group (0.9%) (Figure 32, A). The percentages of neutrophils reached up to 24 % in BALs of mice infected with vOH-4gG, whereas only a slight increase up to 9.9 % could be detected in mice infected with the deletion mutant. The result

for the deletion mutant was close to that obtained for the vOH-03 wild-type infected mice in which up to 8.7 % of the BAL cells were positive for the neutrophil marker. Mice infected with vOH-4hyp1 showed a total percentage of 12.3 % of neutrophils in the BAL, whereas in BAL of mice infected with the vOH-hyp4 virus a low percentage (6.9 %) of neutrophils could be detected on day 2 p.i.

On day 4 p.i. neutrophil percentages were decreased in BALs of all infected mice, irrespective of the virus strain. Values ranged between 1% (vOH-hyp4) and 2.5% (vOH-4gG). The neutrophil percentage in BALs of the control group decreased to 0.2 % (Figure 32, B).

The percentages of macrophages in BALs of infected mice were also increased in comparison to the control group (0.4 %), but did not exceed 6.5 % detected for the vOH-4gG infected mice groups on day 2 post infection. In wild-type (vOH-03) infected mice no more than 5 % of cells positive for macrophages were detectable whilst all other groups (vOH-ΔgG, vOH-4hyp1 and vOH-hyp4) only showed 2 to 3.5 % of the BAL cells positive in the macrophage staining (Figure 32, C)

On day 4 p.i., the percentages of macrophages in BAL ranged between 0.5 % and 4 % and no difference between animals from the different groups was evident (Figure 32, D).

Percentages of B-lymphocytes were clearly increased at day 2 p.i. Still lowest numbers could be counted for the control group with 5.5 % next to vOH-hyp4 with 8.4%, mounting up to 22 % for mice infected with vOH-4gG. Wild-type infected mice in contrast ranged in between at 12 % as well as vOH-ΔgG with 13 % and vOH-4hyp1 showing 15 % positive in the macrophage staining (Figure 32, E).

Percentages of B-lymphocytes remained at higher percentages even at day 4 p.i. ranging between 4 % (Control group) and 11 % (vOH-4hyp1) (Figure 32, F).

The total T-lymphocyte percentages in BAL of infected mice were increased up to 5 % (vOH-03) at day 2 p.i. in contrast to the mock-infected mice where the percentage of T-lymphocytes was below 0,5 % (Figure 32, G). On day 4 p.i. the percentages of T-lymphocytes detectable did not exceed 2.5 % (Figure 32, H).

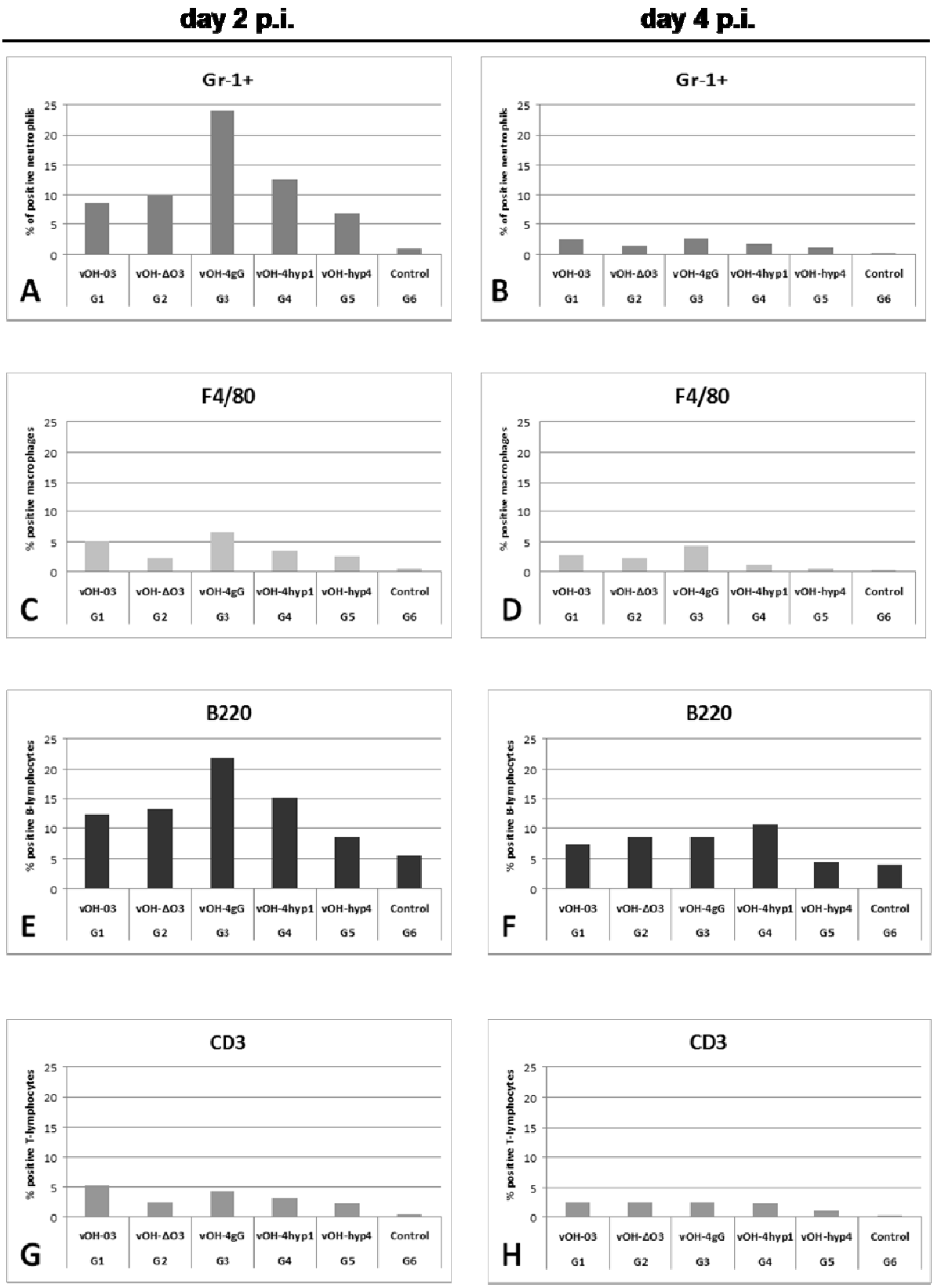

Figure 32: Flow cytometric analysis of BAL cells of mice recovered on day 2 p.i. (left panel) and 4 p.i. (right panel). BALs of 3 mice per group were pooled on each day in two independent experiments. Shown here is the mean percentage of cells positive for the indicated marker from two independent experiments.

e. Cytospins

For comparison with the flow cytometry data, cytospins of the BALs were prepared and analyzed in addition to FACS analyses on day 2 p.i. in one experiment. Stained slides were evaluated by light microscopy after the manipulation. Here, macrophages and neutrophils could be identified as the predominating cell types in cytospins of BALs of mice infected with the various viruses. In mock-infected mice, the total cell count was clearly decreased and primarily macrophages were represented. For mice infected with vOH-4gG, neutrophil percentages reached more than 30% in contrast to vOH-03 wild type infected mice, where not more than 12 % of neutrophils could be seen. The gG deletion virus gave intermediate values and neutrophils represented approximately 17 % of the total cell count. The relative number of neutrophils found in BAL cytospins of mice infected with vOH-4hyp1 remained low at 7 % and BAL of vOH-hyp4 infected mice did not exceed 10 % (Figure 33).

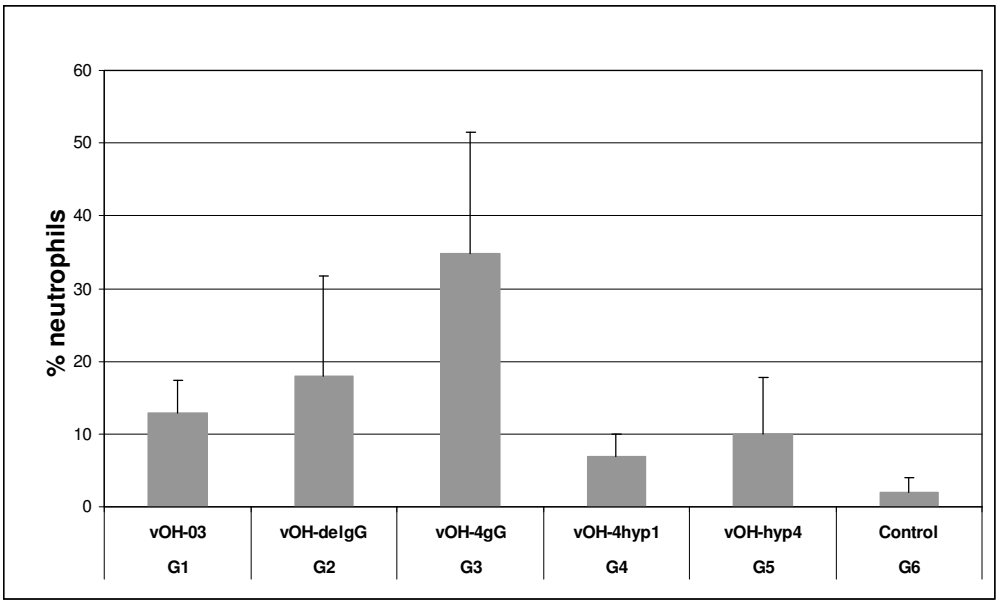

Figure 33: Cytospin of BAL cells of mice infected with vOH-03 (G1), vOH-delgG (G2), vOH-4gG (G3), vOH-4hyp1 (G4), vOH-hyp4 (G5) or MEM alone (G6) at day 2 post infection. Cytospins were photographed; total cells were counted on 10 fields of view and set at 100 %. Total amount of neutrophils were counted and the percentages were calculated in correlation with the total cell count. Shown here are the percentages of neutrophils of one experiment.

4. Discussion

In this study, the role of glycoprotein G of a recently isolated EHV-1 neurovirulent strain (OH-03) [100] and an EHV-4 strain (KT-4) [113] in immune evasion was examined. More specifically, the contribution of the hypervariable region of gG to the protein´s function was adressed *in vitro* as well as in a murine EHV-1 infection model *in vivo*. Previous studies had already investigated the role of gG and its respective hypervariable region with respect to chemokine binding in a different EHV-1 strain (RacL11). Those studies had shown *in vitro* by ELISA that the hypervariable region in fact was able to bind to equine chemokines and therefore contributes to viral immune evasion of RacL11, an EHV-1 strain isolated in the 1950's from an aborted foal [48, 53, 55]. Due to recent outbreaks of EHV-1 neurological disease especially in the United States of America, we focused in this study on a more currently isolated strain, OH-03, obtained from a fatal case of equine herpesvirus myeloencephalopathy (EHM) in Ohio in 2003 [100].

4.1. Characterization of mutant viruses

In this study, the EHV-1 strain OH-03, previously cloned as a bacterial artificial chromosome [66], was used as a backbone to create a set of gG mutants including a null mutant (vOH03ΔgG), a mutant in which EHV-4 gG was inserted in lieu of authentic EHV-1 gG (vOH03-4gG), a mutant harboring EHV-4 gG substituted with the hypervariable region of EHV-1 gG (vOH03-4gGhyp1) and a mutant harboring the hypervariable region of EHV-4 gG in EHV-1 gG.

First, to reveal any contribution of gG and its various mutant forms towards the replication capacity of the virus *in vitro,* plaque size assays as well as single-step-growth-kinetics were conducted. The cytopathic effects of parental wild-type EHV-1 were compared to the constructed mutant viruses by infecting RK13 cells and subsequent staining of plaques with an anti-gM antibody. All viruses induced morphologically similar plaques, which did not significantly differ in size. Also, single-step-growth-kinetics did not reveal any differences in viral titers between the different viruses at any time point after infection. All viruses reached very similar end-point titers as shown for cell-free or cell-associated viruses. This set of experiments could thus confirm the results of a previously conducted study by von Einem et al. on a gG-deletion virus of EHV-1 strain RacL11. This study revealed that gG is not essential for EHV-1 replication *in vitro* [53]. In BHV-1, another alphaherpesvirus affecting cattle and close relative of EHV-1, deletion of gG also did not alter viral growth in cell culture

but appeared to be required for efficient cell-to-cell spread, as reduced plaque sizes could be shown *in vitro* [33, 34]. Various authors have shown that gG is also dispensable for growth of yet another member of the *Varicellovirus* genus, PRV in cell culture [34, 114, 115]. Similar to the situation for EHV-1, determinations of *in vitro* growth kinetics of an ILTV gG deletion virus did not reveal any significant differences either, when compared to wild-type virus [116].

In order to examine the influence of the various gG proteins in terms of inhibition of the migration of neutrophils *in vitro*, chemotaxis assays were performed. A previous study by Van de Walle and colleagues showed that gG of EHV-1 strain RacL11 as well as gG of a revertant virus, where gG was reintroduced after initial deletion in RacL11, were able to significantly decrease neutrophil chemotaxis. In contrast, a gG deletion mutant was shown to be unable to inhibit chemotaxis [48]. In addition it was demonstrated, that gG of EHV-4 strain VLS 829 was not able to interfere with neutrophil chemotaxis [48].

In our study, the various gG mutant viruses created in the background of EHV-1 strain OH-03 were also tested for their potential influence on neutrophil chemotaxis following stimulation by the neutrophil chemoattractant eIL-8 [48]. For this purpose, neutrophils of three independent horses with no history of EHV-1 or EHV-4 infection were isolated and used for a migration assay in duplicates. Evaluation of neutrophil migration in presence or absence of gG showed a clear inhibition of neutrophil migration in presence of wild-type OH-03 gG, which we had surmised functions as a vCKBP. That function of gG, as outlined above, was already shown in a previous study by Van de Walle and coworkers: EHV-1 strain RacL11 could inhibit neutrophil migration by up to 40% [48]. The inhibition observed here was in clear contrast to neutrophil migration in response to the chemoattractant alone, which was used as a positive control. When eIL-8 alone was added to the lower compartment, at least twice as many cells were noted to migrate into this area. Slightly more cells were noted to migrate to the lower compartment when gG was absent from the virus (vOH-ΔgG) or when EHV-1 gG specified the hypervariable region of EHV-4 gG (vOH-4gG), i.e. in absence of the proposed chemokine-binding region. Such a missing effect on chemotaxis had been reported for EHV-4 gG and we therefore expected a similar behavior of the OH-03 variant expressing EHV-4 gG instead of authentic EHV-1 gG [48]. However, we did not observe in the experiments conducted here unaltered neutrophil migration of nearly 100%, as it was previously seen for the EHV-1 RacL11 gG deletion mutant [48]. Also, reinsertion of the hypervariable region of EHV-1 gG into EHV-4 gG (vOH-4hyp1) did not fully restore the ability of gG chemokine binding, which had been expected. Rather, the influx of neutrophils in response to this mutant was even higher as for the deletion mutant. Furthermore, insertion of the hypervariable region of EHV-4 gG into its EHV-1 counterpart did not lead to the predicted complete loss of chemokine-binding function of gG encoded by the mutant virus. These results therefore

suggest that additional parts of gG could be of importance during chemokine binding. They also suggest that the hypervariable region does not exclusively determine binding to chemokines, thereby influencing neutrophil chemotaxis. However, as only three different horses were tested in our study and none of the results showed a statistically significant difference, our results should be corroborated or refuted by testing more neutrophils from blood samples of different horses in chemotaxis assays. In this regard, it could also be of interest to evaluate if previous vaccination against either EHV-1, EHV-4 or both will have any influence on the ability of neutrophils to migrate in response to the presence or absence of various forms gG.

A sensitive *in vitro* test to further elucidate the function of gG as a vCKBP would be an ELISA, which we were unable to perform in this study due to time constraints. With this technique, Van de Walle et al. could determine that amino acids 301 to 340 comprising the hypervariable region of RacL11 gG represent the important domain of gG that confers binding to chemokines of equine origin [55]. For our purposes, the plate would be coated with eIL-8, followed by incubation with supernatants containing the different gGs or medium alone (negative control). If binding of the various gG's to the eIL-8 occurred, the first antibody (rat-anti EHV-1 or rat-anti EHV-4 hypervariable region) should specifically bind to the gG bound to the chemokine coated to the bottom of the plate. Secondary antibody donkey-anti rat coupled with horse radish peroxidase would then bind to the primary antibody and react with the substrate to result in a change of color. The intensity of the color could be determined with an ELISA reader and give us more information of chemokine-gG interactions.

Also, to more specifically determine where the actual binding of chemokines occurs, structural analysis of the gG protein in complex with a chemokine would be of major interest. Crystal structure determinations were already done for the M3 vCKBP encoded by murine gammaherpesvirus-68. The analyses demonstrated that the protein forms a homodimer with two chemokines bound at its distal ends [117].

Taken together, our data reported here suggests that either the hypervariable region alone is not responsible for binding to chemokines or that, by exchanging the hypervariable regions in the gG protein, differences in protein modification or folding might have occurred, which altered the ability of gG for proper binding to chemokines.

4.2. In vivo experiments

The pilot experiment with our generated mutant viruses was carried out in order to establish the murine respiratory model with BALB/c mice in the laboratory in Berlin and to evaluate if the chosen infectious dose of 1 x 10^5 pfu per mouse was in fact sufficient for inducing infection in the respiratory tract of mice. Additionally, due to differences in the pathogenicity of various EHV-1 strains, this experiment should prove if the chosen EHV-1 strain OH-03 is capable of inducing infection in mice at all. In a second mouse experiment we focused on determining the different subsets of immune cells detectable in the BALs of mice infected with the different EHV-1 gG mutant viruses by flow cytometric analyses.

Previous infection experiments with EHV-1 RacL11 and RacL11 gG deletion mutants in BALB/c mice conducted by von Einem and Van de Walle, where infectious doses of 1 x 10^5 and 4 x 10^4 pfu were applied per mouse, demonstrated that mice lost up to 17% of their body weight after infection with the gG deletion virus (vL11ΔgG) and did not gain preinfection weights before day 8 [48, 53]. A statistically significant difference in weight loss of mice infected with RacL11 gG deletion virus in contrast to RacL11 with gG restored was noted by Van de Walle on day 3 post infection [48].

For our study, an infectious dose of 1 x 10^5 pfu per mouse was chosen, as our general interest focused on the functions of gG and its different mutated forms more than on the impact of different infectious doses.

Consistent with the data of previous studies, all mice in our pilot experiment infected with OH-03 mutant viruses lost weight at day 2 p.i. and, following the decrease, gained weight more slowly when compared to the control group. Mice infected with the gG deletion virus also lost weight up to 15 % on day 2 after infection. However, in a second animal experiment, weight loss was not so dramatic and only mice infected with vOH-4gGhyp1 lost weight up to 10 %. The remaining groups of mice infected with vOH-03 wild-type virus and the other mutants only minimally lost weight and their weight curves almost paralleled those of the uninfected control mice.

Histopathological analysis of the lungs clearly showed, however, that viral infection had occurred, but due to the multifocal distribution of the lesions, no clear differences in the infection pattern could be detected between any of the mutated viruses. This outcome is in contrast to the results of some dose response experiments conducted by von Einem and colleagues, where mice infected with 1 x 10^3 or 1 x 10^4 pfu per animal showed a significant reduction in their inflammatory response when infected with the parental RacL11 strain in comparison with the gG deletion mutant [53].

However, when an infectious dose of 1 x 10^5 pfu, the virus concentration chosen for this study, was applied, no difference in the inflammatory response could be noted in these experiments as well [53]. This implies a dosage-dependent effect of gG. It is worth mentioning that it was already noted by these authors that, if lower doses of EHV-1 gG deletion virus were used for infection, a significant increase in pathogenicity occurred [53]. Virus titers in lungs of infected mice determined in our experiments ranged between 10^4 and 10^5 pfu/g lung tissue at day 2 p.i. and remained generally lower in contrast to previously conducted experiments, which might be consistent with our findings that weight reduction did not appear to an extent seen in previous studies [53]. Less pronounced weight loss might correlate with a lower replication rate of the viruses in the respiratory tract leading to a less severe inflammation at the site of infection.

Flow cytometric analyses were performed to determine the composition of immune cells in BALs of mice infected with the various gG mutant viruses on day 2 and 4 after infection. BALs were obtained, and the cells contained in the washes were stained with antibodies detecting neutrophils, macrophages, B- or T lymphocytes. Percentages of the respective cell types were determined. Our analyses showed that all cell types generally remained lower on day 4 p.i. and no statistically significant differences could be detected between the groups of mice infected with the various viruses. In contrast, on day 2 p.i., some tendencies towards differences could be noted with respect to the influx of neutrophils into the lung between groups infected with wild-type virus, the gG deletion mutant and the mutant virus containing EHV-4 gG. The percentage of neutrophils in mice infected with EHV-4gG inserted instead of authentic EHV-1 gG (vOH-4gG) reached up to 24 %, whereas in mice infected with the gG deletion mutant (vOH-ΔgG), neutrophil percentages only slightly increased to 9.9 % when compared with wild-type infected mice for which 8.7 % neutrophils in BALs were determined. The results led us to conclude that insertion of EHV-4 gG instead of its EHV-1 counterpart results in the *de facto* loss of gG's ability to bind to chemokines. The same effect was expected for the gG deletion virus, where the result did not clearly show the absence of vCKBP activity but neutrophil counts remained higher than in BALs of wild-type infected mice. The same trend as with flow cytometry was noted with cytospins of the BALs, which were prepared at day 2 p.i. in one experiment. Here, the largest influx of neutrophils was also determined for mice infected with the vOH-4gG virus, followed by the gG deletion virus and the virus harboring the EHV-4 hypervariable region in an otherwise EHV-1 gG (vOH-hyp4). The results of the cytospin by and large yielded the expected outcome, but, as cells are counted by eye in this method, the flow cytometric analyses results should eventually be more objective and hence, reliable.

Interestingly, complete absence of gG or of its vCKBP properties, i.e. when EHV-4 gG was inserted into EHV-1, seems to have some influence on the B lymphocyte migration, too. The highest percentage of B-lymphocytes in BALs was determined for mice infected with vOH-4gG, correlating with the highest number of migrating neutrophils that were also detected in this group. Similar to the situation with the neutrophil counts, this group is followed by mice infected with the gG deletion virus, where still more than 12 % of B lymphocytes were determined in the BALs, shortly followed by the group infected with the OH-03 wild-type virus.

The flow cytometric results obtained here differ from those derived from a study conducted by Van de Walle et al., where the percentage of positive neutrophils in BALs of mice infected with the gG deletion virus (vL11ΔgG) reached up to 24 % in contrast to wild-type infected mice which showed only 11% of cells staining positive for the neutrophil marker [48]. In the same experiment, we tested here two mutants in which the hypervariable region of EHV-1 and EHV-4 gG, expected to function as the chemokine-binding region in EHV-1, was exchanged. As already seen in the chemotaxis assays, the hypervariable region of EHV-1 gG (vOH-4hyp1) alone apparently was not sufficient to inhibit neutrophil migration in BALs in our experiments as a higher number of neutrophils was measurable when compared with vOH-03ΔgG. Insertion of the hypervariable region of EHV-4 gG into the EHV-1 gG backbone, should lead to a failure of the resulting mutant virus with respect to binding to chemokines and therefore to migration of neutrophils in higher numbers. However, the mutant induced an inhibition of neutrophil migration that was comparable to that of parental EHV-1. Hence inhibition of neutrophil chemotaxis occurred even in the absence of the putative binding domain.

Taken together, our findings suggest that EHV-1 gG might not only influence neutrophil migration, but also influences other immune cells like B lymphocytes. In addition, the hypervariable region does not seem to exclusively determine the immunomodulatory potential of gG of EHV-1 strain OH-03. The immunomodulatory capacity may also be dependent on other protein modifications or protein folding, which seems to be of importance for proper functioning of gG as a vCKBP.

It is important, however, to take into account that there might be some differences in the BALB/c mouse strains regarding susceptibility to EHV-1 infection in Europe and USA, even if they are genetically the same. In addition, various EHV-1 strains differ in pathogenicity - all previous work by von Einem et al. and Van de Walle et al. related to gG was done in the background of RacL11.

Therefore, it would be very interesting to construct the recombinant viruses presented here with exchanged gGs or exchanged hypervariable regions in other neurovirulent and non-neurovirulent EHV-1 strains such as RacL11, Ab4, KyA and to further test the ability of all mutated gGs in binding assays (ELISA) as well as their ability to inhibit chemotaxis of neutrophils.

Also, some limitations of this study are based on the fact that all our *in vivo* experiments were performed in mice, which are not the natural host of EHV-1 infection. Therefore, the model might have some serious limitations, e.g., there is no spread from animal to animal and the system of mice clearly differs from that of horses. In conclusion, the mouse model does not reflect natural EHV-1 infection and can at best provide a first reference point of the pathogenesis of the virus as well as defense mechanisms of the “host”. Only data obtained by testing viruses and their mutants in the natural host, the horse, will allow conclusions on how viruses manage to evade the immune system and which mechanisms the host tries to use in defending the virus.

5. References

1. Frederick A. Murphy, E.P.J.G., Marian C. Horzinek, Michael J. Studdert *Herpesviridae*, in *Veterinary Virology, Third Edition (Hardcover)*1999 Academic press. p. 301 - 325.

2. Philip E. Pellett, B.R., *Fields Virology 5th edition*, in *Fields Virology Fifth Edition*, H.P. Edited by: Knipe DM, Editor 2007 Philadelphia: Lippincott Williams & Wilkins. p. 2479 - 2497.

3. McGeoch, D.J., F.J. Rixon, and A.J. Davison, *Topics in herpesvirus genomics and evolution.* Virus Res, 2006. **117**(1): p. 90-104.

4. Roizman, B., et al., *The family Herpesviridae: an update. The Herpesvirus Study Group of the International Committee on Taxonomy of Viruses.* Arch Virol, 1992. **123**(3-4): p. 425-49.

5. Schrenzel, M.D., et al., *New hosts for equine herpesvirus 9.* Emerg Infect Dis, 2008. **14**(10): p. 1616-9.

6. Telford, E.A., et al., *The DNA sequence of equine herpesvirus-4.* J Gen Virol, 1998. **79 (Pt 5)**: p. 1197-203.

7. Studdert, M.J., T. Simpson, and B. Roizman, *Differentiation of respiratory and abortigenic isolates of equine herpesvirus 1 by restriction endonucleases.* Science, 1981. **214**(4520): p. 562-4.

8. Telford, E.A., et al., *The DNA sequence of equine herpesvirus-1.* Virology, 1992. **189**(1): p. 304-16.

9. Holden, V.R., et al., *The IR3 gene of equine herpesvirus type 1: a unique gene regulated by sequences within the intron of the immediate-early gene.* DNA Seq, 1992. **3**(3): p. 143-52.

10. Crabb, B.S. and M.J. Studdert, *Epitopes of glycoprotein G of equine herpesviruses 4 and 1 located near the C termini elicit type-specific antibody responses in the natural host.* J Virol, 1993. **67**(10): p. 6332-8.

11. Allen, G.P. and J.T. Bryans, *Molecular epizootiology, pathogenesis, and prophylaxis of equine herpesvirus-1 infections.* Prog Vet Microbiol Immunol, 1986. **2**: p. 78-144.

12. Papp-Vid, G. and J.B. Derbyshire, *The protective antigens of equine herpesvirus type 1.* Can J Comp Med, 1978. **42**(2): p. 219-26.

13. Turtinen, L.W. and G.P. Allen, *Identification of the envelope surface glycoproteins of equine herpesvirus type 1.* J Gen Virol, 1982. **63**(2): p. 481-5.

14. Crabb, B.S. and M.J. Studdert, *Comparative studies of the proteins of equine herpesviruses 4 and 1 and asinine herpesvirus 3: antibody response of the natural hosts.* J Gen Virol, 1990. **71 (Pt 9)**: p. 2033-41.

15. Crabb, B.S., G.P. Allen, and M.J. Studdert, *Characterization of the major glycoproteins of equine herpesviruses 4 and 1 and asinine herpesvirus 3 using monoclonal antibodies.* J Gen Virol, 1991. **72 (Pt 9)**: p. 2075-82.

16. Whittaker, G.R., et al., *Antigenic and protein sequence homology between VP13/14, a herpes simplex virus type 1 tegument protein, and gp10, a glycoprotein of equine herpesvirus 1 and 4.* J Virol, 1991. **65**(5): p. 2320-6.

17. Csellner, H., et al., *EHV-1 glycoprotein D (EHV-1 gD) is required for virus entry and cell-cell fusion, and an EHV-1 gD deletion mutant induces a protective immune response in mice.* Arch Virol, 2000. **145**(11): p. 2371-85.

18. Neubauer, A., et al., *Analysis of the contributions of the equine herpesvirus 1 glycoprotein gB homolog to virus entry and direct cell-to-cell spread.* Virology, 1997. **227**(2): p. 281-94.

19. Osterrieder, N., *Construction and characterization of an equine herpesvirus 1 glycoprotein C negative mutant.* Virus Res, 1999. **59**(2): p. 165-77.

20. Stokes, A., et al., *The expression of the proteins of equine herpesvirus 1 which share homology with herpes simplex virus 1 glycoproteins H and L.* Virus Res, 1996. **40**(1): p. 91-107.

21. Van de Walle, G.R., et al., *Equine herpesvirus 1 entry via endocytosis is facilitated by alphaV integrins and an RSD motif in glycoprotein D.* J Virol, 2008. **82**(23): p. 11859-68.

22. Kurtz, B.M., et al., *Equus caballus major histocompatibility complex class I is an entry receptor for equine herpesvirus type 1.* J Virol, 2010. **84**(18): p. 9027-34.

23. Spear, P.G. and R. Longnecker, *Herpesvirus entry: an update.* J Virol, 2003. **77**(19): p. 10179-85.

24. Van de Walle, G.R., K.W. Jarosinski, and N. Osterrieder, *Alphaherpesviruses and chemokines: pas de deux not yet brought to perfection.* J Virol, 2008. **82**(13): p. 6090-7.

25. Costes, B., et al., *Both soluble and membrane-anchored forms of Felid herpesvirus 1 glycoprotein G function as a broad-spectrum chemokine-binding protein.* J Gen Virol, 2005. **86**(Pt 12): p. 3209-14.

26. Engelhardt, T. and G.M. Keil, *Identification and characterization of the bovine herpesvirus 5 US4 gene and gene products.* Virology, 1996. **225**(1): p. 126-35.

27. Keil, G.M., et al., *Bovine herpesvirus 1 U(s) open reading frame 4 encodes a glycoproteoglycan.* J Virol, 1996. **70**(5): p. 3032-8.

28. Kongsuwan, K., et al., *Identification of an infectious laryngotracheitis virus gene encoding an immunogenic protein with a predicted M(r) of 32 kilodaltons.* Virus Res, 1993. **29**(2): p. 125-40.

29. McGeoch, D.J., et al., *DNA sequence and genetic content of the HindIII l region in the short unique component of the herpes simplex virus type 2 genome: identification of the gene encoding glycoprotein G, and evolutionary comparisons.* J Gen Virol, 1987. **68 (Pt 1)**: p. 19-38.

30. Rea, T.J., et al., *Mapping and sequence of the gene for the pseudorabies virus glycoprotein which accumulates in the medium of infected cells.* J Virol, 1985. **54**(1): p. 21-9.

31. Crabb, B.S., H.S. Nagesha, and M.J. Studdert, *Identification of equine herpesvirus 4 glycoprotein G: a type-specific, secreted glycoprotein.* Virology, 1992. **190**(1): p. 143-54.

32. McGeoch, D.J., *Evolutionary relationships of virion glycoprotein genes in the S regions of alphaherpesvirus genomes.* J Gen Virol, 1990. **71 (Pt 10)**: p. 2361-7.

33. Nakamichi, K., et al., *Bovine herpesvirus 1 glycoprotein G is required for viral growth by cell-to-cell infection.* Virus Res, 2000. **68**(2): p. 175-81.

34. Trapp, S., et al., *Mutagenesis of a bovine herpesvirus type 1 genome cloned as an infectious bacterial artificial chromosome: analysis of glycoprotein E and G double deletion mutants.* J Gen Virol, 2003. **84**(Pt 2): p. 301-6.

35. Kaashoek, M.J., et al., *Virulence, immunogenicity and reactivation of bovine herpesvirus 1 mutants with a deletion in the gC, gG, gI, gE, or in both the gI and gE gene.* Vaccine, 1998. **16**(8): p. 802-9.

36. Nakamichi, K., Y. Matsumoto, and H. Otsuka, *Bovine herpesvirus 1 glycoprotein G is necessary for maintaining cell-to-cell junctional adherence among infected cells.* Virology, 2002. **294**(1): p. 22-30.

37. Bryant, N.A., et al., *Glycoprotein G isoforms from some alphaherpesviruses function as broad-spectrum chemokine binding proteins.* Embo J, 2003. **22**(4): p. 833-46.

38. Hartley, C.A., H.E. Drummer, and M.J. Studdert, *The nucleotide sequence of the glycoprotein G homologue of equine herpesvirus 3 (EHV3) indicates EHV3 is a distinct equid alphaherpesvirus.* Arch Virol, 1999. **144**(10): p. 2023-33.

39. Costes, B., et al., *Felid herpesvirus 1 glycoprotein G is a structural protein that mediates the binding of chemokines on the viral envelope.* Microbes Infect, 2006. **8**(11): p. 2657-67.

40. Helferich, D., et al., *The UL47 gene of avian infectious laryngotracheitis virus is not essential for in vitro replication but is relevant for virulence in chickens.* J Gen Virol, 2007. **88**(Pt 3): p. 732-42.

41. Ziemann, K., T.C. Mettenleiter, and W. Fuchs, *Gene arrangement within the unique long genome region of infectious laryngotracheitis virus is distinct from that of other alphaherpesviruses.* J Virol, 1998. **72**(1): p. 847-52.

42. Devlin, J.M., et al., *Evaluation of immunological responses to a glycoprotein G deficient candidate vaccine strain of infectious laryngotracheitis virus.* Vaccine, 2010. **28**(5): p. 1325-32.

43. Devlin, J.M., et al., *Glycoprotein G deficient infectious laryngotracheitis virus is a candidate attenuated vaccine.* Vaccine, 2007. **25**(18): p. 3561-6.

44. Bennett, L.M., et al., *The processing of pseudorabies virus glycoprotein gX in infected cells and in an uninfected cell line.* Virology, 1986. **155**(2): p. 707-15.

45. Viejo-Borbolla, A., et al., *Glycoprotein G from pseudorabies virus binds to chemokines with high affinity and inhibits their function.* J Gen Virol. **91**(Pt 1): p. 23-31.

46. Whalley, J.M., G.R. Robertson, and A.J. Davison, *Analysis of the genome of equine herpesvirus type 1: arrangement of cleavage sites for restriction endonucleases EcoRI, BglII and BamHI.* J Gen Virol, 1981. **57**(Pt 2): p. 307-23.

47. Riggio, M.P., A.A. Cullinane, and D.E. Onions, *Identification and nucleotide sequence of the glycoprotein gB gene of equine herpesvirus 4.* J Virol, 1989. **63**(3): p. 1123-33.

48. Van de Walle, G.R., et al., *Herpesvirus chemokine-binding glycoprotein G (gG) efficiently inhibits neutrophil chemotaxis in vitro and in vivo.* J Immunol, 2007. **179**(6): p. 4161-9.

49. Colle, C.F., 3rd and D.J. O'Callaghan, *Transcriptional analyses of the unique short segment of EHV-1 strain Kentucky A.* Virus Genes, 1995. **9**(3): p. 257-68.

50. Ficorilli, N., M.J. Studdert, and B.S. Crabb, *The nucleotide sequence of asinine herpesvirus 3 glycoprotein G indicates that the donkey virus is closely related to equine herpesvirus 1.* Arch Virol, 1995. **140**(9): p. 1653-62.

51. Crabb, B.S., et al., *A type-specific serological test to distinguish antibodies to equine herpesviruses 4 and 1.* Arch Virol, 1995. **140**(2): p. 245-58.

52. Drummer, H.E., M.J. Studdert, and B.S. Crabb, *Equine herpesvirus-4 glycoprotein G is secreted as a disulphide-linked homodimer and is present as two homodimeric species in the virion.* J Gen Virol, 1998. **79 (Pt 5)**: p. 1205-13.

53. von Einem, J., et al., *In vitro and in vivo characterization of equine herpesvirus type 1 (EHV-1) mutants devoid of the viral chemokine-binding glycoprotein G (gG).* Virology, 2007. **362**(1): p. 151-62.

54. Huang, J., et al., *Glycoprotein G deletion mutants of equine herpesvirus 1 (EHV1; equine abortion virus) and EHV4 (equine rhinopneumonitis virus).* Arch Virol, 2005. **150**(12): p. 2583-92.

55. Van de Walle, G.R., et al., *Analysis of the herpesvirus chemokine-binding glycoprotein G residues essential for chemokine binding and biological activity.* J Biol Chem, 2009. **284**(9): p. 5968-76.

56. Patel, J.R., N. Edington, and J.A. Mumford, *Variation in cellular tropism between isolates of equine herpesvirus-1 in foals.* Arch Virol, 1982. **74**(1): p. 41-51.

57. Pusterla, N., et al., *Equine herpesvirus-1 myeloencephalopathy: a review of recent developments.* Vet J, 2009. **180**(3): p. 279-89.

58. Edington, N., C.G. Bridges, and J.R. Patel, *Endothelial cell infection and thrombosis in paralysis caused by equid herpesvirus-1: equine stroke.* Arch Virol, 1986. **90**(1-2): p. 111-24.

59. Welch, H.M., et al., *Latent equid herpesviruses 1 and 4: detection and distinction using the polymerase chain reaction and co-cultivation from lymphoid tissues.* J Gen Virol, 1992. **73 (Pt 2)**: p. 261-8.

60. Slater, J.D., et al., *The trigeminal ganglion is a location for equine herpesvirus 1 latency and reactivation in the horse.* J Gen Virol, 1994. **75 (Pt 8)**: p. 2007-16.

61. van Maanen, C., *Equine herpesvirus 1 and 4 infections: an update.* Vet Q, 2002. **24**(2): p. 58-78.

62. Perkins, G.A., et al., *Detection of equine herpesvirus-1 in nasal swabs of horses by quantitative real-time PCR.* J Vet Intern Med, 2008. **22**(5): p. 1234-8.

63. Diallo, I.S., et al., *Multiplex real-time PCR for the detection and differentiation of equid herpesvirus 1 (EHV-1) and equid herpesvirus 4 (EHV-4).* Vet Microbiol, 2007. **123**(1-3): p. 93-103.

64. Slater, J.D., *Equine herpesviruses*, in *Equine Infectious Diseases*, L.M. Sellon DC, Editor 2077, Saunders Elsevier: St. Louis. p. 134 - 152.

65. Yeargan, M.R., G.P. Allen, and J.T. Bryans, *Rapid subtyping of equine herpesvirus 1 with monoclonal antibodies.* J Clin Microbiol, 1985. **21**(5): p. 694-7.

66. Rosas, C.T., et al., *Equine herpesvirus type 1 modified live virus vaccines: quo vaditis?* Expert Rev Vaccines, 2006. **5**(1): p. 119-31.

67. Kydd, J.H., H.G. Townsend, and D. Hannant, *The equine immune response to equine herpesvirus-1: the virus and its vaccines.* Vet Immunol Immunopathol, 2006. **111**(1-2): p. 15-30.

68. Minke, J.M., J.C. Audonnet, and L. Fischer, *Equine viral vaccines: the past, present and future.* Vet Res, 2004. **35**(4): p. 425-43.

69. Allen, G., et al., *Major histocompatibility complex class I-restricted cytotoxic T-lymphocyte responses in horses infected with equine herpesvirus 1.* J Virol, 1995. **69**(1): p. 606-12.

70. Hannant, D., et al., *Equid herpesvirus-induced immunosuppression is associated with lymphoid cells and not soluble circulating factors.* Viral Immunol, 1999. **12**(4): p. 313-21.

71. Burki, F., et al., *Viraemia and abortions are not prevented by two commercial equine herpesvirus-1 vaccines after experimental challenge of horses.* Vet Q, 1990. **12**(2): p. 80-6.

72. Meeusen, E.N., et al., *Current status of veterinary vaccines.* Clin Microbiol Rev, 2007. **20**(3): p. 489-510, table of contents.

73. Brune, W., M. Messerle, and U.H. Koszinowski, *Forward with BACs: new tools for herpesvirus genomics.* Trends Genet, 2000. **16**(6): p. 254-9.

74. Messerle, M., et al., *Cloning and mutagenesis of a herpesvirus genome as an infectious bacterial artificial chromosome.* Proc Natl Acad Sci U S A, 1997. **94**(26): p. 14759-63.

75. Shizuya, H., et al., *Cloning and stable maintenance of 300-kilobase-pair fragments of human DNA in Escherichia coli using an F-factor-based vector.* Proc Natl Acad Sci U S A, 1992. **89**(18): p. 8794-7.

76. Adler, H., M. Messerle, and U.H. Koszinowski, *Cloning of herpesviral genomes as bacterial artificial chromosomes.* Rev Med Virol, 2003. **13**(2): p. 111-21.

77. Osterrieder, N., et al., *[Establishment and use of infectious bacterial artificial chromosome (BAC) DNA clones of animal herpesviruses].* Berl Munch Tierarztl Wochenschr, 2003. **116**(9-10): p. 373-80.

78. Rudolph, J., D.J. O'Callaghan, and N. Osterrieder, *Cloning of the genomes of equine herpesvirus type 1 (EHV-1) strains KyA and racL11 as bacterial artificial chromosomes (BAC).* J Vet Med B Infect Dis Vet Public Health, 2002. **49**(1): p. 31-6.

79. Azab, W., et al., *Glycoprotein C of equine herpesvirus 4 plays a role in viral binding to cell surface heparan sulfate.* Virus Res, 2010. **151**(1): p. 1-9.

80. Azab, W., et al., *Cloning of the genome of equine herpesvirus 4 strain TH20p as an infectious bacterial artificial chromosome.* Arch Virol, 2009. **154**(5): p. 833-42.

81. Lusso, P., *Chemokines and viruses: the dearest enemies.* Virology, 2000. **273**(2): p. 228-40.

82. Kenneth Murphy, P.T., Mark Walport, Charles Janeway, *Induced innate responses to infection*, in *Janeway´s immunobiology*2008, Garnand Science, Taylor & Francis Group, LLC: New York. p. 83 - 90.

83. Alcami, A. and S. Efstathiou, *Soluble chemokine binding proteins are also encoded by herpesviruses.* Immunol Today, 2000. **21**(10): p. 526-7.

84. Lalani, A.S., J.W. Barrett, and G. McFadden, *Modulating chemokines: more lessons from viruses.* Immunol Today, 2000. **21**(2): p. 100-6.

85. Webb, L.M. and A. Alcami, *Virally encoded chemokine binding proteins.* Mini Rev Med Chem, 2005. **5**(9): p. 833-48.

86. Mossman, K., et al., *Myxoma virus M-T7, a secreted homolog of the interferon-gamma receptor, is a critical virulence factor for the development of myxomatosis in European rabbits.* Virology, 1996. **215**(1): p. 17-30.

87. Lalani, A.S. and G. McFadden, *Secreted poxvirus chemokine binding proteins.* J Leukoc Biol, 1997. **62**(5): p. 570-6.

88. Graham, K.A., et al., *The T1/35kDa family of poxvirus-secreted proteins bind chemokines and modulate leukocyte influx into virus-infected tissues.* Virology, 1997. **229**(1): p. 12-24.

89. Alcami, A., et al., *Blockade of chemokine activity by a soluble chemokine binding protein from vaccinia virus.* J Immunol, 1998. **160**(2): p. 624-33.

90. van Berkel, V., et al., *Identification and initial characterization of the murine gammaherpesvirus 68 gene M3, encoding an abundantly secreted protein.* J Virol, 1999. **73**(5): p. 4524-9.

91. van Berkel, V., et al., *Identification of a gammaherpesvirus selective chemokine binding protein that inhibits chemokine action.* J Virol, 2000. **74**(15): p. 6741-7.

92. Webb, L.M., V.P. Smith, and A. Alcami, *The gammaherpesvirus chemokine binding protein can inhibit the interaction of chemokines with glycosaminoglycans.* Faseb J, 2004. **18**(3): p. 571-3.

93. Viejo-Borbolla, A., et al., *Glycoprotein G from pseudorabies virus binds to chemokines with high affinity and inhibits their function.* J Gen Virol, 2010. **91**(Pt 1): p. 23-31.

94. Doll, E.R., et al., *Propagation of equine abortion virus in Syrian hamsters.* Cornell Vet, 1956. **46**(1): p. 68-82.

95. Patel, J.R. and N. Edington, *The pathogenicity in mice of respiratory, abortion and paresis isolates of equine herpesvirus-1.* Vet Microbiol, 1983. **8**(3): p. 301-5.

96. Awan, A.R., Y.C. Chong, and H.J. Field, *The pathogenesis of equine herpesvirus type 1 in the mouse: a new model for studying host responses to the infection.* J Gen Virol, 1990. **71 (Pt 5)**: p. 1131-40.

97. Bartels, T., et al., *In situ study on the pathogenesis and immune reaction of equine herpesvirus type 1 (EHV-1) infections in mice.* Immunology, 1998. **93**(3): p. 329-34.

98. Csellner, H., J.M. Whalley, and D.N. Love, *Equine herpesvirus 1 HVS25A isolated from an aborted foetus produces disease in balb/C mice.* Aust Vet J, 1995. **72**(2): p. 68-9.

99. Walker, C., D.N. Love, and J.M. Whalley, *Comparison of the pathogenesis of acute equine herpesvirus 1 (EHV-1) infection in the horse and the mouse model: a review.* Vet Microbiol, 1999. **68**(1-2): p. 3-13.

100. Van de Walle, G.R., et al., *A vectored equine herpesvirus type 1 (EHV-1) vaccine elicits protective immune responses against EHV-1 and H3N8 equine influenza virus.* Vaccine, 2009.

101. Sedgwick, A.D., et al., *Single step purification procedure for the rapid separation of equine leucocytes.* Vet Res Commun, 1986. **10**(6): p. 445-52.

102. Van de Walle, G.R., K. Sakamoto, and N. Osterrieder, *CCL3 and viral chemokine-binding protein gg modulate pulmonary inflammation and virus replication during equine herpesvirus 1 infection.* J Virol, 2008. **82**(4): p. 1714-22.

103. Borchers, K., et al., *Antibodies against equine herpesviruses and equine arteritis virus in Burchell's zebras (Equus burchelli) from the Serengeti ecosystem.* J Wildl Dis, 2005. **41**(1): p. 80-6.

104. Seyboldt, C., H. Granzow, and N. Osterrieder, *Equine herpesvirus 1 (EHV-1) glycoprotein M: effect of deletions of transmembrane domains.* Virology, 2000. **278**(2): p. 477-89.

105. Tischer, B.K., et al., *Two-step red-mediated recombination for versatile high-efficiency markerless DNA manipulation in Escherichia coli.* Biotechniques, 2006. **40**(2): p. 191-7.

106. Tischer, B.K., G.A. Smith, and N. Osterrieder, *En passant mutagenesis: a two step markerless red recombination system.* Methods Mol Biol, 2010. **634**: p. 421-30.

107. Lee, E.C., et al., *A highly efficient Escherichia coli-based chromosome engineering system adapted for recombinogenic targeting and subcloning of BAC DNA.* Genomics, 2001. **73**(1): p. 56-65.

108. Osterrieder, N., et al., *Protection against EHV-1 challenge infection in the murine model after vaccination with various formulations of recombinant glycoprotein gp14 (gB).* Virology, 1995. **208**(2): p. 500-10.

109. Bland, J.M. and D.G. Altman, *Analysis of continuous data from small samples.* BMJ, 2009. **338**: p. a3166.

110. Rudolph, J. and N. Osterrieder, *Equine herpesvirus type 1 devoid of gM and gp2 is severely impaired in virus egress but not direct cell-to-cell spread.* Virology, 2002. **293**(2): p. 356-67.

111. Meyer, H. and P.H. Hubert, *Isolation and characterization of monoclonal antibodies against an attenuated vaccine strain of equine herpesvirus type 1 (EHV-1).* Vet Microbiol, 1988. **18**(1): p. 95-101.

112. Day, L., *Characterisation of selected glycoproteins of equine herpesvirus-1: immune in the murine model*, 1999, University of Leeds, UK.

113. Borchers, K., et al., *Characterisation of three equine influenza A H3N8 viruses from Germany (2000 and 2002): evidence for frozen evolution.* Vet Microbiol, 2005. **107**(1-2): p. 13-21.

114. Devlin, J.M., et al., *Glycoprotein G is a virulence factor in infectious laryngotracheitis virus.* J Gen Virol, 2006. **87**(Pt 10): p. 2839-47.

115. Thomsen, D.R., et al., *Replication and virulence of pseudorabies virus mutants lacking glycoprotein gX.* J Virol, 1987. **61**(1): p. 229-32.

116. Devlin, J.M., G.F. Browning, and J.R. Gilkerson, *A glycoprotein I- and glycoprotein E-deficient mutant of infectious laryngotracheitis virus exhibits impaired cell-to-cell spread in cultured cells.* Arch Virol, 2006. **151**(7): p. 1281-9.

117. Alexander, J.M., et al., *Structural basis of chemokine sequestration by a herpesvirus decoy receptor.* Cell, 2002. **111**(3): p. 343-56.

Acknowledgements

First of all I would like to thank Prof. Klaus Osterrieder for providing me with an interesting topic for my thesis and also for financing and mentoring.

Also, I am deeply grateful to Prof. Gerlinde Van de Walle, who first introduced me to the basic laboratory techniques and the project in Cornell, for helping me with fruitful discussions and advice during the whole study and for always making science look fascinating and interesting again when I most needed it.

I want to thank Dr. Karsten Tischer for explaining the Two-step en passant Red-mediated recombination and for checking the constructed primers, as well as for proof reading parts of this thesis. I highly appreciate the advice of Dr. Matthias Sieber and Veljko Nikolin for the flow cytometric analyses during the in vivo mice experiments. Also, I am very thankful to Dr. Olivia Kershaw for doing the histopathological examinations of the mouse lungs and taking time to sit down with me to look through all the slides.

For the help with the animal experiment I would like to thank Dr. Benedikt Kaufer and our technician Ann Reum, as well as Timo Schippers, especially for giving me moral support during that time.

I am very grateful to all my lab colleges, particularly to Swaantje Roth and Timo Schippers for proof reading most parts of this thesis, Timo Schippers for helping me with the western blots and Annachiara Greco and Inês Veiga for the fruitful discussions. I would like to thank all four not only for giving me moral support at the right time but also for our great shared lunches.

Also, I would like to thank our technicians Tine Leiskau and Ann Reum for all the help provided regarding cell culture work and viral titrations and Silke Feineis for helpful advice in laboratory techniques. I am very grateful to Fabian Lotz (Institute of Biometrics), Annemarie and Odilo Engel and Hanna Plickert for the help in statistics. Furthermore, I want to thank Camillo Krawzcyk (Veterinary Library) for providing me with literature.

I highly appreciate the help of Thomas Kappel with the graphics and layout of this work.

To my roommates, thank you for coping with my moods, giving me moral support and for the plate of food on the table when I came home from the lab late in the evening.

I am also grateful to my physiotherapist Alan, who helped me being able to sit at a desk for a long time.

Also, I want to thank my aunt Irmela Feige for supervision and helping me with my time management.

Last but not least, I want to thank my parents for all the encouragement and support and for showing me that it is always possible to achieve your goals when you put your mind to it.

Selbständigkeitserklärung

Hiermit bestätige ich, dass ich die vorliegende Arbeit selbständig angefertigt habe. Ich versichere, dass ich ausschließlich die angegebenen Quellen und Hilfen in Anspruch genommen habe.

Berlin, 07. Juli 2011

Nora Mariella Thormann